DEVELOPMENT AND APPLICATIONS OF A MICROFLUIDIC VASCULAR MIMIC

By

Paul A. Vogel

A DISSERTATION

Submitted to
Michigan State University
in partial fulfillment of the requirements
for the degree of

DOCTOR OF PHILOSOPHY

Chemistry

2012

ABSTRACT

DEVELOPMENT AND APPLICATIONS OF A MICROFLUIDIC VASCULAR MIMIC

By

Paul A. Vogel

Vascular wall biology and interactions with bloodstream components are areas of continued interest due to the high prevalence of cardiovascular disease and stroke. Cell types comprising the vascular wall, as well as those found in the bloodstream, are frequently isolated and cultured *in vitro* to determine their biological roles, including their involvement in disease progression. Recently, microfluidic systems have emerged as desirable platforms for mimicking biological systems, offering precise control of cellular environments. Here, work is presented that advances microfluidic technology and improves the utility of microfluidic systems for cell-based assays and cell culture.

The endothelium is an important component of the vascular wall due to its role as a protective barrier, as well as its involvement in several important vascular functions. *In vivo*, the endothelium plays a vital role in the regulation of vascular tone by releasing several factors that cause vessel dilation, of which nitric oxide (NO) is one of the most potent. The endothelial cells comprising the endothelium are influenced by many environmental factors, such as shear stress generated by flowing blood and the degree of confluence of the endothelial monolayer. Presented here is the development of novel microfluidic system capable of mimicking the vasculature by incorporating microfluidic channels that enable blood flow past cultured endothelial monolayers. Importantly, this microfluidic vascular mimic is successfully integrated with a transendothelial electrical resistance (TEER) measurement system that allows for the

monitoring of endothelial monolayer confluence and barrier integrity. This microfluidic system is used to highlight the impact of monolayer confluence on cellular behavior by showing that, in response to flowing red blood cells (RBCs), confluent endothelial monolayers produce significantly more NO than less confluent monolayers.

C-peptide, a potential drug for type 1 diabetes, is known to improve blood flow by a previously unknown mechanism. This dissertation hypothesizes that C-peptide is capable of indirectly inducing vessel dilation by stimulating the release of adenosine triphosphate (ATP) from flowing RBCs, which can diffuse to the endothelium to bind purinergic receptors on the endothelial cell surface, ultimately resulting in endothelial NO production. To investigate this hypothesis, the microfluidic vascular mimic is utilized to monitor cell-cell communication, revealing C-peptide is capable of stimulating endothelial NO production by a mechanism mediated by the RBC which requires P2Y purinoreceptor activation by ATP. Importantly, it is shown that in order to observe this NO production, C-peptide must be prepared with Zn^{2+}.

This proposed mechanism describes how Zn^{2+}/C-peptide may improve blood flow indirectly as a result of activity within the bloodstream. However, since C-peptide has never been observed exogenous of the bloodstream *in vivo*, it is unclear whether all C-peptide bioactivity results similarly, or if C-peptide can also escape the bloodstream to directly stimulate cells in surrounding tissue. To assess the ability of C-peptide to penetrate the vascular wall, the microfluidic TEER system is employed to determine the ability of C-peptide to permeate the endothelium, revealing that C-peptide can permeate confluent endothelial monolayers *in vitro*, suggesting that C-peptide may escape the bloodstream *in vivo*. Collectively, this work shows that C-peptide may have a more comprehensive biological role than is currently assumed.

ACKNOWLEDGEMENTS

Firstly, I would like to thank the organizations responsible for funding this research, including Michigan State University for research and travel funding, some of which I have repaid in the form of late registration and enrollment fees. Additionally, I am grateful for research funding provided by the National Institutes of Health and Merck. I appreciate the investments made by each of these organizations in this research, as well as my development as a scientist.

Family members, friends and faculty have helped me complete this dissertation and the work described within. In fact, I was coaxed into attending graduate school by my dear wife Erica, who always has great ideas. In the absence of her persuasion I would not have attended graduate school and, therefore, Erica is primarily responsible for this accomplishment. Luckily, Erica did not abandon me during the course of this work and instead provided consistent encouragement and support throughout. Erica's influence has significantly improved my life, and she was also fundamental to the completion of this dissertation to the extent that she should probably be listed as an author, but this acknowledgement will have to suffice.

Aside from Erica, my family members are the only people who I am certain believed that I was capable of my achievements. Julie, my mother, worked incredibly hard during my childhood, and without this example I am not sure I would have had the dedication required to complete this dissertation. My mom has always urged me to do better, academically and in general, often to no avail. I cannot begin to fathom the stress I have caused my mother over the past quarter century, so I am thankful that she was well enough to endure more during my years as a graduate student. Richard and Sue, my grandparents, have always stressed the importance of an education, both verbally, and by example as career educators. During the

numerous periods of time that I was bored and distracted from school, it was always advice from my grandparents that would motivate me to be a better scholar. Without their advice and support, financial and otherwise, I would most likely not be college educated. My grandpa is the wisest man I know, and I believe that every word he says before 6:00 pm should be written down and studied. Also, my brother Danny has always been excited about my accomplishments and he truly cares about my success, which I find particularly motivating. However, his contributions to this dissertation are questionable when considering the hours we spent playing video games in lieu of studying.

The faculty of this department has provided me with a tremendous graduate education which has enabled me to think about complex problems and approach them as a scientist. As a result of my graduate training, I have gained the skills and confidence necessary for independent research. I am grateful for the advice and critique from my guidance committee. Importantly, I would like to thank Dana Spence, my advisor, for accepting me into his group with my sterling reputation and providing me with exciting scientific opportunities. I truly appreciate his guidance through the work presented in this dissertation. I believe the training I have received from him is invaluable, which will undoubtedly benefit me throughout life, as will the one-liners and limericks that will be forever in my memory.

I would also like to thank the Spence research group for their contributions to this work and for being fun, which made my graduate experience enjoyable. In particular, I would like to thank Kari Anderson and Suzanne Letourneau for always reminding me of my obligations and allowing me to study their superior class notes. I would also like to thank Stephen Halpin for showing me the professional etiquette of national conferences.

TABLE OF CONTENTS

LIST OF TABLE

LIST OF FIGURES

Chapter 1 - Introduction

In vitro cell-based assays have become widely used in the bioscience, biotechnology, and drug discovery fields as they allow precise control of the environment surrounding the cells, enabling the observation of cellular responses to specific environmental queues of interest. Replicating a biological environment *in vitro* greatly simplifies the system under investigation, and also provides an opportunity to monitor specific phenomenon that may not be observable in the more sophisticated environments found *in vivo*. However, in order to successfully extrapolate results derived from *in vitro* studies to the biology of the intact system found *in vivo*, all necessary components that influence the biological activity of interest should be included in an *in vitro* biological mimic. Microfluidic technology provides a platform which most adequately meets these requirements as microfluidic devices can mimic microenvironments found *in vivo* dimensionally, while also allowing precise control of important aspects of the microenvironment, such as chemical signaling[1-3], physiological stresses[4-6], temperature[7-9], and degree of cell-cell interactions,[10, 11].

Biomedically, microfluidic systems have provided valuable platforms for the modeling of cellular monolayers *in vitro*. In order to investigate cell monolayer biology with an *in vitro* model, the layer of cells comprising the wall must be confluent, display a restrictive paracellular pathway, high electrical resistance, physiologically relevant cell architecture, and functional expression of transporter mechanisms while being easy to culture.[12, 13] Microfluidic technology can meet these requirements, providing the successful development of a method to determine monolayer confluence of cells cultured on a microfluidic device. Cellular monolayers are of particular interest because they form barriers *in vivo* that often regulate solute transport.

These barriers are responsible for selectively trafficking some solutes and macromolecules between the distinct regions defined by the barrier, while completely excluding others. Importantly, this activity is often responsible for the exclusion of harmful toxins, maintaining concentration gradients, influencing drug pharmacodynamics, and influencing the physiology of various cell types by manipulating the cellular environment and regulating the introduction of molecules that impact cell behavior. Not surprisingly, the malfunction of cells comprising monolayers, including breakdown of monolayer barrier integrity, has been implicated in various disease states, such as: congenital deafness[14-16], inflammatory bowel disease[17], diabetes[18, 19], multiple sclerosis[20, 21], and even allergies.[22, 23]

Depending on the tissue they developed from *in vivo*, these cellular barriers are comprised of endothelial or epithelial cells. Each of these cell types is similar in function, and, in fact, endothelial cells are often thought of as specialized epithelial cells. Epithelial cells line most structures and cavities in the body, such as the digestive, respiratory, and urinary tracts, as well as many glands, whereas endothelial cells line the lymph and cardiovascular systems. Importantly, endothelial cells line all blood contacting surfaces in the body, from the internal lining of all types of blood vessels, to the outer lining of heart valves. These cells are involved in several distinct and important functions including, but not limited to: regulation of vascular tone[24-26], fluid filtration[27, 28], neutrophil recruitment[29, 30], hemostasis[31, 32], pathogen exclusion and host response[33-35], as well as hormone trafficking.[36, 37] Importantly, since many endothelial functions like these are influenced by the degree of cell confluence, a determination of cell confluence prior to experimentation is imperative and should be routine. Nevertheless, the overwhelming importance of endothelial functions is

continuing to be realized, and as a result, the unsurpassed ability of microfluidic technology to mimic biological systems has been exploited for *in vitro* research of important vascular processes.[38, 39]

1.1 - Monitoring Cell Monolayer Barrier Integrity

Endothelial permeability is frequently studied because it is fundamental for understanding pathological and physiological cardiovascular processes. Molecules can permeate the endothelium by transcellular or paracellular mechanisms.[40] For example, molecules can permeate the endothelium paracellularly by passive diffusion between interendothelial junctions (the space between adjacent endothelial cells). Additionally, the transport of macromolecules, such as plasma proteins, is often accomplished by fluid-phase or absorptive (receptor mediated) transcellular transport mechanisms where the molecule trafficked through the cell. Generally, macromolecules are encapsulated and transported from the apical side (facing the bloodstream) of the cell, through the cellular cytosol, to be endocytosed on the abluminal, or basolateral side (facing the interstitium, or the region opposite of the bloodstream), a process that is receptor mediated. In a similar transcellular mechanism of transport, the fusion of multiple caveolae can transiently form a transcellular channel spanning the entire length of the endothelial cell allowing for passive diffusion of plasma proteins through the cell in a mechanism not requiring receptor mediation. Additionally, aquaporins can form channels across the lipid bilayer that is highly specific for water soluble molecules, thus creating a transendothelial pathway for water and water solutes.

Endothelial cells molecularly regulate permeability by the formation of tight junctions between adjacent endothelial cells, causing the paracellular diffusion of most molecules to be

prohibited.[41, 42] In fact, tight junctions have been discovered to be primarily responsible for the regulation of endothelial permeability.[43] Surprisingly, tight junctions can limit paracellular transport so much that only small water soluble molecules with an ionic radius of less than 3 nm are typically capable of permeating these tight junctions, predominantly limiting interendothelial diffusion to only ions.[40] Tight junctions form a continuous, circumferential barrier surrounding endothelial cells that serves as a boundary between the apical and basolateral domains, as well as a fence within the plasma membrane, offering protection to the cells from the external environment while mediating the paracellular exchange of substances.[43] Structurally, tight junctions are composed of clusters of integral proteins, some of which span the intercellular space and interact with adjacent integral intracellular proteins of nearby cells to complete the protein cluster and form an intercellular boundary.

Several integral transmembrane proteins are responsible for forming cell-cell contacts, including: the claudin family of proteins (1-24), occludin, tricellulin, JAM-A, CAR, CLMP, ESAM, JAM4, and CRB3.[44] These integral proteins are organized based on structure in three classes. The first class includes claudins, occludin, and tricellulin, all of which include four transmembrane regions, two extracellular loops, and two cytoplasmic tails. Another class includes CRB3, which is characterized by a short extracellular domain, a single transmembrane domain, and a short cytoplasmic tail. CRB3 differs from the other integral membrane proteins as the function of the extracellular domain is not yet clear. The remaining integral proteins make up another class, and are characterized by two immunoglobulin-like domains. These integral proteins are linked to the actin cytoskeleton of the cell by classic scaffolding proteins, such as the zonula occludens (ZO) proteins (ZO-1, ZO-2, and ZO-3) among others.[44] Together,

the protein network forms a barrier capable of mediating paracellular transport. Importantly, the complexity of the tight junctional network depends on cell type, yielding differences in barrier integrity and function between different tissues and organs.[45] It is also important to note that tight junctional control of permeability is not statically controlled, but is an organized, dynamic process controlled by molecular signaling.[46] While tight junctions are primarily responsible for regulating monolayer permeability, another protein cluster can also play a role in paracellular transport by forming adherens, but these junctions are primarily responsible for providing structural support to tissue. However, an ideal measure of endothelial barrier integrity will account for any restriction in permeability caused by tight junctions and adherens junctions, since adherens junctions are essential to the maintenance of endothelial barrier function.[47]

Interest in cell monolayer integrity has led to the development of several techniques to evaluate this integrity. Cell confluence and integrity can be determined *in vitro* by a variety of methods, including: the acquisition of an image of the cells by optical microscopy, measuring the permeability of radiolabeled or fluorescently tagged molecules, immunostaining for proteins characteristic of tight junctions, and measuring transendothelial/epithelial electrical resistance. Each of these methods has utility in various situations, however they are drastically different and, therefore, the significance and meaning of results acquired by each method should be well understood.

1.1.1 - Optical Microscopy

A simple method for verifying confluence of cultured cells is by the visual assessment of a bright-field image of the cells acquired via optical microscopy. This method is quite fast and

simple, and requires minimal training to learn. Additionally, visualization of the cells allows for the inspection of cell morphology and detection of undesirable bacteria. While the general health and extent of confluence can be estimated by this method, it is a qualitative and fairly subjective technique. Conclusions resulting from the visual assessment of a cell culture by different individuals are never quantitative and can vary, inevitably introducing bias to the method. Furthermore, it is difficult to detect voids between non-manipulated cells and impossible to verify the presence of tight junctions by optical microscopy. These issues are often compounded when only a small area of the cell culture is examined, as is typical for this method. For these reasons, only a subjective and qualitative estimation of cell health and confluence can be obtained by this method without modification of the cell, whereas a quantitative measure of monolayer barrier integrity is preferred.

Ideally, a quantitative measure of cell confluence is attainable so that bias does not influence the measurement, yielding more accurate and objective conclusions than those derived from qualitative measurements. Furthermore, an analysis that encompasses the area of the entire cell culture is preferable so that areas of compromised barrier integrity are not overlooked. Not surprisingly, developments have been made in order to improve these issues and broaden the utility of the technique, often by modifying the cells prior to analysis, but not always. Recently, a method for quantitatively determining monolayer confluence was reported that involves using optical phase microscopy in conjunction with computer software to detect intercellular voids.[48, 49] Detection of these voids by commonly used bright-field optical microscopy is not plausible due to the minimal variations in light intensity between paracellular voids and areas covered by the transparent cells. In contrast, optical phase microscopy results

in the destructive interference of light that passes through a specimen, causing the areas covered by cells to be dark with a light background allowing for the differentiation and quantification of these different phases by computational image analysis. However, the successful detection of small paracellular voids requires a detailed image, an issue that potentially increases the likelihood that areas of compromised barrier integrity are unnoticed since the analysis of an entire cell culture with a single image is often not feasible. Furthermore, these techniques are limited to verifying monolayer confluence since the modes of transport across the monolayer, or factors associated with proper barrier function, are not investigable by these methods and therefore are not ideal techniques for determining monolayer permeability and barrier function.

An additional method for verifying cell confluence is immunostaining proteins characteristic of tight junctions (occludins, ZO-1, and ZO-2) for detection by fluorescence microscopy.[50] This method has proven useful for verifying barrier function of endothelial monolayers,[51-53] in addition to detecting reductions in barrier function in response to various biological signals.[54-56] Furthermore, this method allows for the visualization of paracellular voids so that areas of barrier compromise can be detected by eye. Undoubtedly, this is a powerful method for determining tight-junctional control of paracellular transport and the extent of monolayer barrier integrity; however this labeling technique is not quantitative. While bias in this measurement is minimized, a visual detection of paracellular voids is still required, which may be accidentally overlooked. Furthermore, this method is limited to a single determination observation for a specific cell culture, eliminating the possibility of a time-lapse analysis of barrier integrity or confluence of the cultured cell monolayer, unless compared to a separate

cell culture that serves as a control. Additionally, a label-free determination of barrier integrity is preferred as labeling techniques can sometimes alter cell behavior, an important consideration if further experimentation is necessary post-labeling. Additionally worth noting is a microscopy technique, ion conductance microscopy, and while it is not an optical technique, it has been adapted for evaluating monolayer barrier integrity since an image in very fine detail of practically any surface can be obtained.[57, 58] However, this method is not yet capable of providing a quantitative measurement of barrier integrity for the complete cell layer.

1.1.2 - Permeability Assays

A straightforward method for the determination of barrier integrity is to monitor the pervasion of an analyte through the monolayer of cells.[59] Typically, endothelial cells are cultured upon a polycarbonate membrane that has been coated with an adhesion molecule such as fibronectin or collagen.[60] After the cells are thought to reach confluency, the membrane is placed in a diffusion cell as shown in Figure 1.1 (typically a cell culture insert placed in the well of a microtiter multiwell plate), while permeation of an analyte from the apical (abluminal) to the basolateral (luminal) compartments is monitored.[60-63] These analytes, or tracers, are typically fluorescently or isotopically labeled.[64] Resulting permeability coefficients are useful for verifying the barrier integrity of a biological mimic, or for estimating the ability of a drug of interest to permeate a barrier *in vivo*.[65] Some typical tracers include sodium fluorescein, lucifer yellow, fluorescein isothiocyanate (FITC) labeled dextrans, [^{14}C] labeled sucrose[66], and [^{3}H] labeled albumin[67]. By determining permeation coefficients of an analyte across a monolayer of cells, a quantitative determination of barrier integrity is achieved that is dependent on the entire cell culture area.

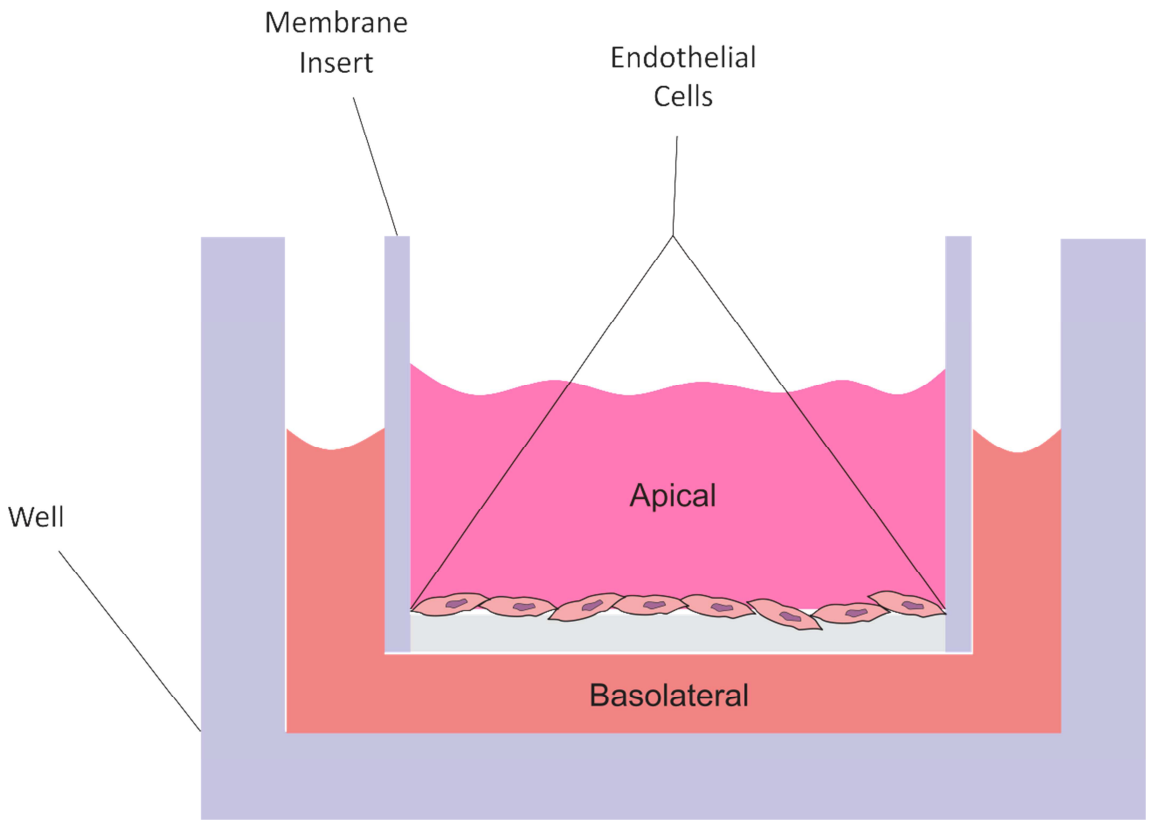

Figure 1.1 - A microtiter cell culture insert (membrane insert) is shown resting in a microtiter well, forming a diffusion cell most commonly used for permeability assays. Typically, a monolayer of cells is cultured upon a collagen or fibronectin coated membrane at the bottom of the membrane insert. The permeation of analytes or drugs of interest from the apical solution to the basolateral solution can be monitored to estimate the *in vivo* permeability of particular cellular barriers, represented by the cultured cells, to the molecules under investigation. Also, the confluence and barrier integrity of the cultured cellular monolayer can be determined by monitoring the permeation of a tracer molecule from the apical compartment to the basolateral compartment and calculating a permeability coefficient, which is proportional to layer barrier integrity. For interpretation of the references to color in this and all other figures, the reader is referred to the electronic version of this dissertation.

The determination of permeation coefficients has become a dominant method for predicting drug absorption *in vivo*.[68] Monitoring drug permeation across a cultured monolayer of cells is often superior to other methods for predicting drug absorption *in vivo* because it accounts for all modes of transport of a drug through a cellular barrier. Drugs are able to permeate cellular barriers in order to reach a desired organ of interest by paracellular and transcellular mechanisms as discussed previously.[40] All possible transcellular mechanisms are accounted for when determining permeation coefficients of a particular analyte, as well as paracellular transport around individual endothelial cells through interendothelial junctions. However, if a confluent endothelial monolayer is intact, transport through interendothelial junctions will be under tight junctional control where typically only small molecules with a molecular radius of less than 3 nm, such as glucose, urea, and small ions, will successfully permeate the monolayer paracellularly.[40]

In addition to drug absorption studies, permeation coefficients of a molecule are particularly also useful for determining factors that can alter or influence monolayer permeability *in vivo*.[69, 70] However, cell monolayer confluence is dependent on complete endothelial coverage and the development of tight junctional intercellular contacts, and since a healthy endothelial barrier will still allow transcellular transport, a superior measurement for monitoring monolayer growth and confluence should involve the permeation of molecules whose permeation is primarily restricted by interendothelial junctions as opposed to transcellular transport. For example, interendothelial junctions under tight junctional control restrict all molecules aside from very small molecules (molecular radius < 3 nm), the interendothelial flux of small water soluble molecules are generally determined primarily by cell

confluence as opposed to transcellular transport and, therefore, a measurement of that flux will adequately gauge cell growth, confluence, and barrier integrity.

1.1.3 - Measuring Transendothelial Electrical Resistance (TEER)

A continuous endothelial monolayer under tight junctional control forms a barrier capable of restricting the motion of molecules as small as ions,[71] and because of this, a straightforward way to determine cell monolayer confluence and barrier integrity is by measuring the ability of the monolayer to restrict the motion of ions. TEER measurements determine the resistance to current induced by an endothelial monolayer when a potential difference is applied across the cellular barrier. The ability of the monolayer to restrict the interendothelial flux of ions, measured by current, is dependent upon the degree of endothelial confluence and barrier integrity induced by the formation of tight junctions between the cells. In this construct, a fully confluent cell monolayer with a high degree of barrier integrity will have a decreased current response, and therefore increased electrical resistance, when compared to a cell monolayer with compromised barrier integrity, assuming that potential applied across each monolayer is of equal magnitude.

By measuring the ability of a monolayer of cells to restrict the motion of ions, a quantitative measure of monolayer confluence and barrier function can be obtained. For example, the most common TEER evaluation is the measurement of the electrical resistance induced by the cellular monolayer. Not only is measuring TEER a quantitative technique, these measurements encompass the entire monolayer and thereby offer a characterization of the overall barrier function of the collective cell culture as opposed to only a portion of the cell layer, as is typical of most optical techniques for determining confluence. Importantly, TEER measurements are

quite useful for verifying monolayer confluence, as TEER values change exponentially during periods of cell growth and death, but remain constant while the cells are at a confluent state. Therefore, comprehensive cell confluence can be verified by multiple sustained TEER measurements over a period of time.

It should be noted that the relationship between transport of solutes (as measured by permeability coefficients) and electrical resistance is nonlinear.[65, 72] This is because solute transport depends on the sum of transport across all transcellular and paracellular pathways[64], while electrical resistance is believed to be dependent on the paracellular permeability of small ions through the interendothelial junctions between endothelial cells.[65] These junctions generally restrict the paracellular transport of hydrophilic and large molecules.[72, 73] While both measurements are indicative of barrier integrity, one must acknowledge the meaning of each measurement when performing experiments.

Obtaining TEER of a cell monolayer to evaluate confluence and barrier integrity is particularly beneficial as it does not damage the cell or alter cell phenotype, and requires only a matter of seconds to perform each measurement. Experimentally, these advantages make TEER measurements uniquely suitable for time-lapse analysis of monolayer integrity due to the ability to repeatedly acquire a quantitative measure of monolayer integrity in a timely fashion without altering cell behavior or phenotype. Consequentially, TEER measurements are frequently involved in investigations of factors affecting cell monolayer barrier solidification[74-76], as well as compromise[77-79], in studies where a basal monolayer integrity can be achieved and verified prior to measuring change in barrier integrity in response to stimuli of interest. These studies have the experimental advantage of confirming monolayer barrier

integrity prior to investigation, yielding the associated benefits mentioned previously, while also eliminating the need for separate cell cultures for negative controls that are often necessary for methods that only allow a one-time measurement of barrier integrity, such as immunostaining tight junctional proteins. This ensures that a change in barrier integrity is truly in response to the intended stimuli, eliminating the assumption that the control cell monolayer exhibits identical barrier integrity as the experimental cell monolayer prior to experimentation. These experimental benefits are in addition to the fundamental advantages granted by the ability to perform multiple measurements without altering cell behavior, resulting in a method that allows for the verification of cell monolayer confluence prior to experimentation which, in turn, ensures proper cellular behavior and increased reproducibility between biological models. As a result of these important experimental advantages, measuring TEER has become the most commonly used method for investigating cell growth and confluence.

The first reports of monitoring TEER across a cultured monolayer of brain endothelial cells were in 1987[80, 81]. Since then, performing TEER measurements has become a common and simple technique with the production of commercial instruments. Most of the commercially based methods for measuring TEER across endothelial cell cultures adhered to microporous filters or culture inserts employ Volt-Ohm resistance meters equipped with “chopstick” electrodes, or chamber electrodes as shown in Figure 1.2. The same microtiter technology used to create a diffusion cell for permeability studies may be used for measuring TEER across a monolayer of cells. However, endothelial cells cover all blood-contacting surfaces of the cardiovascular system and, due to their location, they experience constant exposure to hemodynamic shear stress generated by flowing blood. *In vitro*, applying shear stress on

endothelial cells is critical for the expression of certain cellular responses because shear stress has been shown to regulate many functions of the endothelium *in vivo*.[82] Additionally, many functions of the endothelium are mediated by cell-cell communication,[30, 83-90] so the presence and the degree of cell-cell interactions should be considered in an *in vitro* model of the vasculature.

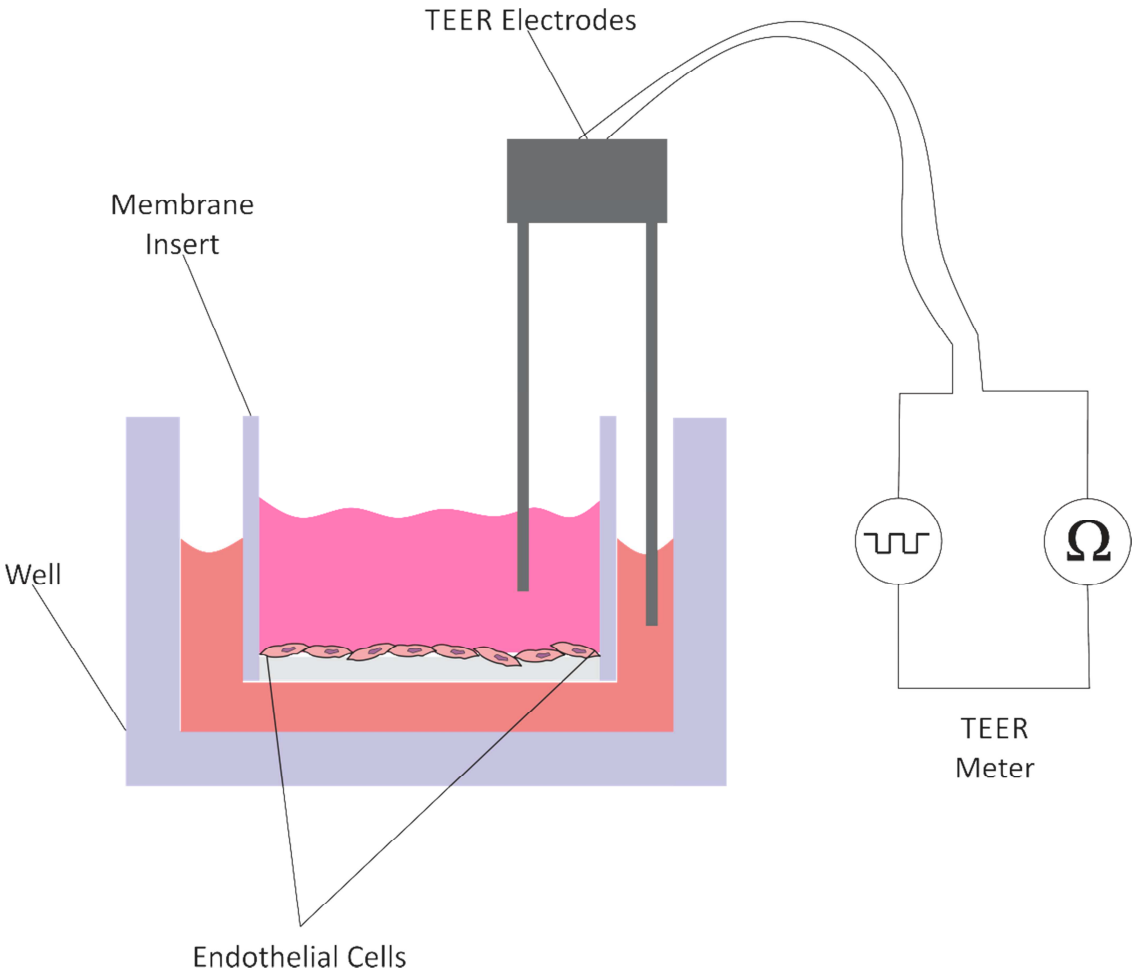

Figure 1.2 - A traditional TEER measurement utilizes a microtiter membrane insert that fits into a traditional well plate. The cell layer is cultured on the polycarbonate membrane at the bottom of the insert and placed into the well, which contains cell media. The TEER measurement is performed by placing electrodes in the basolateral compartment on the outside of the insert and in the apical compartment on the inside of the insert containing the cell layer, and measuring the resistance between the two, which is primarily determined by the barrier integrity of the cultured cells.

1.1.4 - Importance of Monitoring Barrier Integrity in Vascular Mimics

It is fundamentally important that models of biological systems be comprised of fully confluent monolayers of cells to form barriers that each exhibit physiologically relevant paracellular permeability because healthy tissue barriers are comprised of confluent monolayers of cells *in vivo*. Determination of cellular monolayer barrier integrity, specifically tight junctional control of transendothelial permeability, is quite important since cell behavior, including responses to agonists/antagonists and transport of molecules, has been shown to vary with cell confluence and integrity.[91-100] The dependence of cell behavior on barrier integrity highlights the importance of accurately reproducing conditions found *in vivo* when modeling biological systems *in vitro*. As a result, cell monolayer integrity should be determined to more accurately reproduce realistic cell physiology, granting a more appropriate cellular response to stimuli and more realistic monolayer permeability.

Physiologically, conclusions stemming from experimental results involving cellular monolayers that are confirmed to be confluent are generally more accurate due to added physiological relevance in terms of cell behavior and response, adding credibility to the work. Also, measuring barrier integrity to determine monolayer confluence reduces variability between different cell culture models, which is often rather large, allowing for the direct comparison of a particular model to different models, as well as to *in vivo* conditions. Furthermore, verifying monolayer confluence increases reproducibility between models of the same type, which is sometimes low, by ensuring the cultured cells are at the same stage of growth at the time of experimentation. Collectively, these experimental advantages have caused the widespread and common practice of obtaining a determination of confluence in

studies involving monolayers of cells, and furthermore, measurements of barrier integrity are now often requisite for acceptance of results from such studies. Additionally, the ability to monitor cell confluence and barrier integrity in a vascular model introduces a new scope of potential research, specifically the investigation of factors affecting cell proliferation, death, and permeability and corresponding alterations in cellular behavior.

1.2 - Mimicking the Vasculature

The human cardiovascular system is composed of the heart, blood, and the circulatory network of blood vessels, or the vasculature. The blood consists of several components, the red blood cell (RBC), being the most common blood cell, the platelet, the leukocyte, and the plasma, in which the other blood components are suspended. The plasma is primarily water (over 90% by volume), and makes up about 55% of whole blood by volume with the average human having about 5 to 6 liters of whole blood. The blood vessels can be described simply as a network of tubes in which blood can flow throughout the body. Blood vessels are surrounded by smooth muscle that is capable of expansion and contraction. This smooth muscle is lined with a continuous monolayer of endothelial cells to form the endothelium, which completely lines the interior of all blood vessels and surrounds flowing blood as depicted in Figure 1.3. Together, the smooth muscle and the endothelium form the vascular wall, providing separation between flowing blood and the surrounding tissue. The heart pumps blood through the vasculature, first through arteries, which are oxygen rich, to arterioles and finally capillaries. As the blood is pumped farther through the vasculature and away from the heart, the blood vessels begin to decrease in diameter from arterioles to capillaries, which have the smallest diameter. Arterioles and capillaries are considered resistance vessels because they resist the

flow of blood at varying degrees depending on vessel diameter, which ranges from 20 μm to 250 μm, with arterioles generally having larger diameters than capillaries. Importantly, the hematocrit, or percentage of blood occupied by RBCs by volume is typically about 45%, but can be reduced to less than 10% in resistance vessels.[101]

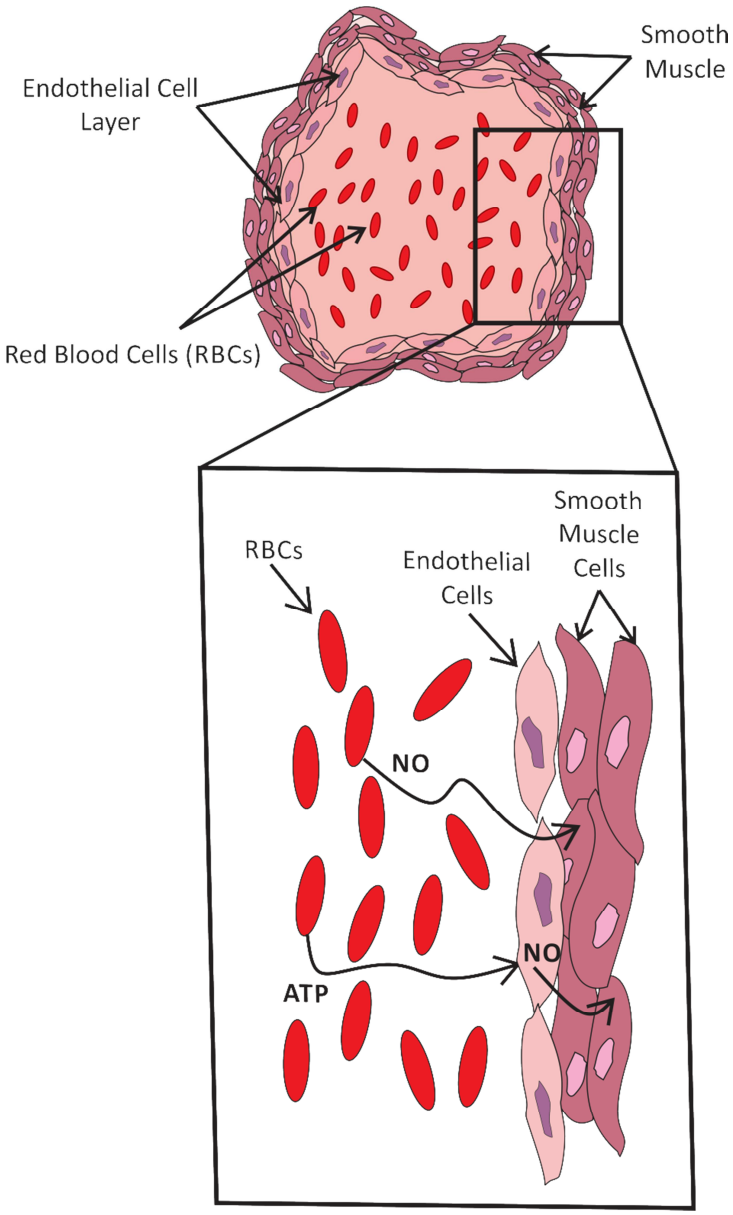

Figure 1.3 - A cross-sectional view of a resistance vessel. Flowing blood components, such as the RBC, are contained in the core of the vessel. Surrounding the flowing blood and lining the interior of all blood vessels is a confluent and continuous monolayer of endothelial cells, which collectively form the endothelium. The endothelium forms a barrier, separating the flowing blood from exterior smooth muscle, which is responsible for contracting and relaxing the blood vessel to regulate vascular tone. In the smooth muscle, the potent vasodilator, NO, is capable of causing vessel relaxation; however the source of this NO is under investigation. In two prominent mechanisms, the primary source is either NO directly released from the RBC, or NO produced in the endothelium in response to ATP released from the RBC.

Interestingly, it is within these resistance vessels, particularly capillaries that nutrients such as oxygen are provided to surrounding tissues and organs, with RBCs being the principal carrier of oxygen in the blood stream. In order to adequately supply nutrients to surrounding tissue, blood vessels are capable of relaxing to accept cardiac output, especially in regions where RBCs (and therefore oxygen supply) may be scarce (often ≤10% hematocrit). After the exchange of nutrients, blood is circulated back up to the heart through veins that increase in diameter as the heart is approached. Importantly, the deoxygenated blood is pumped by the heart to the lungs where the entire cardiac output is accepted for reoxygenation before returning to the heart, completing the cycle, to be once again pumped throughout the body with a renewed oxygen supply.

Perhaps the most important aspect of the cardiac cycle is the ability of resistance vessels to dilate, allowing blood to flow to nutrient poor tissue, and thereby selectively regulating blood flow to increase distribution efficiency. In 1988, groundbreaking work reported that nitric oxide (NO) plays a primary role in regulating vessel dilation through activity in the smooth muscle that results in relaxation of the muscle, increasing vessel diameter and increasing local blood flow. However, in the time since this work, there has been considerable debate as to the source of this NO. Regardless of the specific source of this NO, the most important determinant of continuous NO production, and thus the most important factor in local blood flow and vessel dilation, is shear stress generated by flowing blood. Therefore, the source of this NO is a topic of intense research focus due to its fundamental importance in vascular function and disease. As a result of this research focus, two general arguments have primarily been put forth, the first hypothesis citing the RBC as a direct source of NO, and the second citing the endothelium as

the source of NO as depicted in Figure 1.3. These hypotheses and associated evidence will be discussed in detail within the following sections.

Vascular wall biology, and interactions with bloodstream components (e.g., RBCs, platelets, and leukocytes), is an area of continued interest due to the high prevalence of cardiovascular disease and stroke, as well as the growing realization of its increasingly important roles in many fundamental vascular functions, such as vessel dilation. As stated previously, in order to investigate vascular wall biology with an *in vitro* model, the layer of cells comprising the wall must be confluent and display a restrictive paracellular pathway, high electrical resistance, physiologically relevant cell architecture, and functional expression of transporter mechanisms while being easy to culture.[12, 13] Unfortunately, meeting these criteria is challenging due to the intricate environment found *in vivo* in which various aspects of the environment and sometimes multiple cell types collectively contribute in complex mechanisms to facilitate biological phenomena of interest. As a result, important biological functions are often multifaceted in nature, often being influenced by several environmental queues and cell types while, in turn, influencing other subsequent biological activity. This collective regulation of biological activity where the interplay between several factors ultimately dictates the conception and magnitude of a single biological event is common in the vasculature. As a result, many factors must be considered when attempting to replicate the environment found *in vivo* because the exclusion of elements affecting the desired activity in question will yield biologically irrelevant behavior, potentially resulting in incorrect conclusions based on extraneous results. Unfortunately, the factors affecting a specific biological event are not always known and, in fact, are often the focus of *in vitro* research. Thus, the adequate

reproduction of the biological system of interest is a persistent challenge. Regardless, the fact remains that obtaining meaningful finings *in vitro* that accurately correlate to activity observed *in vivo* hinges on successful reproduction of aspects of the environment that are required for, or play a role in, the activity under investigation.

In order to address these challenges, technologies and methods, including microfluidic technology, have been developed that enable more accurate mimicry of biological systems. For example, microtiter technology is the most commonly used platform to mimic the vasculature, and is described in section 1.1.2. Briefly, endothelial cells are cultured upon a well insert, which is placed in a microtiter well containing a buffer solution, ultimately resulting in a diffusion cell. Alternatively, cells can be simply cultured in the wells of a microtiter plate. These methods allow for the culture of an intact endothelium where many components of an *in vivo* environment can be reproduced, such as pH, molecular content, temperature, and gas content. Additionally, cellular response to added stimuli is easily observable by several methods, including fluorescence or chemiluminescence monitoring, absorption changes, alterations in cell morphology and scintillation counting. Conveniently, a large microtiter based infrastructure exists so that high throughput monitoring of cellular response by these methods is achievable via instrumentation commonly found in typical clinical or biological laboratories. Unfortunately, microtiter technology cannot investigate many vascular functions and activities.

Microtiter technology inadequately reproduces several important biological characteristics of the vasculature that are crucial for producing or regulating an abundance of vascular events involved in normal vascular function, in addition to activities resulting from various diseases, or those involved in the progression of cardiovascular disease. Specifically, microtiter technology

fails to account for the flow of blood, or in some cases the presence of blood whatsoever. Importantly, the fluid shear stress resulting from blood flow is critical for essential vascular functions, such as vasodilation as previously discussed, and is determinant in several fundamental functions of the endothelial cell, as well as the red blood cell. Unfortunately, the majority of studies involving the vascular wall are performed in static systems that do not adequately represent dynamic *in vivo* conditions where shear stress is essential for important biological phenomenon. Furthermore, the inherent geometries of microtiter systems are not capable of reproducing the microenvironments found *in vivo*. For example, these geometries do not adequately reproduce physiologically relevant distances between cells, limiting the ability to derive meaningful conclusions from results where cell-cell communication plays a role. The importance of each of these aspects will be discussed in further detail in the subsequent sections describing important components of the vascular system, especially in the regulation of vascular tone.

1.2.1 - The Endothelial Cell

In order to properly describe various measurements of barrier integrity and the importance of such measurements, the endothelial cell was introduced in Section 1.1 where several cellular functions observed *in vivo* were discussed in addition to important cellular architecture involved in regulating endothelial permeability. To briefly reiterate, endothelial cells cover all blood-contacting tissue in a continuous monolayer which forms a barrier that separates flowing luminal blood from the surrounding tissue. Interestingly, endothelial cells form tight junctional cell-cell contacts that restrict interendothelial permeability, and collectively, these endothelial cells form a continuous monolayer that serves as a protective barrier called the endothelium.

As such, the molecular regulation of vascular permeability prevents pathogen transport to and from the bloodstream, while facilitating the selective transport of macromolecules and solutes between the tissue interstitium and the luminal blood, and vice versa.

In addition to these important biological functions, the endothelium plays a vital role in regulating vascular tone.[102] The first evidence that the endothelium is crucial for vascular tone regulation was the observation by Furchgott and Zawadzki that the endothelial lining was required for the observation of acetylcholine induced relaxation in isolated sections of rabbit aorta.[103] Relaxation induced in the presence of the endothelium was attributed to an endothelial-derived relaxing factor, or EDRF, and that soluble guanylyl cyclase in the surrounding smooth muscle cells was the target of the EDRF upon its calcium-dependent release from the endothelium.[104, 105] Eventually, several observations led Furchgott and Ignarro to independently determine that nitric oxide (NO) was the EDRF, marking the discovery of the first gaseous signaling molecule. Subsequently, it was determined that endothelial NO release indeed did account for the biological activity of the EDRF.[106] Finally, the L-arginine – NO-synthase pathway was identified as the enzymatic source of endothelial NO production.[107, 108] Importantly, endothelial nitric oxide synthase (eNOS) was identified as the enzyme responsible for the conversion of L-arginine to L-citruline and NO as shown in Figure 1.4. [109] Furthermore, eNOS activity was found to be dependent on calmodulin activity and an increase of free intracellular Ca^{2+} levels.[110] In accordance with the impact of the discovered role of the endothelium in vasorelaxation and subsequent identification of NO as the EDRF, Furchgott, Ignarro, and Murad won the Nobel Prize in Medicine in 1998.

Following these important findings, external factors inducing or influencing endothelial NO production are still being investigated, however several stimuli have been identified, including: bradykinin, acetylcholine, prostacyclin, estrogen and adenosine triphosphate (ATP).[111-114] These factors stimulate a signaling cascade resulting in the enzymatic oxidation of L-arginine to L-citruline and NO by eNOS. The catalysis of this reaction requires a number of essential cofactors such as calmodulin (CaM), FAD, NADPH, tetrahydrobiopterin (H4B), and flavin mononucleotide.[115] Upon stimulation by an external factor, these proteins and transduction molecules required for NO production are co-localized in membrane compartments to jointly form the active "eNOS signaling complex" that is responsible for enzymatic endothelial NO production.[115] It is important to note that eNOS exhibits a CaM-binding motif where CaM binds eNOS to facilitate NADPH-mediated electron flux required for NO production by the complex, however, Ca^{2+} binding to CaM enhances the binding of Ca-CaM to eNOS and electron flux of the complex is dependent on CaM phosphorylation and dephosphorylation.[116, 117]

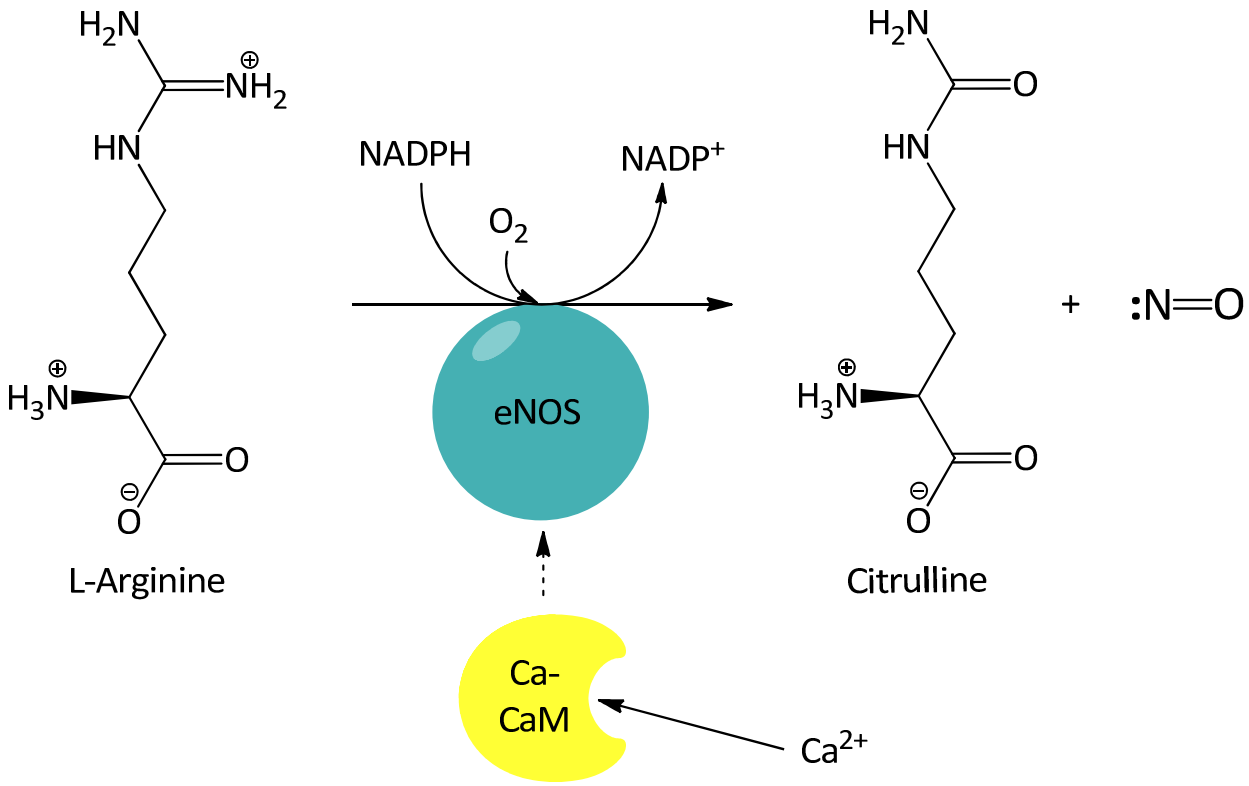

Figure 1.4 - Mechanism describing the production of nitric oxide (NO) in the endothelium. Free intracellular calcium binds calmodulin to form the calcium calmodulin complex (Ca-CaM), which stimulates endothelial nitric oxide synthase (eNOS) by facilitating electron transfer through the complex and thereby increasing the oxidation rate of NADPH to $NADP^+$. The oxygen dependent oxidation of NADPH by eNOS provides electrons for the enzymatic conversion of L-arginine to citruline and NO. Therefore, the increase in electron transfer kinetics resulting from Ca-CaM binding ultimately increases NO production in the endothelium. For simplicity, other essential proteins and signaling molecules which are involved in the signaling complex formed during endothelial NO synthesis are discussed previously, but not pictured.

Prior to the identification of NO as the EDRF, it was shown that its production required an increase in intracellular Ca^{2+} concentration as previously discussed. Additionally, after CaM was shown as a necessary cofactor for eNOS activity, it was shown that Ca^{2+} enhances CaM binding to eNOS. Subsequently, it has been shown that shear induced NO production can be accomplished at basal [Ca^{2+}] levels when eNOS is phosphorylated to increase activity, however free intracellular Ca^{2+} was still required for NO production. Summarily, these results indicate that intracellular [Ca^{2+}] plays an important role in endothelial NO production and regulation of vascular tone. Interestingly, P2 purinergic receptors, specifically the P2Y purinoreceptor located on the endothelial cell membrane,[118] regulates intracellular [Ca^{2+}] by mediating Ca^{2+} influx in response to agonist binding.[119]

The P2 purinoreceptors are G-coupled protein receptors that have a wide distribution of physiological roles throughout the body and in various cell types, most of which have been well established.[120, 121] However, purinergic signaling has recently been implicated in the regulation of vessel tone by a mechanism that is not yet well established.[122] Upon binding of an external agonist, the endothelial P2Y purinoreceptor influences vasodilation by initiating a purinergic signaling cascade that results in the production of smooth muscle relaxing factors by the endothelium, including NO, which seems to be the most potent.[106, 123-130] This activity can be achieved by extracellular ATP levels, as ATP is the primary agonist of the P2Y receptor.[131, 132] Additionally, the resulting endothelial NO upon P2Y activation can be attributed to eNOS activity resulting from purinergic signaling.[133-135] It has been shown that ATP in the blood plasma can increase endothelial NO production and induce vasodilation in

humans via purinergic signaling,[136] and malfunction of this ATP mediated P2 purinergic pathway is observed in several disease states, such as hypertension and diabetes, where vasodilation is dysfunctional leading to blood flow issues.[137]

Upon successful production of NO by endothelial cells, the gaseous radical can only diffuse a short distance as the half-life of NO in physiological solution is short, being on the order of seconds.[138] Within this time frame, NO can diffuse to smooth muscle cells since the endothelium is surrounded by, and in direct contact with, smooth muscle *in vivo*. In smooth muscle cells, NO can activate the soluble guanylyl cyclase resulting in the enzymatic production of cGMP from GTP. Increases in intracellular cGMP levels result in vasorelaxation. This regulation of vascular tone by cGMP may be mediated by a number of mechanisms, but is thought to be primarily due to cGMP induced changes in the concentration of free Ca^{2+} in smooth muscle cells.[139] Physiologically, the most important determinant of the continuous production of NO, and therefore the most important factor in regulating local blood flow and vascular tone is shear stress generated by flowing blood.[115] However, the mechanism of vasodilation in response to shear stress had not yet been well established, although it is clear that shear induced NO is regulatory of vascular tone via its activity in the smooth muscle cell.[140] Regardless of this knowledge, the source of this NO is a topic of considerable debate in the literature. To date, the leading proposed mechanisms of shear induced vasorelaxation involve the red blood cell.

1.2.2 - The Red Blood Cell

RBCs, or erythrocytes, are the most common type of blood component and are the primary carrier of nutrients, primarily oxygen (O_2), through the bloodstream to replenish more hypoxic

(oxygen deprived) tissue and organs as discussed formerly. RBCs consist mainly of water and hemoglobin, a metalloprotein consisting of four subunits. Hemoglobin contains heme groups whose iron reversibly binds oxygen that is subsequently released throughout the body in regions of lower oxygen content and usually replaced by carbon dioxide, a common waste product of tissue. Upon oxygen binding or release, hemoglobin fluctuates between two confirmations called the relaxed and tense states, respectively.[141, 142] Furthermore, NO can also bind oxygenated hemoglobin at a specific cysteine residue as s-nitrosothiol. Interestingly, this NO is released readily when hemoglobin is deoxygenated and in the tense state.[143] As a result of these findings, it has been suggested that the red blood cell regulates vasodilation directly by releasing this NO in regions where the RBC is exposed to low oxygen content. Interestingly, because the RBC releases oxygen, and therefore NO, primarily in resistance vessels where shear stress is experienced by the RBC and the endothelium alike, it is proposed that this RBC derived NO could be the source of shear related NO that is important for blood flow and oxygen replenishment, even though this NO is released in response to hypoxia, or low oxygen content, and not shear.[144]

An additional hypothesis implicating the RBC as the direct source of shear induced NO production is based on the ability of deoxygenated hemoglobin to act as a nitrite reductase, producing NO by the enzymatic reduction of nitrite.[145] This hypothesis is supported by research showing that nitrite injections reduce blood pressure in the human arm.[146] However, it has been shown that nitrite is capable of stimulating ATP release from the RBC, a finding that adds credibility to the hypothesis discussed below.[147] Interestingly, each of these hypotheses that suggest that NO produced in association with shear stress that regulates vessel

dilation is actually a result of the RBCs response to hypoxia and not shear stress. Furthermore, in each hypothesis, it is suggested that this NO originates from the RBC directly. In this construct, the NO released from the RBC would be required to diffuse from a location in the vessel and through the endothelium to reach the smooth muscle cell where NO is known to induce vasodilation. Unpublished data resulting from studies in the Spence lab suggest that NO produced by hypoxic RBCs is essentially blocked by an endothelium. These results are supported by the short half-life of NO in physiological solutions.[148] However, it is important to note that endothelial permeability varies between organs as stated formerly, so the importance of RBC derived NO could potentially vary based on the anatomical location of release.

In a final alternate hypothesis, the ability of the RBC to release ATP can indirectly result in NO production by the endothelium that induces vasodilation. It has been shown that the RBC contains millimolar levels of ATP[149] that can be released in response to several stimuli, including shear stress[150], hypoxia[151, 152], pharmaceutical agents[90, 153], and Zn^{2+}-activated C-peptide[154]. Notably, the mechanism of this ATP release is not a passive process, or a result of cell lysis, but rather an active process mediated by a G-protein coupled receptor, of which the mechanism has been elucidated by Sprague et al.[155-158] Also, it has been shown that this ATP release can be inhibited pharmacologically, verifying that this process is indeed regulated.[155, 159]

As shown in Figure 1.6, ATP is proposed to be an important regulator of vascular tone resulting from its activity in purinergic signaling, which is discussed in Section 1.2.1. In this construct, ATP released in the bloodstream by RBCs can activate the endothelial P2Y

purinoreceptor, resulting in NO production by a mechanism shown to result in vasodilation as discussed previously. Furthermore, by this mechanism, NO is produced in response to shear stress, adding probability that this mechanism is the source of NO produced in association with shear stress, the origin of which has been, and is currently, debated in the literature. Furthermore, the production of endothelial NO has been shown to be capable of, and in some cases, necessary for the relaxation of blood vessels as mentioned earlier. In addition to determining the mechanism of shear induced vasorelaxation, identifying other factors influencing vessel dilation is an active area of research due to the biological importance of the regulation of vascular tone.

1.2.3 - C-peptide

C-peptide, whose sequence is shown in Figure 1.5, is a 31 amino acid peptide produced in the beta cells of the islets of Langerhans within the pancreas and released in equimolar amounts with insulin into the bloodstream.[160, 161] For the first few decades after its discovery in the late 1960's, C-peptide was thought to have minimal physiological effects after release into the bloodstream.[162] However, numerous reports since the mid 1990's have confirmed that C-peptide is a bioactive peptide that can have significant beneficial effects in organs, tissue, and even cultured cells such as endothelial cells.[163-165] Studies involving Type 1 diabetic subjects who are unable to naturally produce C-peptide due to beta cell destruction have shown that C-peptide improves nerve conduction and regeneration[166], renal function[167], inflammation,[168] and blood flow[169, 170] via unknown mechanisms. Diabetic patients are known to develop hypertension as well as other cardiovascular problems, which are often ameliorated by C-peptide treatment, although the mechanism by which C-peptide

impacts diabetic blood flow is currently unknown, as are any influences on blood flow in healthy individuals. However, in light of the importance of NO in the regulation of vascular tone, it is clear that if C-peptide is capable of stimulating endothelial nitric oxide production, it could account for the C-peptide induced improvement in blood flow observed in Type 1 diabetic subjects.

Interestingly, in separate studies, diabetic complications related to blood flow have been shown to be related to endothelial dysfunction,[171] and nitric oxide production, suggesting that C-peptide may be capable of stimulating NO production in the bloodstream that is most likely derived from the endothelium.[172] The fundamental importance of endothelial derived NO for the regulation of vessel tone has been well-established and, as a result, the identification of factors influencing NO production in the endothelium has become a highly active area of research which garners much attention due to the associated biological impact. For these reasons, a potential role for C-peptide in endothelial NO regulation is particularly exciting. This potential activity would not only provide an explanation for observed improvements in diabetic blood flow by a process which has so far eluded identification, but also reveal a fundamentally important and overlooked role of C-peptide in regulating vascular tone.

A relationship between C-peptide and eNOS, the enzyme responsible for regulating endothelial NO concentration, has been reported in many different types of complications associated with diabetes, as well as in various tissues and organs, both *in vivo* and *in vitro*.[173, 174] Reports of C-peptide-stimulated NO production in the endothelium could have great importance, especially in the pulmonary endothelium, where the flow of RBCs through the

pulmonary bed allows re-oxygenation of the RBCs prior to delivery of that oxygen to organs and tissues throughout the body as described previously. In accordance with the importance of pulmonary NO production, Sprague et al. has shown that ATP derived from RBCs stimulates NO production in the pulmonary circulation.[175] Interestingly, C-peptide stimulates the release of ATP from RBCs.[154] However, in order to observe increased ATP release from RBCs, C-peptide was introduced to a metal source, such as zinc, prior to incubation with RBCs. In this construct, C-peptide may have the ability to stimulate NO production in the endothelium indirectly by purinergic signaling, as mediated by C-peptide stimulated release of ATP from RBCs. Importantly, the potential involvement of RBC derived ATP in the proposed mechanism again highlights the importance of flow in *in vitro* vascular experiments, as flowing RBCs under the influence of shear stress release more ATP than static RBCs.[155, 159, 176, 177] However, in order to thoroughly investigate these prospective roles of C-peptide, multiple cell types, separated by physiologically relevant distances, would need to be investigated in a biologically accurate mimic of the vasculature.

Similar to the proposed mechanism for C-peptide induced vasorelaxation, much of the observed biological effects of C-peptide can potentially be attributed to processes occurring in the cardiovascular system resulting indirectly from C-peptide activity within the bloodstream. However, it is unclear if the broad influence of C-peptide is elicited entirely from activity in the bloodstream, or if C-peptide is also capable of escaping the bloodstream to influence cell behavior directly. Some activity stimulated by C-peptide extending beyond the vascular system is difficult to explain in paradigms where C-peptide is confined to the bloodstream, such as the observed improvements in diabetic neuropathy and nerve conduction. While the capability of

C-peptide to escape the bloodstream has yet to be investigated, nor has C-peptide ever been detected exterior to the vasculature *in vivo*, some reports insinuate that C-peptide is potentially trafficked across the endothelium to leave the bloodstream.

For example, It has been previously shown that C-peptide specifically binds to endothelial cells, which is of importance since the transport of macromolecules is generally by transcellular and specific mechanisms.[178] The existence of a binding structure for C-peptide is still in question, however, since this specific binding has not yet been shown by conventional radioligand binding and, furthermore, a specific receptor for C-peptide has not been identified. Additionally, the homology pattern of C-peptide is markedly different from most signaling peptides.[179] However, C-peptide has been shown to be internalized by endosomes to enter human endothelial cells.[180] Additionally, this internalization can be inhibited by nocodazole and monodansylcadaverine (MDC), signifying that C-peptide enters the cell by a mechanism which is receptor mediated and requires microtubule assembly. Interestingly, microtubules have been shown to facilitate transcellular transport and also influence endothelial permeability and integrity.[181-184] Also, some endothelial cell types express PEPT membrane proteins, which promiscuously facilitate the transcellular transport of peptides.[185, 186] In addition to human endothelial cells, C-peptide can also enter fibroblasts and human embryonic kidney cells where it is capable of influencing gene transcription,[187, 188] suggesting that C-peptide is capable of directly influencing cells exogenous of the bloodstream and again demonstrating the ability of C-peptide to permeate cellular membranes. Collectively, these results indicate that C-peptide is potentially selectively trafficked across the endothelium by a transcellular transport mechanism.

When considered jointly, these results indicate that C-peptide can plausibly exit the bloodstream but do not, however, provide sufficient evidence to conclusively confirm or reject this hypothesis. The ability or inability of C-peptide to permeate a cultured endothelium can provide valuable insight as to whether some biological effects of the peptide are initiated directly, or if all of these effects are result indirectly from activity in the bloodstream. However, in order to determine the potential involvement of each of these potential mechanisms, further investigation of the ability of C-peptide to escape the bloodstream is required. In order to more decisively determine the aptitude for C-peptide to leave the bloodstream, an assay of endothelial permeability to C-peptide should be accomplished, since the endothelium serves as the primary barrier separating flowing blood from the interstitium.

Importantly, these permeability studies must account for transcellular transport, which is the probable mode of transport of C-peptide across the endothelium *in vivo*. This requirement is most adequately satisfied by permeability assays, which can be performed to quantitatively monitor the permeation of C-peptide across a cultured endothelium. However, shear has been shown to influence changes in endothelial permeability,[189] and therefore, shear will ideally be incorporated in the permeability assay. More importantly, the endothelial cellular barrier should be characterized in terms of barrier function and confluence to ensure that C-peptide is required to permeate an endothelial monolayer that closely resembles the true endothelium. A more conclusive and accurate deduction of the ability of C-peptide to permeate the endothelium *in vivo* may be accomplished via the utilization of a biological mimic that includes the flow capabilities required to replicate shear stress, as well as RBCs. Unfortunately, these important biological aspects are not accounted for by the microtiter diffusion cell, which is the

conventional platform utilized to perform permeability assays as previously discussed. Therefore, a contrasting platform that accounts for these biological aspects is ideal since conclusions stemming from results obtained using this alternate biological model will likely be significantly more accurate and credible as a result of the enhanced physiological relevance achieved when compared to conventional microtiter platforms.

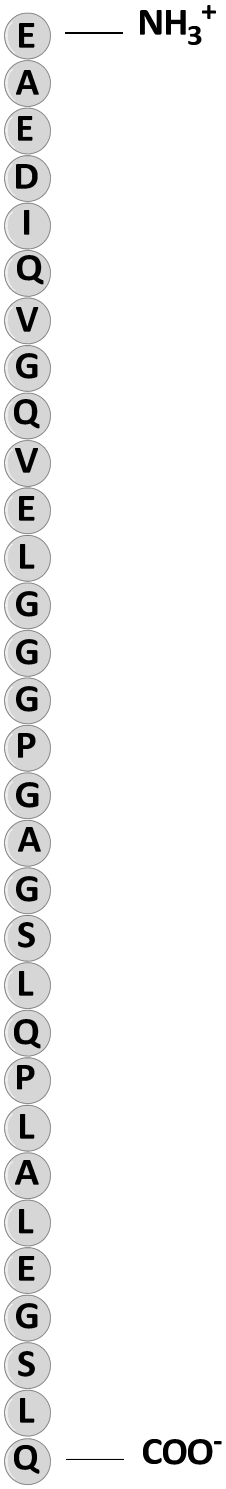

Figure 1.5 - The amino acid sequence of C-peptide. Subsequent to cleavage from insulin, the 31 residue peptide is capable of increasing ATP release from RBCs, an activity which is proposed to mediate NO production in the endothelium.

Recently, our group has shown that if C-peptide is incubated in a solution containing certain divalent metal ions prior to addition to a RBC solution, the resulting metal activated C-peptide was able to facilitate glucose uptake into, and increase ATP release from RBCs.[154, 190] Remarkably, these results could not be reproduced in the absence of a metal, indicating that C-peptide must first be introduced to a metal source for some, if not all bioactivity. These findings were further supported when mass spectrometric analysis of a solution containing active C-peptide not deliberately introduced to a metal, revealed that the peptide had indeed formed an at least one adduct with a metal.[154, 191] Although C-peptide has been shown to be active in the presence of multiple metal ions[154, 190, 192, 193], it has been shown that zinc is present at millimolar levels within beta cells where C-peptide is produced and cleaved from proinsulin prior to release into the bloodstream.[194] Therefore, zinc is the most bioavailable metal source for C-peptide prior to secretion, increasing the probability that zinc is responsible for the bioactivity of C-peptide *in vivo*.

To date, most studies involving the exogenous addition of C-peptide to humans, animal models, and cell models have not directly co-administered a metal as the influence of metal on C-peptide bioactivity is largely under-recognized. Interestingly, some studies report that C-peptide only elicits bioactivity when co-administered with insulin, which often contains Zn^{2+} at levels as high as 0.5% by mass.[195] Furthermore, it has been shown that C-peptide is capable of increasing RBC membrane deformability, however these effects were abolished in the presence of EDTA, which is known to strongly chelate metals.[196] Hypothetically, it is feasible that C-peptide samples often unintentionally contain metals, sometimes rendering C-peptide bioactive, which could explain the inconsistent activity observed in clinical trials. If this is the

case, it could provide an explanation for the surprising lack of findings regarding mechanistic aspects of C-peptide bioactivity, despite the discovery that C-peptide is responsible for many beneficial functions *in vivo*. Due to the development of a now well-established method for C-peptide preparation with Zn^{2+}, our lab is uniquely well suited for investigating the mechanisms of C-peptide bioactivity as indicated by our ability to reproducibly demonstrate various C-peptide bioactivies in the presence of a metal.

1.2.4 - Current Hypothesis Regarding Vasodilation and the Influence of C-peptide

Recent findings have shown that circulating ATP impacts vascular tone by purinergic signaling, specifically as an agonist of the endothelial P2Y receptor, which results in eNOS mediated production of endothelium NO, a potent vasodilator.[197-200] These findings corroborate previous work by Sprague showing that RBC-derived ATP stimulated NO production and vasodilation in the rabbit pulmonary circulation. While it is debated whether this mechanism is primarily responsible for the regulation of vascular tone, it is the only proposed mechanism where NO is derived from the endothelium as opposed to the RBC. Consequential to the short half-life of NO *in vivo*, endothelial derived NO can likely more efficiently stimulate vasorelaxation than NO derived from the RBC since the diffusional distance to the smooth muscle is reduced. Furthermore, RBC derived NO is required to permeate the barrier formed by the endothelium before reaching the smooth muscle, a problem that is largely avoided by NO produced by the endothelium. This assumption is supported by unpublished data from the Spence lab suggesting that RBC derived NO is blocked from reaching the smooth muscle by the pulmonary endothelium. In addition, the continuous production of NO most important for regulating vascular tone has been repeatedly associated with shear stress, which is known to

influence circulating ATP levels by stimulating its release from the RBC. In contrast, the known primary mechanisms proposed in the literature for NO release from the RBC are in response to hypoxia as opposed to shear stress.

Considering these recent developments implicating ATP in the purinergic regulation of vascular tone, factors affecting circulating levels of ATP may be fundamentally important for maintaining healthy blood flow by association. It is well established that the RBC contains millimolar levels of ATP, which can be released into the blood stream by several stimuli. Interestingly, C-peptide, when carefully prepared with a metal source, has been shown to significantly increase ATP release from the RBC. These results are exciting because in patients with type 1 diabetes who have impaired C-peptide production, vascular ailments arise, including hypertension, which can be ameliorated by improved blood flow resulting from C-peptide therapy. However, the mechanism by which C-peptide improves diabetic blood flow is unknown. Figure 1.6 displays the proposed mechanism by which C-peptide regulates vascular tone. In this construct, C-peptide may have the ability to stimulate NO production in the endothelium by purinergic signaling, as mediated by C-peptide stimulated release of ATP from RBCs. As discussed earlier, endothelial derived NO has been shown to be crucial for the regulation of vascular tone.

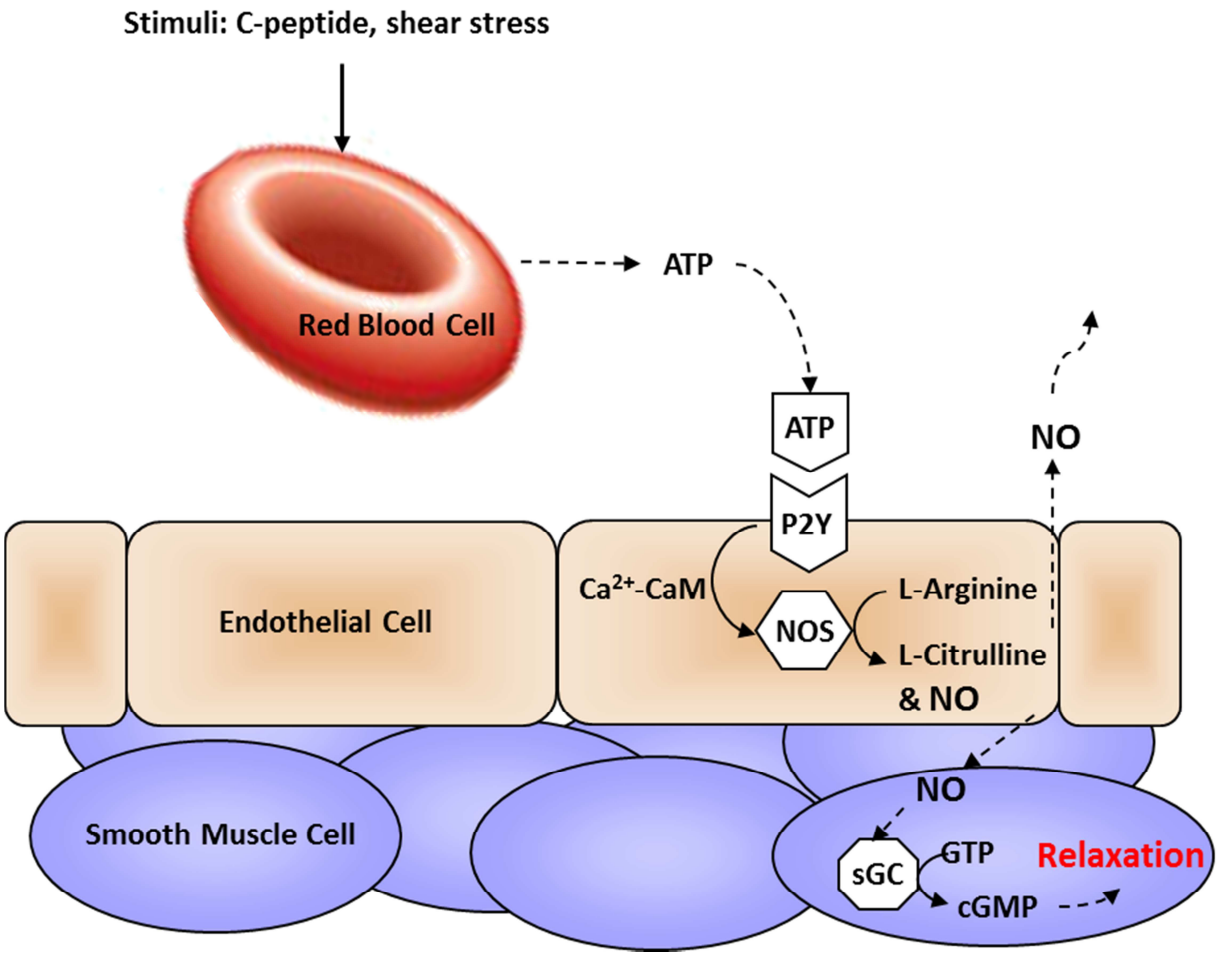

Figure 1.6 - The proposed mechanism of RBC mediated vasorelaxation. In response to a stimulus, such as C-peptide interaction or shear stress, the RBC releases ATP, which is capable of diffusing to the endothelium. As an agonist of the G-coupled P2 purinoreceptors, ATP binds the P2Y purinergic receptors located on the endothelial cell membrane, which initiates a purinergic signaling cascade. In response to ATP agonist, P2Y increases calcium flux into the cell, leading to an increase in free intracellular Ca^{2+}, which can bind CaM to form the Ca-CaM complex. In this active conformation, Ca-CaM is capable of binding the calmodulin-binding domain of eNOS to stimulate the enzymatic conversion of L-arginine to L-Citruline and NO (Figure 1.4). NO produced in the endothelium is able to diffuse to the smooth muscle cells to activate soluble guanylyl cyclase (sGC), resulting in the enzymatic production of cyclic guanosine monophosphate (cGMP) from guanosine triphosphate (GTP) and leading to relaxation of smooth muscle, dilating the blood vessel.

If C-peptide can indeed stimulate endothelial NO production, C-peptide may be revolutionary for the treatment of type 1 diabetes due to the ability to improve blood flow, but also due to its potential ability to mediate glucose clearance from the bloodstream via increased glucose uptake by the RBC. Potentially even more importantly, if shown to influence endothelial NO production, C-peptide may be crucially important for maintaining healthy vascular tone in general. Specifically, C-peptide may play an important role in maintaining appropriate levels of circulating ATP by influencing the degree of ATP release from RBCs, since healthy individuals typically have concentrations of C-peptide varying in the single-digit nanomolar range circulating in the bloodstream at any given time,[201, 202]. Importantly, if C-peptide is shown to potentially influence purinergic regulation of vascular tone, by inference, C-peptide may be fundamentally important for maintaining healthy blood flow, which has so far been overlooked. Of course, in order to verify this hypothesis, an *in vitro* model of the vasculature will need to be developed that is capable of reproducing important aspects of the vasculature. This model will require geometries that mimic resistance vessels and the inclusion of multiple cell types separated by physiological diffusional distances so that biologically relevant cell-cell communication can be monitored. Ideally, a measure of endothelial monolayer confluence will be possible in conjunction with flow capability to reproduce shear stress that is so influential in the vasculature.

1.3 - Microfluidics

1.3.1 - Fabrication and Background

Microfluidic technology has been largely and broadly influential in various fields of science, leaving behind a rich history. For example, microfluidic technology famously made significant

contributions to the successful sequencing of the human genome.[203-207] Microfluidic technology offers several general experimental advantages that are attractive for a vast range of research, causing the preferential use of microfluidic devices in lieu of other well established technology and instrumentation which, in turn, has led to significant and diverse scientific contributions. For example, some of the most appreciated advantages offered by microfluidics are: small sample volume, low reagent consumption, minimal waste, and high throughput.[208-210] In fact, microfluidic technology is commonly called “lab on a chip” technology since often microfluidic devices can accomplish tasks, sometimes with improved results, that usually require whole instruments, of which microfluidic devices are a small fraction of the size. Due to these conveniences, since the 1980s microfluidic technology has been applied in research throughout various scientific fields, however more recently, microfluidic systems have begun to emerge as useful platforms for cell based assays.[30, 88, 113, 211-217]

Arguably, microfluidic technology first became amenable to cell culture research when a soft lithographic technique for the rapid prototyping of polydimethylsiloxane (PDMS) microfluidic devices was developed in the late 1990s by the Whitesides laboratory.[218, 219] PDMS, being a gas permeable polymer, was the first suitable material for use in microfluidic fabrication that also allowed for gas exchange, a requirement for cell survival.[220, 221] Additionally, the fabrication of PDMS microfluidic devices by soft lithography is generally less complicated for the wide range of other materials often utilized for microfluidic construction.[222] While PDMS, as a material for microfluidic fabrication, has several disadvantages, [223] such as hydrophobicity, absorption and adsorption of substances, as well as high flexibility, it has several advantages for cell-based research. Firstly, PDMS is gas

permeable, allowing cellular oxygen and carbon dioxide exchange, which is required for cell survival. Furthermore, PDMS is a transparent material, allowing for visualization of cells, optical analysis, and imaging.[210]

1.3.2 - Microfluidics to Mimic Biological Systems

The inherent geometries and dimensions of microfluidic systems are well suited for mimicking *in vivo* physiological conditions and monitoring cell behavior within these microenvironments. As mentioned previously, microfluidic technology offers precise control of important aspects of the microenvironment, leading to more physiologically relevant models of *in vivo* systems. For these reasons, when considering all technology available for modeling biological systems, a microfluidic platform would serve as an accurate and physiologically relevant model of the vasculature. For example, an *in vitro* cell layer mimic capable of incorporating flow, and other biologically relevant cells, such as the RBC, would be paramount for mimicking a true vascular barrier. However, the various cells would have to be in close proximity to allow for cell-cell communication. These issues are well addressed with microfluidic systems, as it is possible to mimic the small distance between the blood vessel and the endothelium.[211] Blood flow is also easily accomplished by incorporation of channels that have diameters similar to resistance vessels (capillaries and arterioles) found *in vivo*,[211] and thereby incorporating shear stress at a biologically relevant magnitude, a crucially important aspect since shear stress is influential to cell behavior. In accordance with the importance of shear stress, and the ability to simulate this force in microfluidic systems, a myriad of shear-related microfluidic experiments have been accomplished, such as studies on migration,[224] adhesion,[30, 225, 226], enrichment,[227] and shear-induced NO production.[90, 113]

Not surprisingly, microfluidic technology has been used by the Spence group and others to mimic the vasculature.[30, 88, 113, 228-232] Also, as a result of these same beneficial properties of microfluidic systems, several microfluidic organ mimics have been accomplished, including the lung[233, 234], kidney[235, 236], heart[237], and digestive system[238] in work coined "organ on a chip" research. Additionally, microfluidic technology has been utilized to model neurons.[239, 240] Interestingly, a majority of these microfluidic mimics of biological systems feature cellular monolayers comprised of epithelial or endothelial cells, as do numerous other microfluidic biological models, indicating their importance *in vivo*. As previously discussed, it has been shown that the degree of confluence can alter the behavior of these cells, and thus a method for the determination of monolayer barrier integrity is beneficial in all experimental situations and necessary in some. Also, since epithelial and endothelial cells often form barriers *in vivo* that often influence drug delivery, and are implicated in various diseases, measurements of monolayer barrier integrity and permeability are the basis of a majority of research involving these processes.

1.3.3 - Monitoring Barrier Integrity on a Microfluidic Device

Using microfluidic systems for the analysis of cellular monolayers has been contributive and progressive towards understanding complex biological systems, although reliably measuring cell monolayer integrity in these microfluidic devices is challenging. Cell monolayer integrity can be measured in a number of ways that are described previously in Section 1.1. Interestingly, these methods are used in the vast majority of experimentation regarding monolayers, except for those performed using microfluidic systems. Subsequent to the start of the work presented in the following chapters, microfluidic platforms have been reported that are capable of

determining cell monolayer integrity of various cell types by monitoring permeation,[241-243] as well as TEER,[244-246] demonstrating the need for such devices. However, the microfluidic device featured in chapter 2 is the first microfluidic vascular mimic capable of measuring TEER, which is relatively simple and timely to fabricate compared to similar devices.[97] Similarly, microfabricated cell culture chambers have been developed capable of measuring cell monolayer confluence, however these models lack flow capabilities.[247-249] Also, additional devices with this important capability have been reported subsequent to publication of the device presented in Chapter 2.[250-253]

Importantly, the ability to determine monolayer barrier integrity without affecting cells cultured within a microfluidic device, and also simultaneously eliciting shear stress generated by flowing blood, offers the potential for dynamic experiments while accurately mimicking a true biological system. In order to achieve this goal, TEER is a preferred method for determining monolayer barrier robustness since it allows for repeated quantitative measuring without altering cell phenotype or damaging the cells. In addition to the potential for time-lapse microfluidic studies, such a device would further ensure proper cellular behavior by confirming the confluence of cultured cells, adding credibility and accuracy to results. For these reasons, the unprecedented development of a microfluidic vascular mimic with integrated TEER capabilities could be significantly useful for elucidating mechanisms of important physiological events and functions of the vascular system, providing cell-cell interactions are permitted.

1.3.4 - Cell-Cell Communication in Microfluidic Systems

A substantial advantage of microfluidic systems yet unparalleled by other technologies is the ability to incorporate varying cell types separated by physiologically relevant distances,

which are often exceedingly diminutive and therefore challenging to reproduce with alternative technology.[254] Furthermore, microfluidics allows for cell culture, in addition to the flow of cells, reproducing the shear forces experienced by cells *in vivo* in a manner not easily accomplished by other techniques. In the cardiovascular system, it has been shown that shear stress is necessary for certain cellular responses and impacts cellular behavior, including that of the endothelial cell and RBC, and it is one mode by which these cells interact. By employing microfluidics, the Spence group has shown repeatedly that for cell types found in the vasculature, various stimuli, such as shear force, are capable of eliciting a response from one cell type that, in turn, influences the behavior of a second.

For example, it was shown that in addition to C-peptide, shear stress can cause an increase in ATP release from RBCs,[150, 155] which can subsequently stimulate platelet NO production,[90] as well as endothelial NO production.[89, 97, 113, 211, 255] Interestingly, NO is capable of decreasing ATP release from RBCs by a potential feedback mechanism of the endothelial cell and platelet in response to ATP release from the RBC.[256] Additionally, the effects of an anti-adhesion drug were determined by monitoring platelet adhesion to a cultured endothelium under flow conditions.[30] These examples of monitoring cell-cell interactions to elucidate mechanisms of biological events by the Spence group adds to an increasing amount of literature highlighting the utility of microfluidic technology for mimicking biological systems and monitoring cell-cell communication.[257-259] Due to the architectural advantages and flow capabilities of microfluidic systems, a microfluidic device capable of characterizing monolayer barrier integrity can feasibly be developed to elucidate the mechanism by which C-peptide and shear play a role in influencing vascular tone. The displayed ability of microfluidic devices to

mimic biological systems in a manner accurate enough to monitor cell-cell interactions evidences the plausibility of this endeavor.

1.4 - Goals and Motivation

Motivated by the associated impact of elucidating the mechanism by which C-peptide influences vascular tone, specifically by the potential ability to stimulate NO production in the endothelium, the development of a vascular mimic will be attempted in order to investigate the potential involvement of C-peptide in this fundamentally important biological process. Also, the ability of C-peptide to escape the bloodstream is potentially of high biological importance since the direct involvement of C-peptide in biological processes is possible, not only in the vascular system, but throughout the entire body. For example, the biological influence of C-peptide may be restricted to effects that are accomplished indirectly as a result of activity within the bloodstream, or C-peptide may be able to both indirectly and directly stimulate cell types exogenous of the vasculature, provided C-peptide can permeate the vascular wall to physically interact these cells. In the latter case, the scope of the physiological influence of C-peptide may be extensive and diverse, similar to insulin, but also severely under-recognized by the scientific community.

In order to investigate these important possibilities, many important biological aspects must be considered when developing a model of the vasculature in order to achieve meaningful and biologically relevant results. For example, due to the involvement of multiple cell types in the proposed mechanism for C-peptide induced vasorelaxation, specifically the RBC and endothelial cell, a vascular model including these multiple cell types is required. Furthermore, since it is proposed that ATP released from the RBC acts as an extracellular signaling molecule that

directly interacts with endothelial cells to stimulate NO production in the endothelium, the RBC and the endothelial cells must be separated by physiologically relevant distances in the vascular mimic in order to accurately replicate the diffusional distance to the endothelium experienced by ATP released from circulating RBCs *in vivo*. In addition to the release of signaling molecules, endothelial cells and RBCs both respond to shear stress generated from the drag force produced by the direct contact of flowing blood with the stationary endothelium. Importantly, shear stress greatly impacts each cell type *in vivo*, and also directly influences several fundamental aspects of the processes under investigation. For example, shear stress has been shown to impact ATP release from the RBC, and also greatly increase endothelial barrier integrity. Also, since endothelial cells comprising the endothelium form a confluent barrier in vivo, and endothelial behavior and response to environmental queues has been shown to vary with monolayer barrier integrity and confluence and, therefore, the properties of endothelial cells cultured within the vascular mimic should ideally replicate the true endothelium by forming a completely confluent monolayer that exhibits proper barrier integrity. This criterion is important for the successful observation and elucidation of biologically relevant cell-cell communication mechanisms, since physiologically correct cellular responses to stimuli are often dependent on monolayer barrier integrity and confluence. Additionally, the most important factor determining the permeability of cellular monolayers to molecules is the integrity of the barrier formed by the monolayer. Therefore, in order to accurately determine ability of a molecule to permeate a cellular monolayer, conditions found *in vivo* should be replicated and confirmed prior to experimentation by first measuring the barrier integrity and confluence of cultured cells.

To successfully address each of these important aspects of biological systems observed *in vivo*, a microfluidic vascular mimic will be developed to determine a potential mechanism of C-peptide induced endothelial NO production, as well as the endothelial permeability to C-peptide. While microfluidics have recently proven useful for cell based assays, a vascular mimic with integrated flow capabilities, as well as cell layer confluence measurement capabilities, has not yet been developed. The design of the microfluidic vascular mimic will ideally allow for the incorporation of each of the important biological aspects that are often not addressed by conventional microtiter biological models, such as: multiple cell types, physiologically relevant architecture, and shear stress. Additionally, the ability to confirm cell monolayer confluence, which is rarely accomplished in microfluidic platforms, and often easily accomplished in microtiter platforms, will also ideally be integrated in the microfluidic vascular mimic. The development of such a vascular mimic can potentially be utilized to reproduce and decipher highly complicated biological phenomena, including those involving cell-cell communications, with unparalleled accuracy. Therefore, such a device may be capable of replicating conditions found *in vivo* to such an extent that the potential mechanism by which C-peptide stimulates NO production in the endothelium may be elucidated. Furthermore, such a device could be utilized to investigate the ability of C-peptide to permeate the endothelium *in vivo* with a high degree of biological relevance in comparison to conventional techniques.

REFERENCES

REFERENCES

1. Atencia, J. and D.J. Beebe, *Controlled microfluidic interfaces.* Nature, 2005. **437**(7059): p. 648-55.

2. Kuczenski, B., et al., *Probing cellular dynamics with a chemical signal generator.* PLoS ONE, 2009. **4**(3): p. e4847.

3. Faley, S., et al., *Microfluidic platform for real-time signaling analysis of multiple single T cells in parallel.* Lab Chip, 2008. **8**(10): p. 1700-12.

4. Vickerman, V., et al., *Design, fabrication and implementation of a novel multi-parameter control microfluidic platform for three-dimensional cell culture and real-time imaging.* Lab Chip, 2008. **8**(9): p. 1468-77.

5. Walker, G.M., H.C. Zeringue, and D.J. Beebe, *Microenvironment design considerations for cellular scale studies.* Lab Chip, 2004. **4**(2): p. 91-7.

6. Huh, D., et al., *Acoustically detectable cellular-level lung injury induced by fluid mechanical stresses in microfluidic airway systems.* Proc Natl Acad Sci U S A, 2007. **104**(48): p. 18886-91.

7. Lao, A.I.K., et al., *Precise temperature control of microfluidic chamber for gas and liquid phase reactions.* Sensors and Actuators a-Physical, 2000. **84**(1-2): p. 11-17.

8. Guijt, R.M., et al., *Chemical and physical processes for integrated temperature control in microfluidic devices.* Lab on a Chip, 2003. **3**(1): p. 1-4.

9. Roper, M.G., et al., *Infrared temperature control system for a completely noncontact polymerase chain reaction in microfluidic chips.* Anal Chem, 2007. **79**(4): p. 1294-300.

10. Bhatia, S.N., et al., *Effect of cell-cell interactions in preservation of cellular phenotype: cocultivation of hepatocytes and nonparenchymal cells.* FASEB J, 1999. **13**(14): p. 1883-900.

11. Ayliffe, H.E., A.B. Frazier, and R.D. Rabbitt, *Electric impedance spectroscopy using microchannels with integrated metal electrodes.* Journal of Microelectromechanical Systems, 1999. **8**(1): p. 50-57.

12. Gumbleton, M. and K.L. Audus, *Progress and Limitations in the Use of In Vitro Cell Cultures to Serve as a Permeability Screen for the Blood-Brain Barrier.* J. of Pharm. Sci., 2001. **90**(11): p. 1681-1698.

13. Crone, C. and S.P. Olesen, *Electrical resistance of brain microvascular endothelium.* Brain Res FIELD Full Journal Title:Brain research, 1982. **241**(1): p. 49-55.

14. Wilcox, E.R., et al., *Mutations in the gene encoding tight junction claudin-14 cause autosomal recessive deafness DFNB29.* Cell, 2001. **104**(1): p. 165-72.

15. Gow, A., et al., *Deafness in Claudin 11-null mice reveals the critical contribution of basal cell tight junctions to stria vascularis function.* J Neurosci, 2004. **24**(32): p. 7051-62.

16. Riazuddin, S., et al., *Mutations in TRIOBP, which encodes a putative cytoskeletal-organizing protein, are associated with nonsyndromic recessive deafness.* Am J Hum Genet, 2006. **78**(1): p. 137-43.

17. Xavier, R.J. and D.K. Podolsky, *Unravelling the pathogenesis of inflammatory bowel disease.* Nature, 2007. **448**(7152): p. 427-34.

18. Chronopoulos, A., et al., *High glucose-induced altered basement membrane composition and structure increases trans-endothelial permeability: implications for diabetic retinopathy.* Curr Eye Res, 2011. **36**(8): p. 747-53.

19. Sward, P. and B. Rippe, *Acute and sustained actions of hyperglycaemia on endothelial and glomerular barrier permeability.* Acta Physiol (Oxf), 2012. **204**(3): p. 294-307.

20. D'Aversa, T.G., et al., *Myelin Basic Protein Induces Inflammatory Mediators from Primary Human Endothelial Cells and Blood-Brain-Barrier Disruption: Implications for the Pathogenesis of Multiple Sclerosis.* Neuropathol Appl Neurobiol, 2012.

21. Alvarez, J.I., R. Cayrol, and A. Prat, *Disruption of central nervous system barriers in multiple sclerosis.* Biochim Biophys Acta, 2011. **1812**(2): p. 252-64.

22. Perrier, C. and B. Corthesy, *Gut permeability and food allergies.* Clin Exp Allergy, 2011. **41**(1): p. 20-8.

23. Pushparaj, P.N., et al., *The cytokine interleukin-33 mediates anaphylactic shock.* Proceedings of the National Academy of Sciences of the United States of America, 2009. **106**(24): p. 9773-9778.

24. Ignarro, L.J., G. Buga, and G. Dhaudhuri, *EDRF generation and release from perfused bovine pulmonary artery and vein.* Eur. J. Pharmacol, 1988. **149**: p. 79-88.

25. Ignarro, L.J., et al., *Endothelium-derived relaxing factor from pulmonary artery and vein possesses pharmacologic and chemical properties identical to those of nitric oxide radical.* Circulation Research, 1987. **61**(6): p. 866-79.

26. Rees, D.D., R.M. Palmer, and S. Moncada, *Role of endothelium-derived nitric oxide in the regulation of blood pressure.* Proc Natl Acad Sci U S A, 1989. **86**(9): p. 3375-8.

27. Eremina, V., et al., *Glomerular-specific alterations of VEGF-A expression lead to distinct congenital and acquired renal diseases.* J Clin Invest, 2003. **111**(5): p. 707-16.

28. Tolins, J.P., et al., *Role of endothelium-derived relaxing factor in regulation of renal hemodynamic responses.* Am J Physiol, 1990. **258**(3 Pt 2): p. H655-62.

29. Witko-Sarsat, V., et al., *Neutrophils: molecules, functions and pathophysiological aspects.* Laboratory Investigation, 2000. **80**(5): p. 617-53.

30. Ku, C.J., T. D'Amico Oblak, and D.M. Spence, *Interactions between multiple cell types in parallel microfluidic channels: monitoring platelet adhesion to an endothelium in the presence of an anti-adhesion drug.* Anal Chem, 2008. **80**(19): p. 7543-8.

31. Becker, B.F., et al., *Endothelial function and hemostasis.* Z Kardiol, 2000. **89**(3): p. 160-7.

32. Kim, J.A., et al., *Brain endothelial hemostasis regulation by pericytes.* Journal of Cerebral Blood Flow and Metabolism, 2006. **26**(2): p. 209-217.

33. Aird, W.C., *The role of the endothelium in severe sepsis and multiple organ dysfunction syndrome.* Blood, 2003. **101**(10): p. 3765-3777.

34. Amar, S., et al., *Periodontal disease is associated with brachial artery endothelial dysfunction and systemic inflammation.* Arterioscler Thromb Vasc Biol, 2003. **23**(7): p. 1245-9.

35. Tuomanen, E., *Entry of pathogens into the central nervous system.* FEMS Microbiol Rev, 1996. **18**(4): p. 289-99.

36. Luttun, A. and P. Carmeliet, *De novo vasculogenesis in the heart.* Cardiovasc Res, 2003. **58**(2): p. 378-89.

37. Hoekstra, M., et al., *Specific gene expression of ATP-binding cassette transporters and nuclear hormone receptors in rat liver parenchymal, endothelial, and Kupffer cells.* The Journal of biological chemistry, 2003. **278**(28): p. 25448-53.

38. van der Meer, A.D., et al., *Microfluidic technology in vascular research.* J Biomed Biotechnol, 2009. **2009**: p. 823148.

39. Wong, K.H., et al., *Microfluidic Models of Vascular Functions.* Annu Rev Biomed Eng, 2012.

40. Mehta, D. and A.B. Malik, *Signaling mechanisms regulating endothelial permeability.* Physiological Reviews, 2006. **86**(1): p. 279-367.

41. Gumbiner, B.M., *Breaking through the Tight Junction Barrier.* Journal of Cell Biology, 1993. **123**(6): p. 1631-1633.

42. Gonzalez-Mariscal, L., et al., *Tight junction proteins.* Progress in Biophysics & Molecular Biology, 2003. **81**(1): p. 1-44.

43. Forster, C., *Tight junctions and the modulation of barrier function in disease.* Histochem Cell Biol, 2008. **130**(1): p. 55-70.

44. Ebnet, K., *Organization of multiprotein complexes at cell-cell junctions.* Histochem Cell Biol, 2008. **130**(1): p. 1-20.

45. Staehelin, L.A., *Further observations on the fine structure of freeze-cleaved tight junctions.* J Cell Sci, 1973. **13**(3): p. 763-86.

46. Dejana, E., et al., *Organization and signaling of endothelial cell-to-cell junctions in various regions of the blood and lymphatic vascular trees.* Cell Tissue Res, 2009. **335**(1): p. 17-25.

47. Alcaide, P., et al., *p120-Catenin regulates leukocyte transmigration through an effect on VE-cadherin phosphorylation.* Blood, 2008. **112**(7): p. 2770-9.

48. Curl, C.L., et al., *Quantitative phase microscopy: a new tool for investigating the structure and function of unstained live cells.* Clin Exp Pharmacol Physiol, 2004. **31**(12): p. 896-901.

49. Kobayashi, H., et al., *Angiocrine factors from Akt-activated endothelial cells balance self-renewal and differentiation of haematopoietic stem cells.* Nature Cell Biology, 2010. **12**(11): p. 1046-U32.

50. Furuse, M., et al., *OCCLUDIN - A NOVEL INTEGRAL MEMBRANE-PROTEIN LOCALIZING AT TIGHT JUNCTIONS.* Journal of Cell Biology, 1993. **123**(6): p. 1777-1788.

51. Furuse, M., et al., *A single gene product, claudin-1 or -2, reconstitutes tight junction strands and recruits occludin in fibroblasts.* Journal of Cell Biology, 1998. **143**(2): p. 391-401.

52. Chen, Y.H., et al., *Restoration of tight junction structure and barrier function by down-regulation of the mitogen-activated protein kinase pathway in Ras-transformed Madin-Darby canine kidney cells.* Molecular Biology of the Cell, 2000. **11**(3): p. 849-862.

53. Wang, W., W.L. Dentler, and R.T. Borchardt, *VEGF increases BMEC monolayer permeability by affecting occludin expression and tight junction assembly.* American Journal of Physiology-Heart and Circulatory Physiology, 2001. **280**(1): p. H434-H440.

54. Harhaj, N.S. and D.A. Antonetti, *Regulation of tight junctions and loss of barrier function in pathophysiology.* international journal of biochemistry & cell biology, 2004. **36**(7): p. 1206-1237.

55. Bolton, S.J., D.C. Anthony, and V.H. Perry, *Loss of the tight junction proteins occludin and zonula occludens-1 from cerebral vascular endothelium during neutrophil-induced blood-brain barrier breakdown in vivo.* Neuroscience, 1998. **86**(4): p. 1245-1257.

56. Hirase, T., et al., *Occludin as a possible determinant of tight junction permeability in endothelial cells.* Journal of Cell Science, 1997. **110**: p. 1603-1613.

57. Chen, C.C., Y. Zhou, and L.A. Baker, *Scanning ion conductance microscopy.* Annu Rev Anal Chem (Palo Alto Calif), 2012. **5**(1): p. 207-28.

58. Morris, C.A., A.K. Friedman, and L.A. Baker, *Applications of nanopipettes in the analytical sciences.* Analyst, 2010. **135**(9): p. 2190-202.

59. Deli, M.A., et al., *Permeability studies on in vitro blood-brain barrier models: physiology, pathology, and pharmacology.* Cell Mol Neurobiol, 2005. **25**(1): p. 59-127.

60. Borchardt, R.T., et al., *Models for Assessing Drug Absorption and Metabolism. [In: Pharm. Biotechnol., 1996; 8]*1996. 444 pp.

61. Dehouck, M.P., et al., *Drug transfer across the blood-brain barrier: correlation between in vitro and in vivo models.* Journal of Neurochemistry, 1992. **58**(5): p. 1790-7.

62. Dehouck, M.P., et al., *In vitro reconstituted blood-brain barrier.* Journal of Controlled Release, 1992. **21**(1-3): p. 81-91.

63. Audus, K.L. and R.T. Borchardt, *Characterization of an in vitro blood-brain barrier model system for studying drug transport and metabolism.* Pharmaceutical Research, 1986. **3**(2): p. 81-7.

64. Deli, M.A., et al., *Permeability studies on in vitro blood-brain barrier models: Physiology, pathology, and pharmacology.* Cellular and Molecular Neurobiology, 2005. **25**(1): p. 59-127.

65. Gaillard, P.J. and A.G. de Boer, *Relationship between permeability status of the blood-brain barrier and in vitro permeability coefficient of a drug.* European Journal of Pharmaceutical Sciences, 2000. **12**(2): p. 95-102.

66. Bowman, P.D., et al., *Brain microvessel endothelial cells in tissue culture: a model for study of blood-brain barrier permeability.* Annals of Neurology, 1983. **14**(4): p. 396-402.

67. Plateel, M., E. Teissier, and R. Cecchelli, *Hypoxia dramatically increases the nonspecific transport of blood-borne proteins to the brain.* Journal of Neurochemistry, 1997. **68**(2): p. 874-877.

68. Audus, K.L., et al., *Brain microvessel endothelial cell culture systems.* Pharm Biotechnol, 1996. **8**: p. 239-58.

69. Brown, R.C., et al., *Protection against hypoxia-induced increase in blood-brain barrier permeability: role of tight junction proteins and NFkappaB.* J Cell Sci, 2003. **116**(Pt 4): p. 693-700.

70. Qaum, T., et al., *VEGF-initiated blood-retinal barrier breakdown in early diabetes.* Invest Ophthalmol Vis Sci, 2001. **42**(10): p. 2408-13.

71. Butt, A.M., H.C. Jones, and N.J. Abbott, *Electrical resistance across the blood-brain barrier in anaesthetized rats: a developmental study.* The Journal of physiology, 1990. **429**: p. 47-62.

72. Madara, J.L., *Regulation of the movement of solutes across tight junctions.* Annual Review of Physiology, 1998. **60**: p. 143-159.

73. Wong, V. and B.M. Gumbiner, *A synthetic peptide corresponding to the extracellular domain of occludin perturbs the tight junction permeability barrier.* Journal of Cell Biology, 1997. **136**(2): p. 399-409.

74. Madsen, K.L., et al., *Interleukin 10 prevents cytokine-induced disruption of T84 monolayer barrier integrity and limits chloride secretion.* Gastroenterology, 1997. **113**(1): p. 151-9.

75. Garcia, J.G., et al., *Sphingosine 1-phosphate promotes endothelial cell barrier integrity by Edg-dependent cytoskeletal rearrangement.* J Clin Invest, 2001. **108**(5): p. 689-701.

76. Birukova, A.A., et al., *Afadin controls p120-catenin-ZO-1 interactions leading to endothelial barrier enhancement by oxidized phospholipids.* J Cell Physiol, 2012. **227**(5): p. 1883-90.

77. Hurst, R.D., et al., *Nitric-oxide-induced inhibition of glyceraldehyde-3-phosphate dehydrogenase may mediate reduced endothelial cell monolayer integrity in an in vitro model blood-brain barrier.* Brain Research, 2001. **894**(2): p. 181-8.

78. Imaizumi, S., et al., *The influence of oxygen free radicals on the permeability of the monolayer of cultured brain endothelial cells.* Neurochem Int, 1996. **29**(2): p. 205-11.

79. Xu, M., et al., *Ethanol disrupts vascular endothelial barrier: implication in cancer metastasis.* Toxicol Sci, 2012. **127**(1): p. 42-53.

80. Hart, M.N., et al., *Differential opening of the brain endothelial barrier following neutralization of the endothelial luminal anionic charge in vitro.* Journal of Neuropathology and Experimental Neurology, 1987. **46**(2): p. 141-53.

81. Rutten, M.J., R.L. Hoover, and M.J. Karnovsky, *Electrical resistance and macromolecular permeability of brain endothelial monolayer cultures.* Brain Research, 1987. **425**(2): p. 301-10.

82. Davies, P.F., *Flow-mediated endothelial mechanotransduction.* Physiol Rev, 1995. **75**(3): p. 519-60.

83. Nagaraja, S., A. Kapela, and N.M. Tsoukias, *Intercellular communication in the vascular wall: A modeling perspective.* Microcirculation, 2012.

84. Sprague, R.S., et al., *ATP: the red blood cell link to NO and local control of the pulmonary circulation.* Am. J. Physiol, 1996. **271**: p. H2717-H2722.

85. Ellsworth, M.L., et al., *Erythrocytes: Oxygen Sensors and Modulators of Vascular Tone.* Physiology, 2009. **24**(2): p. 107-116.

86. Sprague, R.S., Olearczyk, Jeffrey J., Spence, Dana M., Stephenson, Alan H., Sprung, Robert W., Lonigro, Andrew J., *Extracellular ATP signaling in the rabbit lung: erythrocytes as determinants of vascular resistance.* American Journal of Physiology-Heart and Circulatory Physiology, 2003. **285**: p. H693-H700.

87. Dietrich, H.H., et al., *Red blood cell regulation of microvascular tone through adenosine triphosphate.* Am. J. Physiol, 2000. **278**: p. H1294-H1298.

88. Tolan, N.V., et al., *Personalized Metabolic Assessment of Erythrocytes Using Microfluidic Delivery to an Array of Luminescent Wells.* Analytical Chemistry, 2009. **81**(8): p. 3102-3108.

89. Halpin, S.T., et al., *The Red Blood Cell and Nitric Oxide: Derived, Stimulated, or Both?* The Open Nitric Oxide Journal, 2011. **3**(Suppl 1-M2): p. 8-15.

90. Carroll, J.S., et al., *Red blood cell stimulation of platelet nitric oxide production indicated by quantitative monitoring of the communication between cells in the bloodstream.* Anal Chem, 2007. **79**(14): p. 5133-8.

91. Masszi, A., et al., *Integrity of cell-cell contacts is a critical regulator of TGF-beta 1-induced epithelial-to-myofibroblast transition: role for beta-catenin.* Am J Pathol, 2004. **165**(6): p. 1955-67.

92. Pentland, A.P., et al., *Cellular confluence determines injury-induced prostaglandin E2 synthesis by human keratinocyte cultures.* Biochim Biophys Acta, 1987. **919**(1): p. 71-8.

93. Fleisher, L.N., et al., *Stimulation of arterial endothelial cell prostacyclin synthesis by high density lipoproteins.* The Journal of biological chemistry, 1982. **257**(12): p. 6653-5.

94. Drexler, H.C., W. Risau, and M.A. Konerding, *Inhibition of proteasome function induces programmed cell death in proliferating endothelial cells.* FASEB J, 2000. **14**(1): p. 65-77.

95. Yalcin, H.C., S.F. Perry, and S.N. Ghadiali, *Influence of airway diameter and cell confluence on epithelial cell injury in an in vitro model of airway reopening.* Journal of applied physiology (Bethesda, Md. 1985), 2007. **103**(5): p. 1796-807.

96. Govers, R., et al., *Endothelial nitric oxide synthase activity is linked to its presence at cell-cell contacts.* The Biochemical journal, 2002. **361**(Pt 2): p. 193-201.

97. Vogel, P.A., et al., *Microfluidic transendothelial electrical resistance measurement device that enables blood flow and postgrowth experiments.* Anal Chem, 2011. **83**(11): p. 4296-301.

98. Corvera, S., C. DiBonaventura, and H.S. Shpetner, *Cell confluence-dependent remodeling of endothelial membranes mediated by cholesterol.* The Journal of biological chemistry, 2000. **275**(40): p. 31414-21.

99. Vinals, F. and J. Pouyssegur, *Confluence of vascular endothelial cells induces cell cycle exit by inhibiting p42/p44 mitogen-activated protein kinase activity.* Mol Cell Biol, 1999. **19**(4): p. 2763-72.

100. Lampugnani, M.G., et al., *Cell confluence regulates tyrosine phosphorylation of adherens junction components in endothelial cells.* J Cell Sci, 1997. **110 (Pt 17)**: p. 2065-77.

101. Pries, A.R. and T.W. Secomb, *Microvascular blood viscosity in vivo and the endothelial surface layer.* American journal of physiology. Heart and circulatory physiology, 2005. **289**(6): p. H2657-64.

102. Feletou, M., Y. Huang, and P.M. Vanhoutte, *Endothelium-mediated control of vascular tone: COX-1 and COX-2 products.* Br J Pharmacol, 2011. **164**(3): p. 894-912.

103. Furchgott, R.F. and J.V. Zawadzki, *The Obligatory Role of Endothelial-Cells in the Relaxation of Arterial Smooth-Muscle by Acetylcholine.* Nature, 1980. **288**(5789): p. 373-376.

104. Ignarro, L.J., et al., *Association between cyclic GMP accumulation and acetylcholine-elicited relaxation of bovine intrapulmonary artery.* J Pharmacol Exp Ther, 1984. **228**(3): p. 682-90.

105. Rapoport, R.M. and F. Murad, *Agonist-induced endothelium-dependent relaxation in rat thoracic aorta may be mediated through cGMP.* Circ Res, 1983. **52**(3): p. 352-7.

106. Palmer, R.M., A.G. Ferrige, and S. Moncada, *Nitric oxide release accounts for the biological activity of endothelium-derived relaxing factor.* Nature, 1987. **327**(6122): p. 524-6.

107. Palmer, R.M., et al., *L-arginine is the physiological precursor for the formation of nitric oxide in endothelium-dependent relaxation.* Biochem Biophys Res Commun, 1988. **153**(3): p. 1251-6.

108. Palmer, R.M., D.S. Ashton, and S. Moncada, *Vascular endothelial cells synthesize nitric oxide from L-arginine.* Nature, 1988. **333**(6174): p. 664-6.

109. Pollock, J.S., et al., *Purification and characterization of particulate endothelium-derived relaxing factor synthase from cultured and native bovine aortic endothelial cells.* Proc Natl Acad Sci U S A, 1991. **88**(23): p. 10480-4.

110. Forstermann, U., et al., *Calmodulin-dependent endothelium-derived relaxing factor/nitric oxide synthase activity is present in the particulate and cytosolic fractions of bovine aortic endothelial cells.* Proc Natl Acad Sci U S A, 1991. **88**(5): p. 1788-92.

111. Chataigneau, T., et al., *Acetylcholine-induced relaxation in blood vessels from endothelial nitric oxide synthase knockout mice.* Br J Pharmacol, 1999. **126**(1): p. 219-26.

112. Osanai, T., et al., *Cross talk of shear-induced production of prostacyclin and nitric oxide in endothelial cells.* Am J Physiol Heart Circ Physiol, 2000. **278**(1): p. H233-8.

113. D'Amico Oblak, T., P. Root, and D.M. Spence, *Fluorescence monitoring of ATP-stimulated, endothelium-derived nitric oxide production in channels of a poly(dimethylsiloxane)-based microfluidic device.* Anal Chem, 2006. **78**(9): p. 3193-7.

114. Chen, Z., et al., *Estrogen receptor alpha mediates the nongenomic activation of endothelial nitric oxide synthase by estrogen.* J Clin Invest, 1999. **103**(3): p. 401-6.

115. Fleming, I. and R. Busse, *Molecular mechanisms involved in the regulation of the endothelial nitric oxide synthase.* Am J Physiol Regul Integr Comp Physiol, 2003. **284**(1): p. R1-12.

116. Busse, R. and A. Mulsch, *Calcium-dependent nitric oxide synthesis in endothelial cytosol is mediated by calmodulin.* FEBS Lett, 1990. **265**(1-2): p. 133-6.

117. Fisslthaler, B., et al., *Phosphorylation and activation of the endothelial nitric oxide synthase by fluid shear stress.* Acta Physiol Scand, 2000. **168**(1): p. 81-8.

118. Olsson, R.A. and J.D. Pearson, *Cardiovascular purinoceptors.* Physiol Rev, 1990. **70**(3): p. 761-845.

119. Raqeeb, A., et al., *Purinergic P2Y2 receptors mediate rapid Ca(2+) mobilization, membrane hyperpolarization and nitric oxide production in human vascular endothelial cells.* Cell Calcium, 2011. **49**(4): p. 240-8.

120. Abbracchio, M.P. and G. Burnstock, *Purinergic signalling: pathophysiological roles.* Jpn J Pharmacol, 1998. **78**(2): p. 113-45.

121. Burnstock, G., *Purinergic signalling--an overview.* Novartis Found Symp, 2006. **276**: p. 26-48; discussion 48-57, 275-81.

122. Burnstock, G., *Purinergic regulation of vascular tone and remodelling.* Auton Autacoid Pharmacol, 2009. **29**(3): p. 63-72.

123. Saenz de Tejada, I., et al., *Cholinergic neurotransmission in human corpus cavernosum. I. Responses of isolated tissue.* Am J Physiol, 1988. **254**(3 Pt 2): p. H459-67.

124. Kimoto, Y., R. Kessler, and C.E. Constantinou, *Endothelium dependent relaxation of human corpus cavernosum by bradykinin.* J Urol, 1990. **144**(4): p. 1015-7.

125. Kim, N., et al., *A nitric oxide-like factor mediates nonadrenergic-noncholinergic neurogenic relaxation of penile corpus cavernosum smooth muscle.* J Clin Invest, 1991. **88**(1): p. 112-8.

126. Azadzoi, K.M. and I. Saenz de Tejada, *Diabetes mellitus impairs neurogenic and endothelium-dependent relaxation of rabbit corpus cavernosum smooth muscle.* J Urol, 1992. **148**(5): p. 1587-91.

127. Burnett, A.L., et al., *Nitric oxide: a physiologic mediator of penile erection.* Science, 1992. **257**(5068): p. 401-3.

128. Trigo-Rocha, F., et al., *Nitric oxide and cGMP: mediators of pelvic nerve-stimulated erection in dogs.* Am J Physiol, 1993. **264**(2 Pt 2): p. H419-22.

129. Saiag, B., et al., *Study of the mechanisms involved in adenosine-5'-O-(2-thiodiphosphate) induced relaxation of rat thoracic aorta and pancreatic vascular bed.* Br J Pharmacol, 1996. **118**(3): p. 804-10.

130. Shalev, M., et al., *Stimulation of P2y purinoceptors induces, via nitric oxide production, endothelium-dependent relaxation of human isolated corpus cavernosum.* J Urol, 1999. **161**(3): p. 955-9.

131. Needham, L., et al., *Characteristics of the P2 purinoceptor that mediates prostacyclin production by pig aortic endothelial cells.* Eur J Pharmacol, 1987. **134**(2): p. 199-209.

132. Mitchell, J.A., et al., *Different patterns of release of endothelium-derived relaxing factor and prostacyclin.* Br J Pharmacol, 1992. **105**(2): p. 485-9.

133. Kalinowski, L., et al., *Third-generation beta-blockers stimulate nitric oxide release from endothelial cells through ATP efflux: a novel mechanism for antihypertensive action.* Circulation, 2003. **107**(21): p. 2747-52.

134. da Silva, C.G., et al., *Mechanism of purinergic activation of endothelial nitric oxide synthase in endothelial cells.* Circulation, 2009. **119**(6): p. 871-9.

135. Xu, H.L., et al., *Agonist-specific differences in mechanisms mediating eNOS-dependent pial arteriolar dilation in rats.* American journal of physiology. Heart and circulatory physiology, 2002. **282**(1): p. H237-43.

136. Mortensen, S.P., et al., *ATP-induced vasodilation and purinergic receptors in the human leg: roles of nitric oxide, prostaglandins, and adenosine.* Am J Physiol Regul Integr Comp Physiol, 2009. **296**(4): p. R1140-8.

137. Erlinge, D. and G. Burnstock, *P2 receptors in cardiovascular regulation and disease.* Purinergic Signal, 2008. **4**(1): p. 1-20.

138. Griffith, T.M., et al., *The nature of endothelium-derived vascular relaxant factor.* Nature, 1984. **308**(5960): p. 645-7.

139. Lincoln, T.M., N. Dey, and H. Sellak, *Invited review: cGMP-dependent protein kinase signaling mechanisms in smooth muscle: from the regulation of tone to gene expression.* Journal of applied physiology (Bethesda, Md. 1985), 2001. **91**(3): p. 1421-30.

140. Nossaman, B., E. Pankey, and P. Kadowitz, *Stimulators and activators of soluble guanylate cyclase: review and potential therapeutic indications.* Crit Care Res Pract, 2012. **2012**: p. 290805.

141. Vucetic, M., P.K. Jensen, and E.C. Jansen, *Diameter variations of retinal blood vessels during and after treatment with hyperbaric oxygen.* Br J Ophthalmol, 2004. **88**(6): p. 771-5.

142. Lampe, J. and K. Pommerening, *[Oxygen binding of hemoglobin following covalent fixation in the deoxy- and oxy- conformation].* Acta Biol Med Ger, 1975. **34?710**: p. 1603-8.

143. Stamler, J.S., et al., *Blood flow regulation by S-nitrosohemoglobin in the physiological oxygen gradient.* Science, 1997. **276**(5321): p. 2034-2037.

144. Jia, L., et al., *S-Nitrosohemoglobin: a dynamic activity of blood involved in vascular control.* Nature (London), 1996. **380**(6571): p. 221-6.

145. Doyle, M.P., D.M. LePoire, and R.A. Pickering, *Oxidation of hemoglobin and myoglobin by alkyl nitrites inhibition by oxygen.* The Journal of biological chemistry, 1981. **256**(23): p. 12399-404.

146. Cosby, K., et al., *Nitrite reduction to nitric oxide by deoxyhemoglobin vasodilates the human circulation.* Nat Med, 2003. **9**(12): p. 1498-505.

147. Garcia, J.I., et al., *Nitrite and nitroglycerin induce rapid release of the vasodilator ATP from erythrocytes: Relevance to the chemical physiology of local vasodilation.* J Inorg Biochem, 2010. **104**(3): p. 289-96.

148. Aisaka, K., et al., *NG-methylarginine, an inhibitor of endothelium-derived nitric oxide synthesis, is a potent pressor agent in the guinea pig: does nitric oxide regulate blood pressure in vivo?* Biochem Biophys Res Commun, 1989. **160**(2): p. 881-6.

149. Beutler, E., *Biochemistry of the erythrocyte.* Experientia, 1969. **25**(5): p. 470-3.

150. Edwards, J.L., et al., *Chemiluminescence detection of ATP release from red blood cells upon deformation in microbore tubing.* Analyst, 2001. **126**: p. 1257-1260.

151. Faris, A. and D.M. Spence, *Measuring the simultaneous effects of hypoxia and deformation on ATP release from erythrocytes.* Analyst (Cambridge, United Kingdom), 2008. **133**(5): p. 678-682.

152. Bergfeld, G.R. and T. Forrester, *Release of ATP from human erythrocytes in response to a brief period of hypoxia and hypercapnea.* Cardiovasc. Res., 1992. **26**: p. 40-47.

153. Raththagala, M., et al., *Hydroxyurea stimulates the release of ATP from rabbit erythrocytes through an increase in calcium and nitric oxide production.* Eur J Pharmacol, 2010. **645**(1-3): p. 32-8.

154. Meyer, J.A., et al., *Metal-activated C-peptide facilitates glucose clearance and the release of a nitric oxide stimulus via the GLUT1 transporter.* Diabetologia, 2008. **51**(1): p. 175-82.

155. Sprague, R.S., et al., *Deformation-induced ATP release from red blood cells requires cystic fibrosis transmembrane conductance regulator activity.* Am. J. Physiol, 1998. **275**: p. H1726-H1732.

156. Olearczyk, J.J., et al., *Heterotrimeric G protein Gi is involved in a signal transduction pathway for ATP release from erythrocytes.* American Journal of Physiology, 2004. **286**(3, Pt. 2): p. H940-H945.

157. Sprague, R.S., et al., *Participation of cAMP in a signal-transduction pathway relating erythrocyte deformation to ATP release.* American Journal of Physiology, 2001. **281**(4, Pt. 1): p. C1158-C1164.

158. Olearczyk, J.J., Stephenson, Alan H., Lonigro, Andrew J., Sprague, Randy S., *Receptor-mediated activation of the heterotrimeric G-protein Gs results in ATP release from erythrocytes.* Medical Science Monitor, 2001. **7**(4): p. 669-674.

159. Price, A., K., et al., *Deformation-induced release of ATP from erythrocytes in a poly(dimethylsiloxane)-based microchip with channels that mimic resistance vessels.* Analytical Chemistry, 2004. **76**(16): p. 4849-55.

160. Steiner, D.F., et al., *Proinsulin and the biosynthesis of insulin.* Recent Prog Horm Res, 1969. **25**: p. 207-82.

161. Rubenstein, A.H., et al., *Proinsulin and C-peptide in blood.* Diabetes, 1972. **21**(2 Suppl): p. 661-72.

162. Hoogwerf, B.J., et al., *Infusion of synthetic human C-peptide does not affect plasma glucose, serum insulin, or plasma glucagon in healthy subjects.* Metabolism, Clinical and Experimental, 1986. **35**(2): p. 122-5.

163. Jensen, M.E. and E.J. Messina, *C-peptide induces a concentration-dependent dilation of skeletal muscle arterioles only in presence of insulin.* Am J Physiol, 1999. **276**(4 Pt 2): p. H1223-8.

164. Scalia, R., et al., *C-peptide inhibits leukocyte-endothelium interaction in the microcirculation during acute endothelial dysfunction.* FASEB J, 2000. **14**(14): p. 2357-64.

165. Young, L.H., et al., *C-peptide exerts cardioprotective effects in myocardial ischemia-reperfusion.* Am J Physiol Heart Circ Physiol, 2000. **279**(4): p. H1453-9.

166. Pierson, C.R., W. Zhang, and A.A. Sima, *Proinsulin C-peptide replacement in type 1 diabetic BB/Wor-rats prevents deficits in nerve fiber regeneration.* Journal of Neuropathology and Experimental Neurology, 2003. **62**(7): p. 765-79.

167. Maezawa, Y., et al., *Influence of C-peptide on early glomerular changes in diabetic mice.* Diabetes/metabolism research and reviews, 2006. **22**(4): p. 313-22.

168. Sima, A.A., et al., *Inflammation in Diabetic Encephalopathy is Prevented by C-Peptide.* Rev Diabet Stud, 2009. **6**(1): p. 37-42.

169. Lindstrom, K., et al., *Acute effects of C-peptide on the microvasculature of isolated perfused skeletal muscles and kidneys in rat.* Acta Physiol Scand, 1996. **156**(1): p. 19-25.

170. Hansen, A., et al., *C-peptide exerts beneficial effects on myocardial blood flow and function in patients with type 1 diabetes.* Diabetes, 2002. **51**(10): p. 3077-3082.

171. Schalkwijk, C.G. and C.D. Stehouwer, *Vascular complications in diabetes mellitus: the role of endothelial dysfunction.* Clin Sci (Lond), 2005. **109**(2): p. 143-59.

172. Johansson, B.L., J. Wahren, and J. Pernow, *C-peptide increases forearm blood flow in patients with type 1 diabetes via a nitric oxide-dependent mechanism.* Am J Physiol Endocrinol Metab, 2003. **285**(4): p. E864-70.

173. Wallerath, T., et al., *Stimulation of endothelial nitric oxide synthase by proinsulin C-peptide.* Nitric Oxide, 2003. **9**(2): p. 95-102.

174. Kitamura, T., et al., *Proinsulin C-peptide activates cAMP response element-binding proteins through the p38 mitogen-activated protein kinase pathway in mouse lung capillary endothelial cells.* Biochemical Journal, 2002. **366**(3): p. 737-744.

175. Sprague, R.S., et al., *Extracellular ATP signaling in the rabbit lung: erythrocytes as determinants of vascular resistance.* Am J Physiol Heart Circ Physiol, 2003. **285**(2): p. H693-700.

176. Sprung, R.J., R.S. Sprague, and D.M. Spence, *Determination of ATP release from erythrocytes using microbore tubing as a model of resistance vessels in vivo.* Anal. Chem., 2002. **74**: p. 2274-2278.

177. Wan, J., W.D. Ristenpart, and H.A. Stone, *Dynamics of shear-induced ATP release from red blood cells.* Proc Natl Acad Sci U S A, 2008. **105**(43): p. 16432-7.

178. Rigler, R., et al., *Specific binding of proinsulin C-peptide to human cell membranes.* Proc. Natl. Acad. Sci., 1999. **96**: p. 13318-13323.

179. Henriksson, M., et al., *Separate functional features of proinsulin C-peptide.* Cell Mol Life Sci, 2005. **62**(15): p. 1772-8.

180. Luppi, P., et al., *C-peptide is internalised in human endothelial and vascular smooth muscle cells via early endosomes.* Diabetologia, 2009. **52**(10): p. 2218-28.

181. Minshall, R.D. and A.B. Malik, *Transport across the endothelium: regulation of endothelial permeability.* Handb Exp Pharmacol, 2006(176 Pt 1): p. 107-44.

182. Minshall, R.D., et al., *Vesicle formation and trafficking in endothelial cells and regulation of endothelial barrier function.* Histochem Cell Biol, 2002. **117**(2): p. 105-12.

183. Lossinsky, A.S. and R.R. Shivers, *Structural pathways for macromolecular and cellular transport across the blood-brain barrier during inflammatory conditions. Review.* Histol Histopathol, 2004. **19**(2): p. 535-64.

184. Le Sueur, L.P., C.B. Collares-Buzato, and M.A. da Cruz-Hofling, *Mechanisms involved in the blood-brain barrier increased permeability induced by Phoneutria nigriventer spider venom in rats.* Brain Research, 2004. **1027**(1-2): p. 38-47.

185. Groneberg, D.A., et al., *Distribution and function of the peptide transporter PEPT2 in normal and cystic fibrosis human lung.* Thorax, 2002. **57**(1): p. 55-60.

186. Meredith, D. and C.A. Boyd, *Dipeptide transport characteristics of the apical membrane of rat lung type II pneumocytes.* Am J Physiol, 1995. **269**(2 Pt 1): p. L137-43.

187. Lindahl, E., et al., *Cellular internalization of proinsulin C-peptide.* Cell. Mol. Life Sci., 2007. **64**: p. 479-486.

188. Lindahl, E., et al., *Proinsulin C-peptide regulates ribosomal RNA expression.* J Biol Chem, 2010. **285**(5): p. 3462-9.

189. Jo, H., et al., *Endothelial albumin permeability is shear dependent, time dependent, and reversible.* Am J Physiol, 1991. **260**(6 Pt 2): p. H1992-6.

190. Meyer, J.A., et al., *Zinc-activated C-peptide resistance to the type 2 diabetic erythrocyte is associated with hyperglycemia-induced phosphatidylserine externalization and reversed by metformin.* Mol Biosyst, 2009. **5**(10): p. 1157-62.

191. Keltner, Z., et al., *Mass spectrometric characterization and activity of zinc-activated proinsulin C-peptide and C-peptide mutants.* Analyst, 2010. **135**(2): p. 278-288.

192. Brooks, P., J. Meyer, and D.M. Spence, *Metal (Zn^{2+}) Activated C-Peptide Induced ATP Release Via Red Blood Cells with the Addition of Albumin.* Abstracts, 60th Southeast Regional Meeting of the American Chemical Society, Nashville, TN, United States, November 12-15, 2008: p. SERM-680.

193. Medawala, W., et al., *A Molecular Level Understanding of Zinc Activation of C-peptide and its Effects on Cellular Communication in the Bloodstream.* Rev Diabet Stud, 2009. **6**(3): p. 148-58.

194. Hutton, J.C., *The insulin secretory granule.* Diabetologia, 1989. **32**(5): p. 271-81.

195. Shafqat, J., et al., *Proinsulin C-peptide elicits disaggregation of insulin resulting in enhanced physiological insulin effects.* Cell Mol Life Sci, 2006. **63**(15): p. 1805-11.

196. Kunt, T., et al., *The effect of human proinsulin C-peptide on erythrocyte deformability in patients with type I diabetes mellitus.* Diabetologia, 1999. **42**(4): p. 465-471.

197. Rieg, T., et al., *P2Y(2) receptor activation decreases blood pressure and increases renal Na(+) excretion.* Am J Physiol Regul Integr Comp Physiol, 2011. **301**(2): p. R510-8.

198. Gonzalez-Alonso, J., *ATP as a mediator of erythrocyte-dependent regulation of skeletal muscle blood flow and oxygen delivery in humans.* The Journal of physiology, 2012.

199. Burnstock, G., *Control of vascular tone by purines and pyrimidines.* Br J Pharmacol, 2010. **161**(3): p. 527-9.

200. Sprague, R.S. and M.L. Ellsworth, *Erythrocyte-derived ATP and perfusion distribution: Role of intracellular and intercellular communication.* Microcirculation, 2012.

201. Kuzuya, H., et al., *Heterogeneity of circulating C-peptide.* The Journal of clinical endocrinology and metabolism, 1977. **44**(5): p. 952-62.

202. Horwitz, D.L., et al., *Proinsulin, insulin, and C-peptide concentrations in human portal and peripheral blood.* J Clin Invest, 1975. **55**(6): p. 1278-83.

203. Dovichi, N.J. and J. Zhang, *How Capillary Electrophoresis Sequenced the Human Genome This Essay is based on a lecture given at the Analytica 2000 conference in Munich (Germany) on the occasion of the Heinrich-Emanuel-Merck Prize presentation.* Angew Chem Int Ed Engl, 2000. **39**(24): p. 4463-4468.

204. Kidd, J.M., et al., *Haplotype sorting using human fosmid clone end-sequence pairs.* Genome Res, 2008. **18**(12): p. 2016-23.

205. Kidd, J.M., et al., *Mapping and sequencing of structural variation from eight human genomes.* Nature, 2008. **453**(7191): p. 56-64.

206. Easley, C.J., et al., *A fully integrated microfluidic genetic analysis system with sample-in-answer-out capability.* Proc Natl Acad Sci U S A, 2006. **103**(51): p. 19272-7.

207. Easley, C.J., et al., *Rapid DNA amplification in glass microdevices.* Methods Mol Biol, 2006. **339**: p. 217-32.

208. Dittrich, P., S. and A. Manz, *Lab-on-a-chip: Microfluidics in Drug Discovery.* Nature Reviews Drug Discovery, 2006. **5**: p. 210-218.

209. Dittrich, P.S., K. Tachikawa, and A. Manz, *Micro Total Analysis Systems. Latest Advancements and Trends.* Anal. Chem., 2006. **ASAP**.

210. Whitesides, G.M., *The origins and the future of microfluidics.* Nature, 2006. **442**(7101): p. 368-373.

211. Genes, L., I., et al., *Adressing a Vascular Endothelium Array with Blood Components using Underlying Microfluidic Channels.* Lab on a Chip, 2007. **7**(10): p. 1256-1259.

212. Song, J.W., et al., *Microfluidic endothelium for studying the intravascular adhesion of metastatic breast cancer cells.* PLoS ONE, 2009. **4**(6): p. e5756.

213. Barbulovic-Nad, I., et al., *Digital microfluidics for cell-based assays.* Lab on a Chip, 2008. **8**(4): p. 519-526.

214. Pihl, J., et al., *Microfluidics for cell-based assays.* Materials Today, 2005. **8**(12): p. 46-51.

215. Oblak, T.D., J.A. Meyer, and D.M. Spence, *A microfluidic technique for monitoring bloodstream analytes indicative of C-peptide resistance in type 2 diabetes.* Analyst, 2009. **134**(1): p. 188-193.

216. Hung, P.J., et al., *Continuous perfusion microfluidic cell culture array for high-throughput cell-based assays.* Biotechnol Bioeng, 2005. **89**(1): p. 1-8.

217. Kim, M.S., J.H. Yeon, and J.K. Park, *A microfluidic platform for 3-dimensional cell culture and cell-based assays.* Biomed Microdevices, 2007. **9**(1): p. 25-34.

218. McDonald, J.C., et al., *Fabrication of microfluidic systems in poly(dimethylsiloxane).* Electrophoresis, 2000. **21**(1): p. 27-40.

219. Duffy, D.C., et al., *Rapid prototyping of microfluidic systems in poly(dimethylsiloxane).* Analytical Chemistry, 1998. **70**(23): p. 4974-4984.

220. Mehta, G., et al., *Quantitative measurement and control of oxygen levels in microfluidic poly(dimethylsiloxane) bioreactors during cell culture.* Biomed Microdevices, 2007. **9**(2): p. 123-34.

221. Leclerc, E., Y. Sakai, and T. Fujii, *Microfluidic PDMS (polydimethylsiloxane) bioreactor for large-scale culture of hepatocytes.* Biotechnol Prog, 2004. **20**(3): p. 750-5.

222. Soper, S.A., et al., *Polymeric microelectromechanical systems.* Anal Chem, 2000. **72**(19): p. 642A-651A.

223. Regehr, K.J., et al., *Biological implications of polydimethylsiloxane-based microfluidic cell culture.* Lab Chip, 2009. **9**(15): p. 2132-9.

224. Shamloo, A., et al., *Endothelial cell polarization and chemotaxis in a microfluidic device.* Lab on a Chip, 2008. **8**(8): p. 1292-1299.

225. Young, E.W., A.R. Wheeler, and C.A. Simmons, *Matrix-dependent adhesion of vascular and valvular endothelial cells in microfluidic channels.* Lab Chip, 2007. **7**(12): p. 1759-66.

226. Lu, H., et al., *Microfluidic shear devices for quantitative analysis of cell adhesion.* Anal Chem, 2004. **76**(18): p. 5257-64.

227. Sin, A., et al., *Enrichment using antibody-coated microfluidic chambers in shear flow: model mixtures of human lymphocytes.* Biotechnol Bioeng, 2005. **91**(7): p. 816-26.

228. Wong, K.H.K., et al., *Microfluidic Models of Vascular Functions.* Annual Review of Biomedical Engineering, 2012. **14**(1): p. null.

229. Srigunapalan, S., et al., *A microfluidic membrane device to mimic critical components of the vascular microenvironment.* Biomicrofluidics, 2011. **5**(1): p. 13409.

230. Kaihara, S., et al., *Silicon micromachining to tissue engineer branched vascular channels for liver fabrication.* Tissue Eng, 2000. **6**(2): p. 105-17.

231. Lim, D., et al., *Fabrication of microfluidic mixers and artificial vasculatures using a high-brightness diode-pumped Nd:YAG laser direct write method.* Lab Chip, 2003. **3**(4): p. 318-23.

232. Borenstein, J.T., et al., *Microfabrication of three-dimensional engineered scaffolds.* Tissue Eng, 2007. **13**(8): p. 1837-44.

233. Huh, D., et al., *Reconstituting organ-level lung functions on a chip.* Science, 2010. **328**(5986): p. 1662-8.

234. Tavana, H., et al., *Epithelium damage and protection during reopening of occluded airways in a physiologic microfluidic pulmonary airway model.* Biomed Microdevices, 2011. **13**(4): p. 731-42.

235. Suwanpayak, N., et al., *Blood cleaner on-chip design for artificial human kidney manipulation.* Int J Nanomedicine, 2011. **6**: p. 957-64.

236. Jang, K.J. and K.Y. Suh, *A multi-layer microfluidic device for efficient culture and analysis of renal tubular cells.* Lab Chip, 2010. **10**(1): p. 36-42.

237. Grosberg, A., et al., *Ensembles of engineered cardiac tissues for physiological and pharmacological study: heart on a chip.* Lab Chip, 2011. **11**(24): p. 4165-73.

238. Kim, H.J., et al., *Human gut-on-a-chip inhabited by microbial flora that experiences intestinal peristalsis-like motions and flow.* Lab Chip, 2012. **12**(12): p. 2165-74.

239. Chronis, N., M. Zimmer, and C.I. Bargmann, *Microfluidics for in vivo imaging of neuronal and behavioral activity in Caenorhabditis elegans.* Nat Methods, 2007. **4**(9): p. 727-31.

240. Chung, K., M.M. Crane, and H. Lu, *Automated on-chip rapid microscopy, phenotyping and sorting of C. elegans.* Nat Methods, 2008. **5**(7): p. 637-43.

241. Shao, J., et al., *A microfluidic chip for permeability assays of endothelial monolayer.* Biomed Microdevices, 2010. **12**(1): p. 81-8.

242. Young, E.W., et al., *Technique for real-time measurements of endothelial permeability in a microfluidic membrane chip using laser-induced fluorescence detection.* Anal Chem, 2010. **82**(3): p. 808-16.

243. Imura, Y., et al., *A microfluidic system to evaluate intestinal absorption.* Anal Sci, 2009. **25**(12): p. 1403-7.

244. Douville, N.J., et al., *Fabrication of two-layered channel system with embedded electrodes to measure resistance across epithelial and endothelial barriers.* Anal Chem, 2010. **82**(6): p. 2505-11.

245. Ferrell, N., et al., *A microfluidic bioreactor with integrated transepithelial electrical resistance (TEER) measurement electrodes for evaluation of renal epithelial cells.* Biotechnol Bioeng, 2010. **107**(4): p. 707-16.

246. Nalayanda, D.D., et al., *An open-access microfluidic model for lung-specific functional studies at an air-liquid interface.* Biomed Microdevices, 2009.

247. Sun, T., et al., *On-chip epithelial barrier function assays using electrical impedance spectroscopy.* Lab on a Chip, 2010. **10**(12): p. 1611-1617.

248. Hediger, S., et al., *Biosystem for the culture and characterisation of epithelial cell tissues.* Sensors and Actuators B-Chemical, 2000. **63**(1-2): p. 63-73.

249. Hediger, S., et al., *Modular microsystem for epithelial cell culture and electrical characterisation.* Biosens Bioelectron, 2001. **16**(9-12): p. 689-94.

250. Booth, R. and H. Kim, *Characterization of a microfluidic in vitro model of the blood-brain barrier (muBBB).* Lab Chip, 2012. **12**(10): p. 1784-92.

251. Esch, M.B., et al., *Characterization of in vitro endothelial linings grown within microfluidic channels.* Tissue Eng Part A, 2011. **17**(23-24): p. 2965-71.

252. Gaspar, S., et al., *Simultaneous impedimetric and amperometric interrogation of renal cells exposed to a calculus-forming salt.* Analytica Chimica Acta, 2012. **713**: p. 115-20.

253. Nan, Y.S., et al., *Different effects of dibutyryl cAMP on monolayer permeability in human aortic and coronary arterial endothelial cells.* African Journal of Microbiology Research, 2012. **6**(5): p. 897-903.

254. Khademhosseini, A., et al., *Microscale technologies for tissue engineering and biology.* Proceedings of the National Academy of Sciences of the United States of America, 2006. **103**(8): p. 2480-2487.

255. Letourneau, S., et al., *Evaluating the effects of estradiol on endothelial nitric oxide stimulated by erythrocyte-derived ATP using a microfluidic approach.* Anal Bioanal Chem, 2010. **397**(8): p. 3369-75.

256. Olearczyk, J.J., et al., *NO inhibits signal transduction pathway for ATP release from erythrocytes via its action on heterotrimeric G protein Gi.* American Journal of Physiology, 2004. **287**(2, Pt. 2): p. H748-H754.

257. El-Ali, J., P.K. Sorger, and K.F. Jensen, *Cells on chips.* Nature, 2006. **442**(7101): p. 403-11.

258. Skelley, A.M., et al., *Microfluidic control of cell pairing and fusion.* Nat Methods, 2009. **6**(2): p. 147-52.

259. Paguirigan, A.L. and D.J. Beebe, *Microfluidics meet cell biology: bridging the gap by validation and application of microscale techniques for cell biological assays.* BioEssays, 2008. **30**(9): p. 811-21.

Chapter 2 - Development of a Microfluidic Device Capable of Measuring TEER

2.1 - TEER Measurements on a Microfluidic Vascular Mimic

Studying vascular wall biology and interactions with blood components is an important area of research due to the prevalence of cardiovascular diseases in which these interactions are implicated in disease progression. Efforts to understand the cardiovascular system has led to the development of vascular models that replicate conditions found *in vivo*. The goal of these models is to simplify the system so that a more detailed and convenient analysis can be performed with focus placed completely on certain components of the system that are convoluted in whole organisms. In an *in vivo* situation, flowing blood is always surrounded by an endothelial cell monolayer that forms a vascular wall. The endothelial cells and the blood components are continuously interacting in a dynamic fashion via cell-cell communication where flowing blood is able to elicit endothelial cellular responses, and the endothelial cells are also capable of influencing cellular behavior of various blood components. Examples of important biological events caused by these interactions between different cell types in the vascular system are continually emerging. These interactions between various cell types are biologically important and, as a result, a drive for the development of technologies capable of elucidating the mechanisms of cell-cell communications is underway. Also, cell types that are found in close proximity *in vivo* are often cultured together *in vitro* so that interactions between the cells are accounted for, yielding more physiologically relevant cellular responses and, therefore, increasing the validity of experimental results.

TEER measurements have been universally established as a non-invasive and reliable method for evaluating and monitoring the growth of cellular monolayers. As such, a simple way of performing TEER measurements on *in vitro* biological systems was made commercially available by World Precision Instruments in the mid-1980's as discussed previously in section 1.1.3. A version of this instrumentation is still available and is commonly used for cell based assays. This TEER system was previously integrated into microfabricated cell culture systems in an important step towards integrating TEER measurements with microfluidic technology.[1, 2] Unfortunately, the resulting microsystem did not allow for flow, an important requirement for adequately mimicking certain biological systems as discussed in section 1.3.2.

Microfluidic systems have recently proven useful for mammalian cell culture and cell-based assays,[3-6] including the culture and subsequent cellular assay of cell types found in the vasculature.[5, 7-10] The inherent geometries and dimensions of microfluidic systems are well suited for mimicking *in vivo* physiological conditions and monitoring cell behavior within these microenvironments. An *in vitro* cell layer mimic capable of incorporating flow, and other biologically relevant cells, such as the RBC, would be paramount for mimicking a true vascular barrier. However, the various cells would have to be in close proximity to allow for cell-cell communication. These issues are well addressed through microfluidic systems, as it is possible to mimic the small distance between the blood vessel and the endothelium.[7] Blood flow is also easily accomplished by incorporation of channels that have diameters similar to capillaries.[7] Furthermore, microfluidic systems lend themselves to high throughput techniques,[11-14] and could provide a more realistic model of a vascular wall. Microfluidics have the unique ability to adequately model *in vivo* conditions to the extent that cell-cell

communications can be observed, an ideal property that is absent in many conventional biological mimics.

Microfluidics have recently been utilized for vascular research by our group and others, highlighting the utility of microfluidics as *in vitro* models of the vasculature.[5, 10, 15-20] However, since many vascular mimics include an endothelial monolayer of cells, it is important to remember that cellular responses have been shown to vary with cell monolayer confluence as discussed in Section 1.1. Because of this, a measure of cell barrier integrity, such as TEER determination, is common practice during studies involving cell monolayers, including those often found in models of biological systems, prior to experimentation involving these monolayers. A confirmation of cell monolayer confluence prior to experimentation adds credibility to experimental results by ensuring more physiologically appropriate cellular behavior, which is quite advantageous for elucidating the mechanisms of cell-cell communication where cell responses may be difficult to detect. These benefits offer ample incentive for the integration of a TEER measurement system with a microfluidic vascular model. However, this work illustrates the first microfluidic vascular mimic capable of performing TEER measurements.[21] Perhaps more importantly, this work describes the first microfluidic device capable of measuring TEER that also includes flow capabilities.[22] Since this work began, other examples of microfluidic devices capable of monitoring barrier integrity of various cell types have appeared in the literature, suggesting the potential importance of such devices.[23-25]

2.2 - Methods

2.2.1 - Device Fabrication

Soft lithography techniques are used to produce PDMS slabs from silicon masters. Briefly, silicon masters are spin coated with 4 mL of SU8-50 photoresist (MicroChem Corp.) at 500 rpm for 15 seconds, followed by a 1000 rpm spin cycle for 30 seconds. The wafer is then allowed to rest on a hotplate at 95°C for 15 minutes. A transparency mask is placed over the wafer, and subsequently exposed to UV light for 1 minute for a 100 µm thick feature[26]. The wafer is then transferred again to a hotplate at 95°C for 7 minutes before it is developed in propylene glycol methyl ether acetate (Sigma) to remove excess photoresist. The resulting completed silicon master is suitable for rapid prototyping of PDMS slabs with embedded features. The process for fabricating a silicon master is depicted in Figure 2.1a.

PDMS slabs are prepared by mixing Dow Corning's Sylgard 184 bulk polymer (Ellsworth Adhesives, Germantown WI) with curing agent in a desired ratio by mass. A 20:1 ratio of bulk polymer to curing agent mixture is used where sealing is desired, whereas a more rigid 5:1 mixture is utilized on edges, or wherever a more rigid area was desired. The PDMS mixture is well stirred and then degassed by vacuum prior to pouring onto a silicon master. Each layer of PDMS is subsequently cured by heating for 12 minutes at 75°C.[27] The cured PDMS slab can be removed from the silicon master. Any raised features on the silicon master will be embedded in the PDMS slab. The process of rapid prototyping PDMS slabs from a silicon master is depicted in Figure 2.1b. Outlets and wells are punched in the PDMS slabs using 1/8 in. and 1/4 in. paper hole punches. A 23 gauge luer stub adapter is employed to punch inlets, and then plumbed using 20 gauge stainless steel tubing to allow for connectivity to syringe pumps. After the microfluidic device is constructed, it is irreversibly sealed by heating for 30 minutes at 75°C.

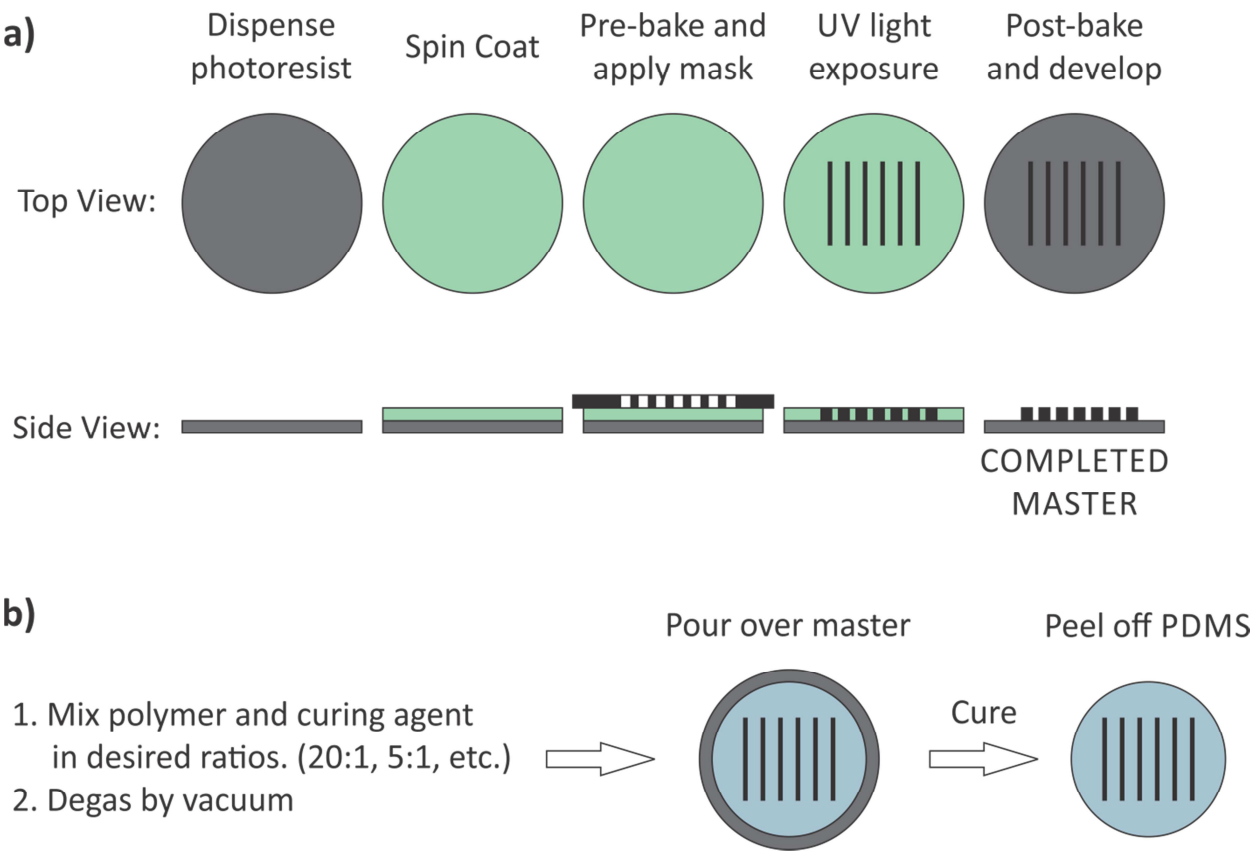

Figure 2.1 - Soft lithography techniques are used for the rapid prototyping of PDMS slabs from silicon masters. Briefly, as shown in (a), a silicon wafer is spin-coated with SU-8 photoresist, and a negative mask is placed over the photoresist prior to UV light exposure. The photoresist exposed to light cross links to form a rigid polymer structure, and the remaining SU-8 polymer is dissolved by a developing agent, resulting in a silicon master with raised features. As shown in (b), PDMS polymer and curing agent is mixed in a desired ratio and degased prior to pouring over the silicon master. The PDMS is then cured at 75° C for 15 minutes and subsequently removed from the master, yielding a PDMS slab with embedded features.

The construction of the microfluidic device requires three PDMS slabs as shown in figure 2.2. The middle slab of PDMS has channels whose dimensions are 200 µm wide by 100 µm tall, which are prepared using standard soft lithographic techniques as described above. At one end of each channel, inlets are punched, and in the center of each channel, a 1/8 in. hole is punched to act as a well. The top PDMS slab has no channels or other features, but does contain two columns of wells, one column that aligns with the wells punched in the center of each channel, and one column that aligns with the end of each channel on the middle slab of PDMS. The column of wells in the center of each channel on the middle PDMS slab is separated by the column of wells on the upper PDMS slab by a polycarbonate membrane. The pore size of the membrane is typically 0.22 µm, but 0.1-1.0 µm pore sizes have been used in our group. The column of wells on the upper PDMS slab lying above the end of the channels on the middle PDMS slab act as waste wells for excess solution that has passed beneath the polycarbonate membrane. An aluminum strip is placed underneath the column of wells that are punched in the center of the channels on the middle PDMS slab. The aluminum strip is then sealed in place with a bottom slab of PDMS that has been halved using a scalpel, also without any channels or other features. The bottom slab of PDMS is cut in half in order to allow access to the inlets that are punched in the middle slab of PDMS, which is required for plumbing of the channels.

The aluminum strip running beneath each of the membranes serves as a stationary common electrode that is sufficient for TEER measurements across every membrane. The well punched in the center of each channel on the middle PDMS slab allows solution that is flowing through the channel to contact the electrode. The electrode can be polished by sanding the electrode surface with a Dremel tool to remove debris and subsequently reused.

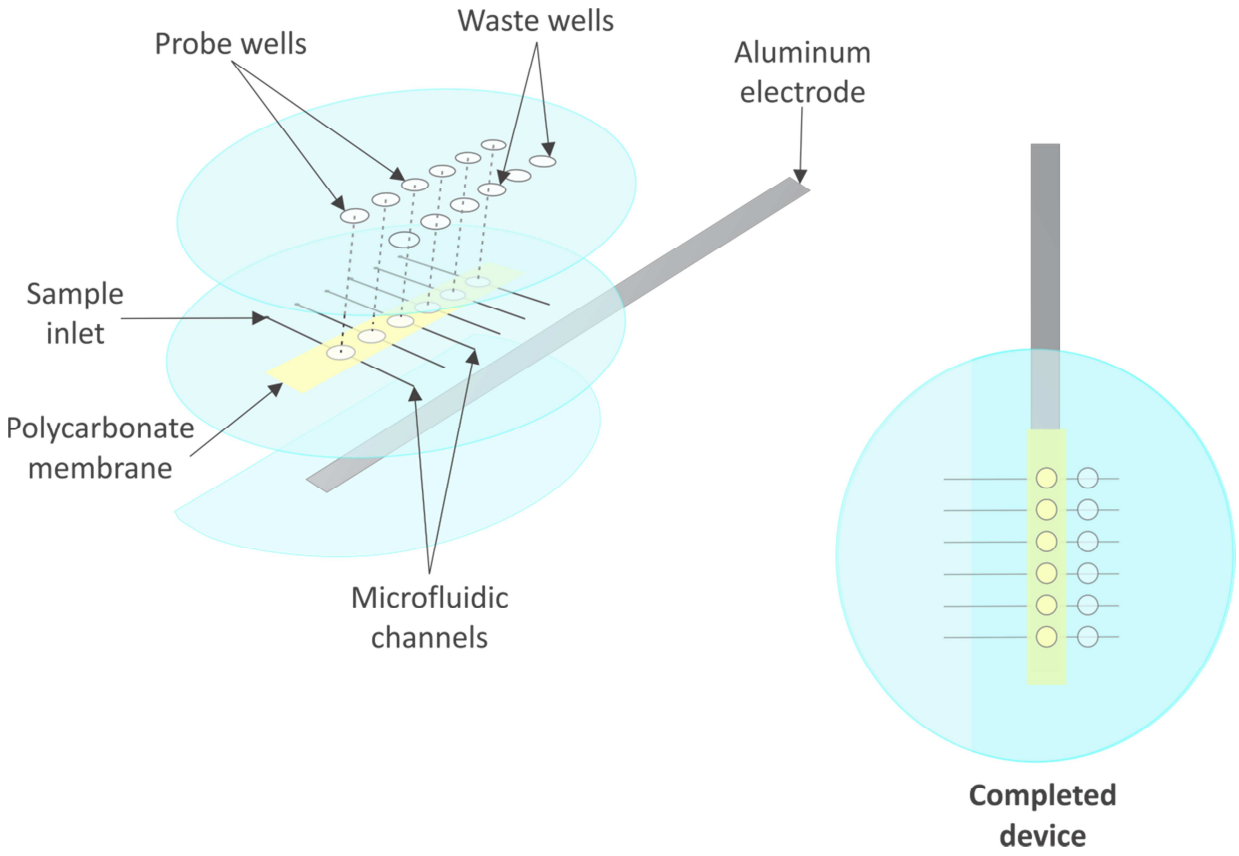

Figure 2.2 - The microfluidic TEER device is fabricated from 3 PDMS slabs. The device contains a series of flow channels integrated with a common electrode below the cell layer, which is cultured on the polycarbonate membrane. A second copper top electrode (not pictured) is placed in the wells of the top layer of PDMS to perform a TEER measurement directly across the cell monolayer.

2.2.2 - Pumping and Attachments

Syringe pumps (Harvard Apparatus) are employed to drive 500 µL Hamilton Gastight syringes for controlled flow of solution in the microfluidic channels. Tygon tubing is interfaced to the syringes using an adapter connecting a male luer syringe to a female 1/16 in. compression fitting (Upchurch/IDEX scientific). The Tygon tubes are interfaced with the microfluidic device using 20 gauge stainless steel tubing (New England Small Tube Company), which fits securely into both the Tygon tubing and the microfluidic inlets described in 2.2.1.

A top electrode consists of a 16 gauge copper wire that has been secured with epoxy to a pipet tip, forming a disk electrode. The epoxy is used to secure the wire in the pipet tip to prevent capillary effects of the solution and likely improving the reproducibility between measurements by maintaining a constant effective electrode area (area of the electrode allowed to contact solution). The top electrode is then clamped in place using a ring stand, and the microfluidic device is raised until the top disk electrode rests inside of the well in which a TEER measurement is desired. The outer diameter of the pipette tip and the inner diameter of the 1/8 in. well are nearly identical, so the electrode rests directly in the center of the well for every measurement.

2.2.3 - bPAEC Culture

Bovine pulmonary artery endothelial cells (bPAEC) are purchased from Lonza and arrive frozen. They are cryogenically frozen for storage, and are thawed to room temperature and then added to a T-75 tissue culture flask containing 12 mL of cell culture media that has been equilibrated at 37°C. Cell culture media is prepared from Lonza's EGM MV media containing 5% fetal bovine serum with gentamicin and phenol red. Subsequently, bPAECs are incubated at 37

°C and 5% CO_2 atmosphere until confluence is reached. Media is changed the day after plating the cells, and then every two to three days thereafter. When the cells reach approximately 80% confluence as identified by optical microscopy, subculturing is performed.

Seeding cells in the wells of a microfluidic device is accomplished by first coating the polycarbonate membrane with fibronectin. Fibronectin (Invitrogen) is dissolved in phosphate buffered saline (PBS) to prepare a 1000 μg/mL stock solution. The stock solution is aliquoted and frozen until use. When cell seeding is desired, an aliquot of stock solution is thawed and diluted to 100 μg/mL and 10 μL of solution are added to each microfluidic well. The solution is allowed to completely evaporate to yield a fibronectin coating on the polycarbonate membrane.

bPAECs are cultured in T-75 tissue culture flasks, and are removed by pipetting 2 mL of a 0.25% trypsin solution onto the cells and incubated for 2 minutes. The trypsin solution is removed by aspiration and immediately replaced with 6 mL of cell media. The cells are repeatedly rinsed and the bottom of the flask is gently rapped to promote removal of the adhered cells. The resulting cell suspension is centrifuged at 500 *g* for 5 min. and the supernatant removed. The cells are then resuspended in 1 mL of cell media and 10 μL of the suspension are added to each well of the microfluidic device. Cell media is replaced after 1.5 hours, and then again every 3 hours afterwards. If the cells are allowed to incubate overnight, 18 μL of cell media are added to each well, and the device is stored in a covered petri dish with a Kimwipe saturated with water in order to prevent evaporation of the cell media. Media is also replaced prior to each TEER measurement in order to maintain electrolyte concentration in the electrochemical cell for each measurement.

2.3 - Results

2.3.1 - TEER Measurement Method Development

A custom LabView (National Instruments) program was written in-house and implemented to perform TEER measurements. The software applies a 20 Hz square wave with a magnitude of 0.75 V across the membrane for 2 seconds as shown in Figure 2.3a. This potential is applied using the analog output of a DAQ board (National Instruments), and the resulting current is measured at an acquisition rate of 1000 Hz. The resultant current signal (Figure 2.3b) is then analyzed via MATLAB (Mathworks), automatically performing curve fitting and integration in real time. The resultant current signal is averaged and integrated to provide charge, which is plotted as a function of time as in Figure 2.4.

A typical TEER device, discussed in section 1.2.3, is comprised of a small volume cup that contains a membrane. This cup then sits in a larger well and, when both are filled with liquid (e.g., a physiological buffer), a voltage can be applied and the current passing through the membrane can be determined. Specifically, a standard TEER measurement is performed with a four electrode system, and consists of an instrument that applies a potential through a battery-powered square wave generator at approximately 12 Hz. Additional sensing electrodes are employed to measure the resulting current through a built-in traditional multimeter.

To simplify fabrication of our device and eliminate the need for four electrodes, the device shown in Figure 2.2 was constructed. Current resulting from a potential applied across cellular monolayers cultured in the wells of the completed device can be measured and characterized. When the system is operational with added electrolyte solutions and endothelial cell layers

cultured upon the polycarbonate membranes, it can be modeled as an RC circuit. As such, applying a steady potential should yield a current profile as predicted by Equation 2.1,

$$I(t) = I_o e^{-\frac{t}{RC}} \tag{2.1}$$

where I is current, t is time, I_o is the initial current, R is resistance, and C is capacitance. The resulting current decays were averaged and integrated with respect to time, the result of which is the average charge passed through the circuit in a single pulse as described by equation 2.2

$$\int I \partial t = \frac{\partial Q}{\partial t} + c = \frac{V}{R}. \tag{2.2}$$

where Q is charge, and V is voltage. Equation 2.2 describes the inverse relationship between resistance and average charge. Therefore, TEER values are reported in units of coulombs, which are inversely proportional to resistance, and represent the average charge passed through the electrochemical cell during a single potential pulse as described by Equation 2.2. Due to the inverse relationship of average charge and resistance, the average charge will reach a minimum charge at maximum cell confluence, which is indicative of the maximum resistance measured by commercial systems when maximum cell confluence is achieved.

In order to report an estimate of resistance in the electrochemical cell, total current was determined by

$$Q = \int_0^t I \partial t + c \tag{2.4}$$

where Q is the average charge determined by the TEER system, I is the total current, and ∂t is the time interval of the applied square wave. After the total current is determined, resistance can be determined by

$$R = \frac{V}{I} \tag{2.5}$$

where R is resistance, V is the magnitude of the applied square wave potential, and I is the total current determined by Equation 2.4. While measurements acquired using the microfluidic TEER system introduced in this chapter are typically reported in units of charge, TEER values are conventionally reported in units of ohms·cm^2, which requires normalization to the area of the cultured cell monolayer. In order to accurately determine the area of microfluidic wells, calipers are employed to measure the diameter of each well, from which the cross-sectional area of the well is determined in units of cm^2. It was determined that the microfluidic wells had an average well diameter of 1.76 ± 0.08 mm (n=10 wells), which is used to calculate TEER estimates in Figure 2.6. The TEER data can then be presented in ohms·cm^2, by finding resistance as discussed previously, and multiplying by the area of the microfluidic well.

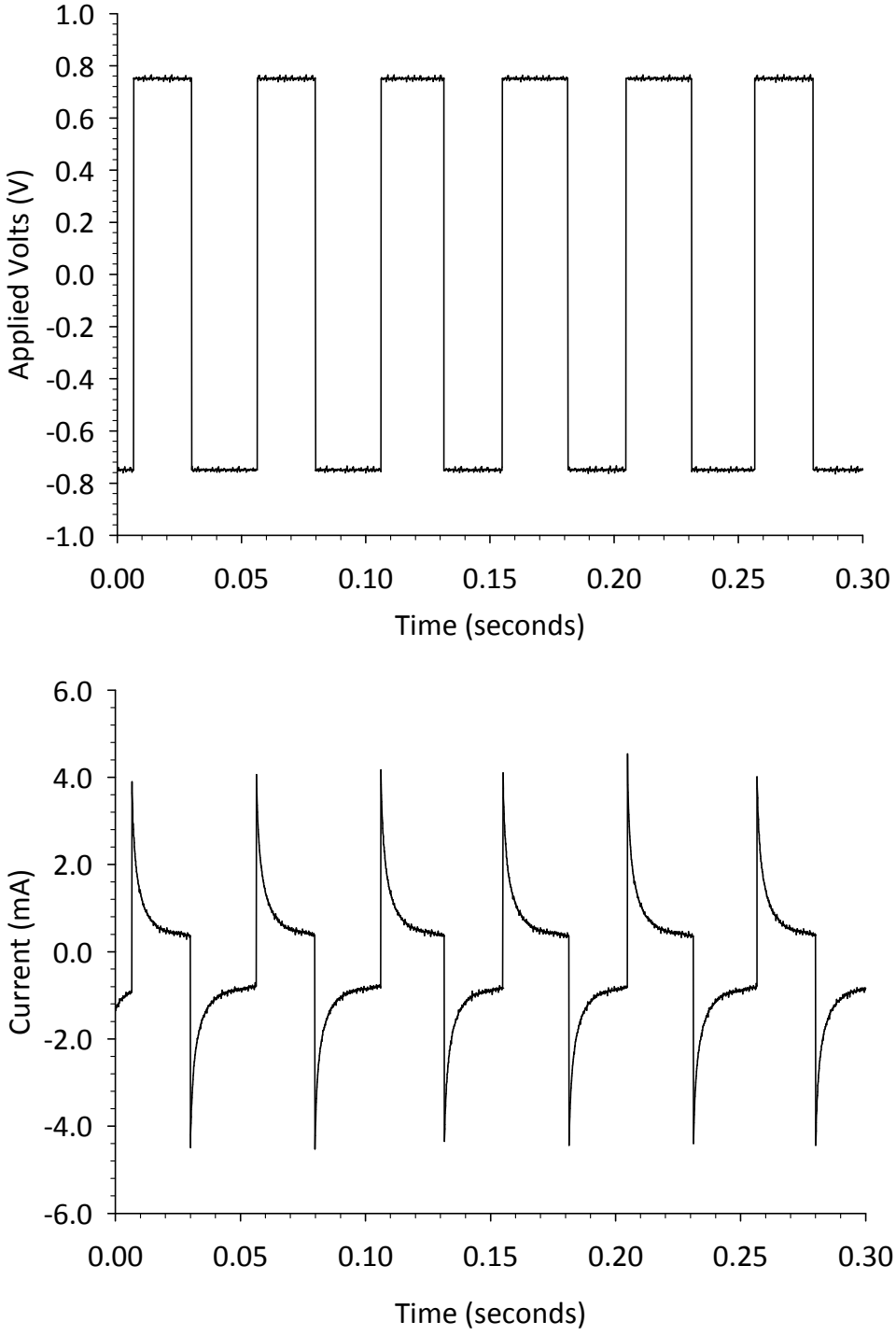

Figure 2.3 - Shown in the top graph is the bipolar pulsed perturbation signal used in the system, a 20 Hz square wave. The resulting current is then measured as a function of time as shown in the bottom graph, yielding current decays that resemble those typically seen in an RC circuit. These current decays are then averaged and integrated, and the resulting charge value is presented as a TEER signal in units of charge.

2.3.2 - Validation of TEER Measurements

The ability to measure resistance using the integrated TEER system was first examined by performing measurements across solutions containing various KCl concentrations. Since salts, such as KCl, completely dissociate in aqueous solutions to form ions, the concentration of ions in the resulting solution is proportional to the amount of salt dissolved, assuming the solvent does not contain ions initially. Therefore, by applying a constant potential across an ionic solution, a resulting current will be induced that can be measured, which is directly proportional to the conductivity of the solution and inversely proportional to solution resistance. The data in Figure 2.3a represents the applied quare wave potentials (ranging from -750 mV to 750 mV at 20 Hz for 2 seconds), while the data in Figure 2.3b is the resultant current decay profiles that coincide with the applied potentials. Charge is obtained by averaging the current decays resulting from the 20 negative applied potential pulses, and integrating with respect to time. The curve in Figure 2.4 shows charge plotted as a function of KCl concentration above and below the membrane. Summarily, as the salt concentration increases in the device, the current passed per potential pulse increases, resulting in an increased charge as shown in 2.4. The waveforms shown in 2.3a, the current profiles in 2.3b and the resultant integration of averaged area in 2.4 were all performed using the computer controlled interface to generate the waveforms, collect the resultant current data, and analyze the data.

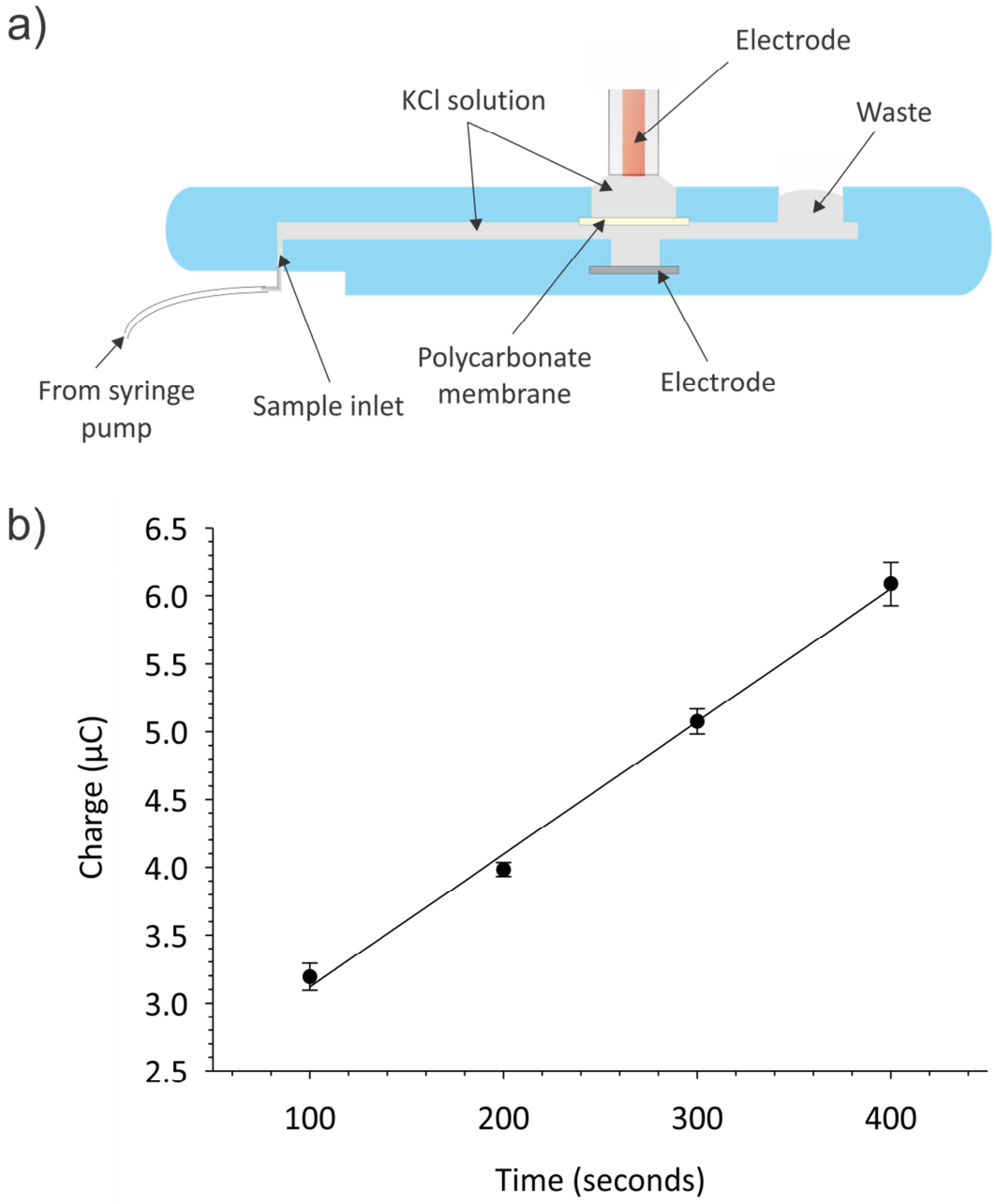

Figure 2.4 - A cross-sectional view of the microfluidic device is shown in (a). Solutions containing various concentrations of potassium chloride (KCl) are pumped into the channels of the microfluidic device, and a solution of the same concentration is pipetted into the overlying wells. TEER measurements are shown to correlate linearly with KCl concentration in (b), displaying the ability of the device to measure conductance, which is inversely proportional to resistance, and therefore indicative of resistance between the two electrodes. (n=4, errors are SD)

The methods for performing conventional TEER measurements using microtiter based techniques vary somewhat from the methodology we used to accomplish TEER measurements on a microfluidic platform. For instance, microtiter based measurements utilize a four electrode system in order to eliminate junction potentials. The necessity to simplify the system in a smaller microfluidic based platform required the incorporation of only two electrodes, so junction potentials are present in the microfluidic system. Additionally, a two electrode system restricts the addition of a proper reference electrode. These inherent differences account for TEER values being reported in units of coulombs, which are easier to calculate in our case, and are still a satisfactory measurement of barrier integrity, and relative changes in that integrity, as shown in Figure 2.5. However, the data is also presented in Figure 2.6 using conventional TEER units of ohms·cm^2.

2.3.3 - Monitoring bPAEC Monolayer Barrier Integrity on a Microfluidic Device

After it was determined that the total charge passed correlated with conductivity of an electrochemical cell, the device was employed to estimate confluence of a monolayer of bPAECs. In order to culture the cells within the wells of the microfluidic device, a fibronectin coating was first added to the polycarbonate membrane representing the bottom of the well to promote cell adhesion, as described in section 2.2.3. Cells are then added to each well, and cell barrier integrity is monitored by performing TEER measurements as the cells become confluent. A side view of the device with the cells in place on the polycarbonate membrane is shown in figure 2.5. After seeding on the membrane, the bPAECs were given time to adhere to the fibronectin matrix. During adhesion, the cells ability to develop into a confluent layer was monitored at various time points using the integrated TEER measurement system. The

resulting data, shown in Figures 2.5, demonstrates that the cells are able to form a more resistive barrier with time, reaching a plateau after approximately 8 hours. Initially, after cell seeding on the fibronectin-coated membrane, the applied potential resulted in approximately 22.3 ± 1.6 μC (40.9 ± 2.9 ohms·cm^2). However, after 8 h, this value dropped to 3.5 ± 0.4 μC (259.1 ± 27.4 ohms·cm^2), a statistically significant decrease ($p<0.001$, $n = 4$ devices). A statistically non-significant change between 8 h and 17 h suggested that the cells had reached an optimum resistivity.

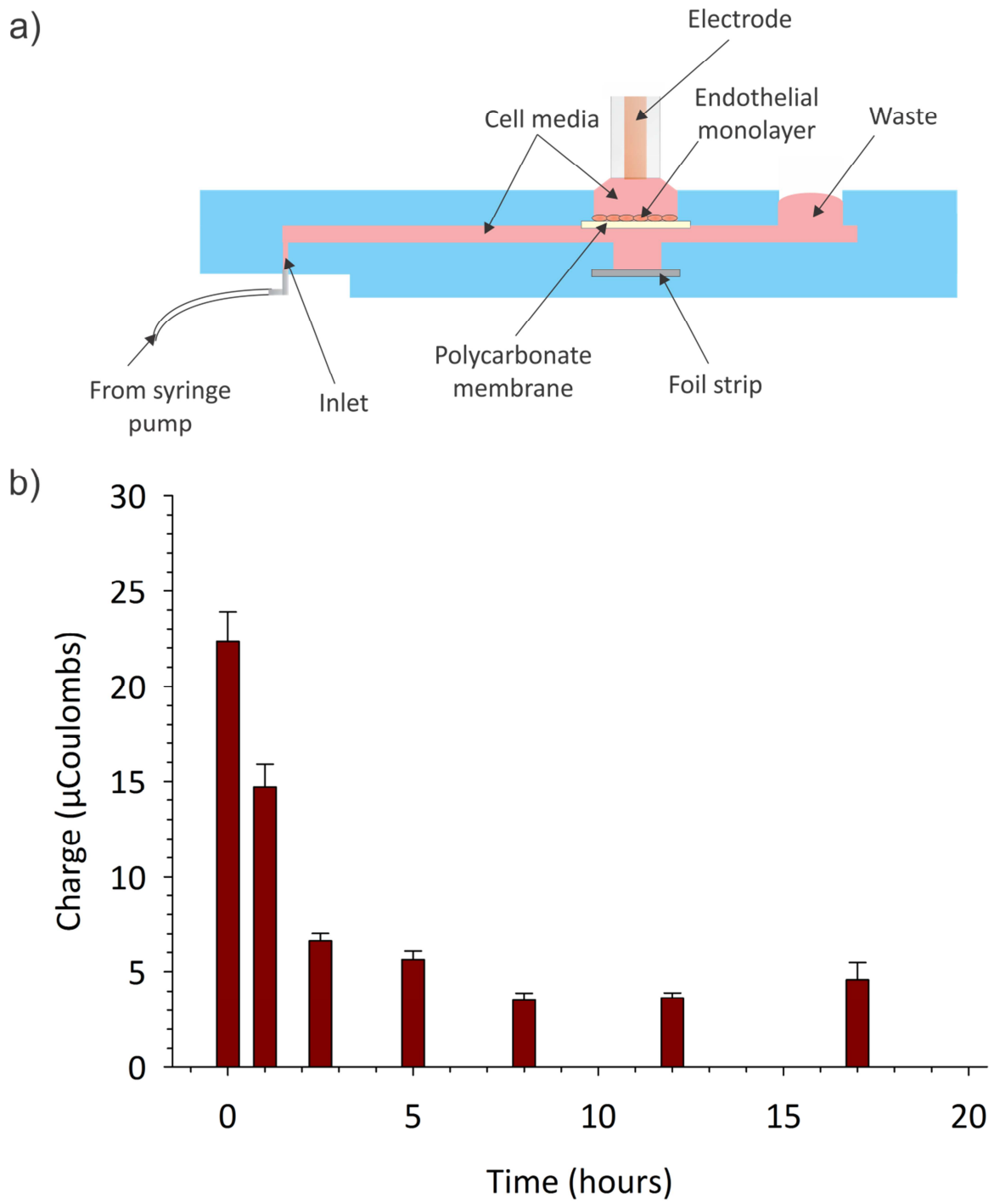

Figure 2.5 - A cross-sectional view of one channel of the microfluidic device, where TEER measurements are performed directly across an endothelial monolayer cultured on a polycarbonate membrane. Shown in (b) are the results of TEER measurements performed on endothelial cells over the course of 17 h in units of µCoulombs, demonstrating the cells reach confluence at approximately 8 h. (n=4, errors are SD)

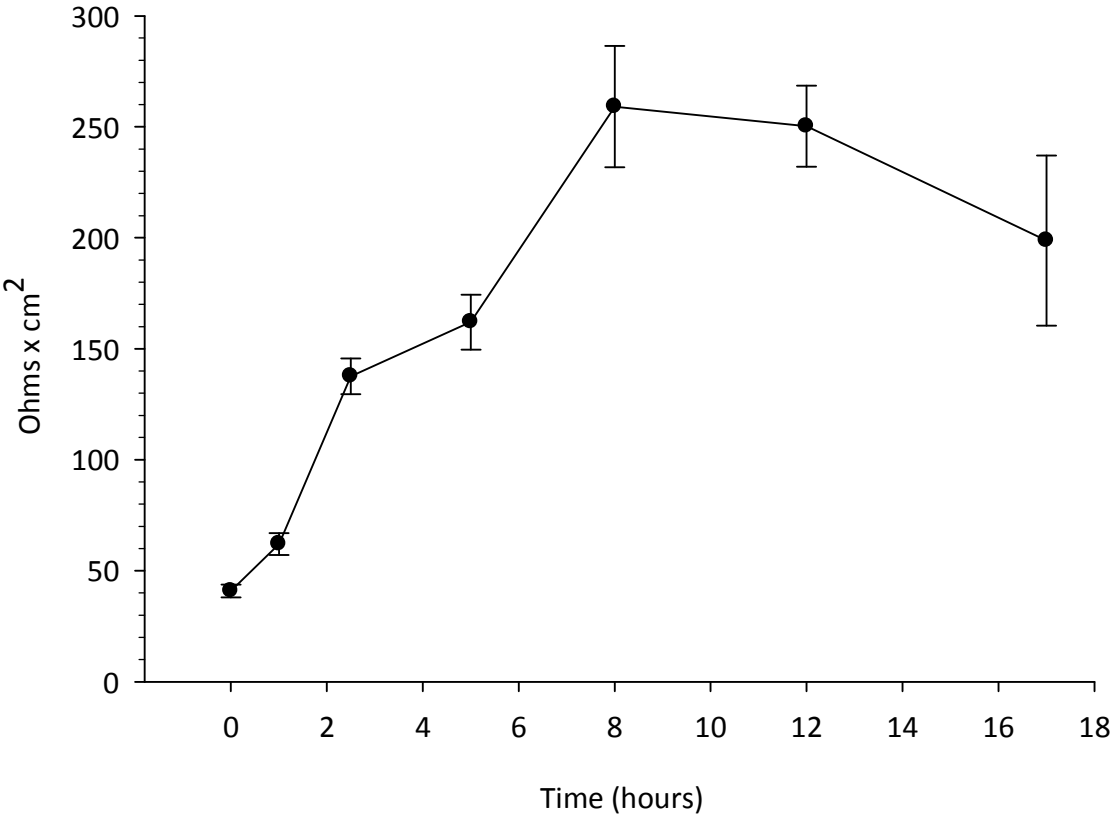

Figure 2.6 - TEER measurements performed on endothelial cells over the course of 17 h are reported in conventional TEER units of ohms·cm^2. These values are estimated from the TEER measurements displayed in Figure 2.5b. These results again demonstrate that the cells reach confluence at approximately 8 h, as suggested by the peak in TEER signal at that time. (n=4, errors are SD)

2.4 - Discussion

The method for constructing the microfluidic device is depicted in Figure 2.2. Utilizing a single aluminum strip as a single electrode for each microfluidic well eliminated the need for including an individual electrode for every microfluidic well, simplifying the design and software requirements compared to other microfluidic devices capable of TEER measurements that have emerged since the development of our device.[23, 24, 28] Additionally, minimizing the number of individual electrodes also eliminates the need to make numerous electrical connections, simplifying experimental setup while decreasing the probability of errors that arise from device handling and interfacing the device to external hardware. Designing the microfluidic TEER device in a non-complex manner was intentional so that the device can be easily reproduced and implemented for work in our laboratory, and in other research laboratories that intend to culture cell monolayers in microfluidic devices. Also, since the device can be fabricated and utilized simply and quickly, with minimal experimental setup and automated data collection and analysis, the device can be prepared and used by researchers with only modest experience in microfluidics.

In general, microfluidics are evolving towards more intricate devices that can be used for complicated analyses involving increasingly complex research interests. As a result, microfluidic devices are better suited for solving sophisticated and interesting questions in research, but often entail a complicated and timely fabrication procedure that can only be accomplished by microfluidics experts. Additionally, microfluidic devices that include sophisticated design features requiring difficult and time consuming fabrication processes often limits the widespread use of the technology. Furthermore, important experimental results are often

convoluted by complex microfluidic designs, as is the likelihood of device errors arising from design flaws. For these reasons, the microfluidic TEER device was designed simply, however it is still capable of performing complex analyses to study multifaceted research problems as shown by experimental results obtained by the device over the course of this work. Fortunately, the microfluidic device presented in this work can be constructed relatively quickly, requiring only 3-4 hours for fabrication, and is comprised of materials, such as PDMS, that are well studied and frequently used in microfluidics. The microfluidic design showcased in this work was, however, modified to maximize simplicity, reliability and reproducibility of the devices.

In order to fabricate the device, PDMS was selected as a fabrication material for several reasons. Firstly, the device is intended to contain biological samples containing live cells, which require a supply of gases, such as oxygen and carbon dioxide, in order to survive and behave properly.[29] Healthy cell culture is most amenable in PDMS microfluidic devices because it is a non-toxic, gas permeable polymer that does not compromise cell health by restricting the diffusion of gases to and from cells within the device. Also, PDMS is well-studied and frequently used for microfluidic device construction because soft lithography permits highly detailed microfluidic features and rapid prototyping.[30] PDMS is also optically clear, enabling optical measurements.

Furthermore, track etched polycarbonate membranes were selected as a cell culture support because the support should be porous, allowing for diffusion of molecules between the flowing solution and the cultured cells, which is required for cell-cell communication and permeability assays. Additionally, polycarbonate membranes have been integrated into PDMS

microfluidic devices for years in the Spence group.[20] These aspects of the device remained unchanged during development of the device.

Microfluidic devices with integrated electrodes commonly entail a complicated design in order to successfully incorporate the electrodes, as well as lengthy fabrication times (on the order of days). However, the benefits provided by the ability to measure TEER in a vascular mimic provide incentive to overcome these challenges. Integration of the TEER system ultimately increased the quality of experimental results obtained using the device, and also addressed the overall absence of TEER measurements in microfluidic research. Initially, the device was constructed with wire electrodes sealed in PDMS that addressed each channel individually, a design that was modified for several reasons. Additionally, each wire had to be interfaced to external hardware sequentially, which forces repeated handling of the device and often compromised structural integrity. Here, the design was improved by using a single wire that ran perpendicular to the channels so that each well could be addressed using one electrode, similar to the aluminum electrode in the optimized final design, which reduced fabrication time, device complexity, and handling during experiments. Unfortunately the resulting microfluidic device was unreliable because upon solution contacted with the wire, the solution would leak along the length of the wire due to capillary effects resulting from the inability to completely seal a round wire in a PDMS microfluidic device.

The issues that arise by attempting to seal a metal electrode in PDMS were also encountered by others when constructing a microfluidic TEER device.[23] The problem was ultimately resolved by adding a channel to the PDMS design that was completely dedicated to containing the wire. The wire is pushed into the channel, and the voids in the channel

surrounding the wire were filled with uncured PDMS mortar by syringe injections. The wire was then able to be secured into place after the completed device was cured. This method successfully resolves the issue, but requires a complicated fabrication procedure coupled with a long fabrication time where the device must be allowed to cure overnight for two consecutive nights. This issue was alternatively avoided this work by choosing an aluminum foil as an electrode material because it is able to lie flush between two PDMS slabs, and with a thickness of less than 200 μm, adequate sealing is accomplished. The width of the aluminum foil strip is also always prepared in dimensions so that the width of the foil is greater than that of the overlying wells. This helps prevent leakage in the device, and ensures that the electrode area that makes contact with the solutions contained in the channels is as similar as possible from channel to channel, leading to more reliable and reproducible TEER measurements.

The electrode areas resulting from using foil instead of wire were greatly increased. The average effective electrode areas of the bottom electrodes in the microfluidic device are a result of the size of well that is punched in the center of each channel. These wells are punched with a 1/16 in. hole punch, resulting in an average electrode area of about 2.4 mm^2. The resulting macroelectrodes are often avoided in electrochemistry due to the production of large charging currents required to form a double layer at the electrode surface. These charging currents are sometimes so large that any faradaic current is not observable, which is not ideal when using faradaic current to determine characteristics of an electrochemical cell, such as resistance. However, the perturbation potential used in the TEER system, displayed in Figure 2.4a, is a 20 Hz square wave applied for 2 seconds. Because a potential pulse is applied for only 0.05 sec before being reversed, the resulting current response provides primarily kinetic

information. It is hypothesized that cell monolayer confluence in the electrochemical cell affects the kinetics of faradaic processes, as well as the kinetics of double layer formation, resulting in an ideal situation where even charging current can be used to measure TEER. The validity of this hypothesis is supported by the TEER measurements performed using the device where successful determination of conductivity and cell monolayer barrier integrity were accomplished as shown in Figures 2.4 and 2.5, respectively. In a situation that is unique to our microfluidic TEER system due to our measurement methods, the integration of macroelectrodes in the device design was acceptable since charging current can be used in addition to faradaic current the determine TEER. For these reasons, we were able to forego the complications of integrating microelectrodes into the device, such as sealing wires in PDMS.

Interestingly, the applied perturbation potential, shown in Figure 2.4a, was not chosen because of the advantages discussed previously, but rather for three other reasons. Firstly, the measurement technique was implemented as one of the first successful methods for determining resistance in a small electrochemical cell, including the microscale electrochemical cells that are basically inevitable in microfluidic devices.[31, 32] Secondly, the square wave potential is an ideal choice because it can only polarize the cells for a short time interval, an important feature because polarization of cells for extended periods of time has been shown to influence cell behavior[33, 34], and even cause cell lysis.[35] Lastly, since TEER measurements have become a commercialized and standard measurement technique outside of microfluidic research, we were able to use well established methods to develop our method for determining TEER. A simple way of performing TEER measurements on *in vitro* biological systems was made commercially available by World Precision Instruments in the mid-1980's. A version of this

instrumentation is still available and is commonly used in microtiter based experiments as discussed in section 2.1. The square wave potential applied by the microfluidic TEER system shown closely resembles the perturbation potential used in the commercially available TEER system, which applies a 12 Hz square wave potential and measures current to determine TEER. However, the methodology used to determine TEER in the microfluidic system varies somewhat from the traditional TEER device, where a four electrode system is employed to determine TEER rather than the two electrode system utilized in the microfluidic TEER system.

The development of a two electrode system arose from the necessity to simplify the method on a smaller microfluidic platform. A four electrode system is used in a standard TEER system in order to eliminate junction potentials, which are present in the microfluidic TEER device. Also, the resistance in an electrochemical cell in response to an amperometric potential is typically determined by analyzing steady state current. However, for reasons discussed previously, the nature of the applied square wave potential restricts the system from reaching a steady state. Consequently, estimations of resistance in the microfluidic electrochemical cell are determined when the system is kinetically controlled and charging current contributes to the current. As a result of these differences, we can only estimate TEER in units of ohms·cm^2 because determination of resistance is required. Regardless, TEER data is presented in ohms·cm^2 in figure 2.6 in an effort to compare our system to traditional measurements, resulting in measurements similar to literature values.[36, 37] Even as estimates of TEER values with units of ohms·cm^2 tend to match literature values, presenting TEER values in units of μCoulombs avoid estimation, and still provide a measurement of cell monolayer confluence, and changes in that confluence, as shown in Figure 2.5.

The current response to the applied square wave in Figure 2.4b resembles a current decay commonly seen in a typical RC circuit. These types of responses to a constant DC potential are common and well characterized, allowing for simple isolation of important properties of the electrochemical cell as discussed in section 2.3.1. Due to the predictability of the current response observed, the manipulation of data to determine TEER values was able to be completely automated allowing for the development of a simple user interface in which a TEER value can be determined in seconds without the need for additional manipulation of data.

The data presented in Figure 2.5 displays the ability of the microfluidic device to successfully perform measurements to quantitatively determine conductance in an electrochemical cell. A microfluidic system capable of measuring conductance is not novel, but it is a powerful tool used previously in vascular mimics, primarily to isolate rare cells from circulating blood samples.[38] The purpose of determining the conductance of our microfluidic electrochemical cell was to verify that our specific method for determining TEER was valid, as the technique for determining conductance in the microfluidic device is the same as used to determine TEER. The ability to measure conductance with a wide linear range indicates that the software employed to perform TEER measurements, as well as the microfluidic design, was robust enough to interrogate the barrier integrity cell monolayer.

The data presented in Figures 2.5 and 2.6 demonstrates the capacity for quantitatively determining endothelial cell barrier integrity using the microfluidic TEER system. The initial TEER measurement at 0 hours was taken immediately after the cells had been added to the microfluidic well, and before seeding on the fibronectin network was possible. This initial TEER measurement yielded an average charge of 22.3 ± 1.6 μC (or 40.9 ± 2.9 ohms·cm^2) , a value over

6 fold greater than that obtained at 8 hours of 3.5 ± 0.4 μC (or 259.1 ± 27.4 ohms·cm^2) when the cells had reached optimal confluence. These findings illustrate the sensitivity of the TEER system, and the ability to detect slight variations in cell monolayer confluence. Furthermore, a non-statistical change in TEER measurements obtained from 8 h to 17 h shows that the bPAEC monolayer had reached an optimal confluence that was verifiable by the device. Prior to the these findings, our group would allow 1.5 to 2 hours for bPAEC seeding on microfluidic devices, which does not allow for complete confluence according to the data in Figure 2.5. After obtaining this data, cells were allowed to seed overnight to ensure confluence, which greatly increased the reproducibility of cell based experiments in our lab.

An additional important feature of the device, aside from the ability to measure TEER, is the ability to culture endothelial cells that are separated in a biologically relevant distance from a capillary that allows for the flow of solution, such as a blood sample, producing a potential microfluidic vascular mimic. The ability to mimic the vasculature using microfluidics has been accomplished previously[20, 39, 40], however this work is the first example of a microfluidic vascular mimic capable of measuring TEER.[21] Utilization of the microfluidic TEER device as a vascular mimic will be the topic of the upcoming chapters. Since publication of this work, one other microfluidic vascular mimic capable of performing TEER measurements has appeared in literature[28], re-emphasizing the importance of confirming and monitoring cell monolayer integrity, even in microfluidic devices. Since the primary incentives for inventing the device was to perform endothelial permeability studies and to study cell-cell communication between flowing RBCs and a vascular wall comprised of a monolayer of endothelial cells, integrating TEER measurement capabilities was a priority in the development and fabrication of the device.

Often, when performing research involving monolayers of cells, a quantitative measure of monolayer barrier integrity is essentially prerequisite to any investigation involving the cell layer, an aspect not previously addressed in microfluidic research. Additionally, confirmation of cell monolayer confluence is important for proper cellular behavior as discussed in Section 1.2.4.

Data presented in Figure 2.5 exhibits the ability of the microfluidic device to confirm the barrier integrity of bPAECs, which is a cell type particularly interesting to our group due to our intention to mimic the cardiovascular system. However, other biological research has recently been performed using microfluidics to mimic specific organs, resulting in a new genre of research termed "organ on a chip" research. Organ on a chip research involves employing microfluidic devices in order to create crude reproductions of important organs, ideally reducing the need for animal models. Several microfluidic organ mimics have been accomplished, including the lung[41], kidney[42, 43], heart[44], and digestive system[45]. Importantly, all of these models join numerous previously developed microfluidic systems that require a monolayer of cells. While the importance of verifying cell monolayer confluence prior to experimentation has been well understood for decades[46], an alarmingly small number of microfluidic platforms capable of performing such measurements have been developed, especially considering that cell monolayers have been cultured in microfluidic devices for over a decade.[47] Hypothetically, the lack of microfluidic devices capable of performing these simple measurements is due to the engineering challenge of including the required components in a microfluidic platform. Therefore, a simple method for including TEER measurement capabilities in microfluidic experiments where cell monolayers are required would be paramount for

confirming the validity of experiments performed. We anticipate that the microfluidic TEER device is capable of performing TEER measurements across cell barriers comprised of any cell, in addition to bPAEC monolayers. The integration of a TEER measurement system would surely aid in validating experiments performed in organ on a chip research and any research involving cell monolayers cultured in microfluidic devices.

2.5 - Conclusions

Summarily, the work presented here describes the fabrication of a novel microfluidic vascular mimic that can determine TEER of endothelial monolayers, providing a reliable and sensitive method for monitoring cell barrier integrity. When performing microfluidic permeability assays, this ability to measure cell monolayer barrier integrity is essentially required to validate results by confirming proper barrier function of the cell layer. Importantly, this novel device is the first example a microfluidic platform with integrated TEER capabilities that also enables flow. Therefore, this device, in contrast to other similar devices, takes advantage of desirable flow characteristics that are typical of microfluidic platforms, and that have led to the widespread use of microfluidics. Furthermore, the flow of solutions through microfluidic channels which are dimensionally similar to resistance vessels is easily accomplished, yielding the first microfluidic vascular mimic with integrated TEER capabilities. These desirable properties are unique to the microfluidic TEER system presented here and, therefore, this device can be used to mimic the vasculature with unparalleled accuracy.

Verifying cell confluence prior to experimentation is crucial to validating results, and since microfluidics have become a popular platform for cellular assays, the device presented here is a powerful tool for providing credibility to microfluidic research involving cell monolayers. Since

the microfluidic TEER system is simply designed and fabricated, integration into other microfluidic platforms used to study cell monolayers should be trivial. Additionally, using the microfluidic TEER system is intuitive since experimental setup is minimal, and obtaining TEER values is completely automated. Also, the device can potentially be integrated with microtiter technology since the microfluidic wells are arranged in an array format, similar to a 96-well plate. In this construct, conventional microtiter instrumentation can be used to perform high throughput cell-based assays, while still taking advantage of the flow and TEER measurement capabilities of the microfluidic device that are not permitted by microtiter platforms. This work provides a simple method for ensuring proper cellular response in a vascular mimic, thus increasing the value and accuracy of experimental results, including the results presented in upcoming chapters. These benefits are particularly favorable when studying cell-cell communication, cell monolayer permeation, or any other cellular response involving the monolayer.

REFERENCES

REFERENCES

1. Hediger, S., et al., *Modular microsystem for epithelial cell culture and electrical characterisation.* Biosens Bioelectron, 2001. **16**(9-12): p. 689-94.

2. Hediger, S., et al., *Biosystem for the culture and characterisation of epithelial cell tissues.* Sensors and Actuators B-Chemical, 2000. **63**(1-2): p. 63-73.

3. Lee, P.J., et al., *Microfluidic System for Automated Cell-based Assays.* JALA Charlottesv Va, 2007. **12**(6): p. 363-367.

4. Barbulovic-Nad, I., S.H. Au, and A.R. Wheeler, *A microfluidic platform for complete mammalian cell culture.* Lab Chip, 2010. **10**(12): p. 1536-42.

5. Tolan, N.V., et al., *Personalized Metabolic Assessment of Erythrocytes Using Microfluidic Delivery to an Array of Luminescent Wells.* Analytical Chemistry, 2009. **81**(8): p. 3102-3108.

6. Yu, Z.T., et al., *Integrated microfluidic devices for combinatorial cell-based assays.* Biomed Microdevices, 2009. **11**(3): p. 547-55.

7. Genes, L., I., et al., *Adressing a Vascular Endothelium Array with Blood Components using Underlying Microfluidic Channels.* Lab on a Chip, 2007. **7**(10): p. 1256-1259.

8. Song, J.W., et al., *Microfluidic endothelium for studying the intravascular adhesion of metastatic breast cancer cells.* PLoS ONE, 2009. **4**(6): p. e5756.

9. Halpin, S.T. and D.M. Spence, *Direct Plate-Reader Measurement of Nitric Oxide Released from Hypoxic Erythrocytes Flowing through a Microfluidic Device.* Analytical Chemistry, 2010. **82**(17): p. 7492-7497.

10. Ku, C.J., T. D'Amico Oblak, and D.M. Spence, *Interactions between multiple cell types in parallel microfluidic channels: monitoring platelet adhesion to an endothelium in the presence of an anti-adhesion drug.* Anal Chem, 2008. **80**(19): p. 7543-8.

11. McClain, M.A., et al., *Microfluidic devices for the high-throughput chemical analysis of cells.* Analytical Chemistry, 2003. **75**(21): p. 5646-5655.

12. O'Neill, A.T., N.A. Monteiro-Riviere, and G.M. Walker, *Microfabricated curtains for controlled cell seeding in high throughput microfluidic systems.* Lab Chip, 2009. **9**(12): p. 1756-62.

13. White, A.K., et al., *High-throughput microfluidic single-cell RT-qPCR.* Proc Natl Acad Sci U S A, 2011. **108**(34): p. 13999-4004.

14. Lecault, V., et al., *High-throughput analysis of single hematopoietic stem cell proliferation in microfluidic cell culture arrays.* Nat Methods, 2011. **8**(7): p. 581-6.

15. Wong, K.H.K., et al., *Microfluidic Models of Vascular Functions.* Annual Review of Biomedical Engineering, 2012. **14**(1): p. null.

16. Srigunapalan, S., et al., *A microfluidic membrane device to mimic critical components of the vascular microenvironment.* Biomicrofluidics, 2011. **5**(1): p. 13409.

17. Kaihara, S., et al., *Silicon micromachining to tissue engineer branched vascular channels for liver fabrication.* Tissue Eng, 2000. **6**(2): p. 105-17.

18. Lim, D., et al., *Fabrication of microfluidic mixers and artificial vasculatures using a high-brightness diode-pumped Nd:YAG laser direct write method.* Lab Chip, 2003. **3**(4): p. 318-23.

19. Borenstein, J.T., et al., *Microfabrication of three-dimensional engineered scaffolds.* Tissue Eng, 2007. **13**(8): p. 1837-44.

20. D'Amico Oblak, T., P. Root, and D.M. Spence, *Fluorescence monitoring of ATP-stimulated, endothelium-derived nitric oxide production in channels of a poly(dimethylsiloxane)-based microfluidic device.* Anal Chem, 2006. **78**(9): p. 3193-7.

21. Vogel, P.A., et al., *Microfluidic transendothelial electrical resistance measurement device that enables blood flow and postgrowth experiments.* Anal Chem, 2011. **83**(11): p. 4296-301.

22. Vogel, P.A., et al., *Microfluidic Transendothelial Electrical Resistance Measurement Device that Enables Blood Flow and Postgrowth Experiments.* Analytical Chemistry, 2011. **83**(11): p. 4296-4301.

23. Douville, N.J., et al., *Fabrication of two-layered channel system with embedded electrodes to measure resistance across epithelial and endothelial barriers.* Anal Chem, 2010. **82**(6): p. 2505-11.

24. Ferrell, N., et al., *A microfluidic bioreactor with integrated transepithelial electrical resistance (TEER) measurement electrodes for evaluation of renal epithelial cells.* Biotechnol Bioeng, 2010. **107**(4): p. 707-16.

25. Young, E.W., et al., *Technique for real-time measurements of endothelial permeability in a microfluidic membrane chip using laser-induced fluorescence detection.* Anal Chem, 2010. **82**(3): p. 808-16.

26. Duffy, D.C., et al., *Rapid prototyping of microfluidic systems in poly(dimethylsiloxane).* Analytical Chemistry, 1998. **70**(23): p. 4974-4984.

27. McDonald, J.C., et al., *Fabrication of microfluidic systems in poly(dimethylsiloxane).* Electrophoresis, 2000. **21**: p. 27-40.

28. Booth, R. and H. Kim, *Characterization of a microfluidic in vitro model of the blood-brain barrier (muBBB).* Lab Chip, 2012.

29. Obradovic, B., et al., *Gas exchange is essential for bioreactor cultivation of tissue engineered cartilage.* Biotechnol Bioeng, 1999. **63**(2): p. 197-205.

30. Qin, D., Y.N. Xia, and G.M. Whitesides, *Rapid prototyping of complex structures with feature sizes larger than 20 mu m.* Advanced Materials, 1996. **8**(11): p. 917-&.

31. Johnson, D.E. and C.G. Enke, *Bipolar Pulse Technique for Fast Conductance Measurements.* Analytical Chemistry, 1970. **42**(3): p. 329-&.

32. Caserta, K.J., et al., *Computer controlled bipolar pulse conductivity system for applications in chemical rate determinations.* Anal. Chem., 1978. **50**(11): p. 1534-41.

33. Kralj, J.M., et al., *Optical recording of action potentials in mammalian neurons using a microbial rhodopsin.* Nat Methods, 2012. **9**(1): p. 90-5.

34. McCaig, C.D., et al., *Controlling cell behavior electrically: current views and future potential.* Physiol Rev, 2005. **85**(3): p. 943-78.

35. Lee, D.W. and Y.H. Cho, *A continuous electrical cell lysis device using a low dc voltage for a cell transport and rupture.* Sensors and Actuators B-Chemical, 2007. **124**(1): p. 84-89.

36. Ali, M.H., et al., *Endothelial permeability and IL-6 production during hypoxia: role of ROS in signal transduction.* Am J Physiol, 1999. **277**(5 Pt 1): p. L1057-65.

37. Wilhelm, I., C. Fazakas, and I.A. Krizbai, *In vitro models of the blood-brain barrier.* Acta Neurobiol Exp (Wars), 2011. **71**(1): p. 113-28.

38. Adams, A.A., et al., *Highly efficient circulating tumor cell isolation from whole blood and label-free enumeration using polymer-based microfluidics with an integrated conductivity sensor.* Journal of the American Chemical Society, 2008. **130**(27): p. 8633-8641.

39. Letourneau, S., et al., *Evaluating the effects of estradiol on endothelial nitric oxide stimulated by erythrocyte-derived ATP using a microfluidic approach.* Anal Bioanal Chem, 2010. **397**(8): p. 3369-75.

40. Huang, J.H., et al., *Rapid Fabrication of Bio-inspired 3D Microfluidic Vascular Networks.* Advanced Materials, 2009. **21**(35): p. 3567-+.

41. Huh, D., et al., *Reconstituting organ-level lung functions on a chip.* Science, 2010. **328**(5986): p. 1662-8.

42. Suwanpayak, N., et al., *Blood cleaner on-chip design for artificial human kidney manipulation.* Int J Nanomedicine, 2011. **6**: p. 957-64.

43. Jang, K.J. and K.Y. Suh, *A multi-layer microfluidic device for efficient culture and analysis of renal tubular cells.* Lab Chip, 2010. **10**(1): p. 36-42.

44. Grosberg, A., et al., *Ensembles of engineered cardiac tissues for physiological and pharmacological study: heart on a chip.* Lab Chip, 2011. **11**(24): p. 4165-73.

45. Kim, H.J., et al., *Human gut-on-a-chip inhabited by microbial flora that experiences intestinal peristalsis-like motions and flow.* Lab Chip, 2012. **12**(12): p. 2165-74.

46. Hart, M.N., et al., *Differential opening of the brain endothelial barrier following neutralization of the endothelial luminal anionic charge in vitro.* Journal of Neuropathology and Experimental Neurology, 1987. **46**(2): p. 141-53.

47. Patel, N., et al., *Spatially controlled cell engineering on biodegradable polymer surfaces.* FASEB J, 1998. **12**(14): p. 1447-54.

Chapter 3 - Monitoring Cell-Cell Communication in a Microfluidic-Based Vascular Mimic

3.1 - Microfluidics to Mimic the Vasculature

As discussed in Chapter 1, vascular wall biology, and interactions with bloodstream components, such as the red blood cell, is an area of continued interest due to the high prevalence of cardiovascular disease and stroke. In order to investigate vascular wall biology with an *in vitro* model, the layer of cells comprising the wall must be confluent, display a restrictive paracellular pathway, high electrical resistance, physiologically relevant cell architecture, and functional expression of transporter mechanisms while being easy to culture.[1, 2] Additionally, a determination of cell confluence prior to experimentation is important because cellular activity (i.e., responses to agonists/antagonists, transport of molecules, etc.) has been shown to vary with cell confluence and integrity.[3-12] While these criteria for an *in vitro* mimic of the vascular wall seem straightforward, reproducing the actual environment found *in vivo* is quite challenging.

Most *in vitro* models reported in the literature are based on stationary cultures or co-cultures (multiple cell types cultured together) to attempt to reproduce the intricate environment of the true vascular barrier. Generally, isolated endothelial cells are cultured within a microtiter insert upon a polycarbonate membrane that has been coated with an adhesion molecule such as fibronectin or collagen to promote cell adhesion to the membrane.[13] The cells are allowed to reach confluence, and the membrane is placed in a diffusion cell where a cell-based assay is performed.[13] These methods are discussed in detail within section 1.1.2. While this methodology has proven useful, the use of buffer in the

diffusion cell and lack of flow on the apical side of the model fail to adequately mimic the microvasculature. In an even simpler experimental design, cell-based assays are commonly performed on cells cultured within wells of a microtiter plate. These methods for studying cell biology are adequate in many situations, resulting in their widespread use, however these platforms again lack important properties required to accurately mimic the vasculature.

Endothelial cells cover all blood contacting areas of the cardiovascular system and, due to their location, are constantly exposed to the hemodynamic shear stress of flowing blood. Shear stress is known to regulate endothelial cell behavior, and is a determinant in the expression of certain cellular responses.[14] It is also known that other cell types, such as the RBC, can alter endothelial cell behavior and vice versa via cell-cell communication.[15-18] Therefore, an accurate vascular mimic should include flow to account for shear stress, multiple cell types in close proximity to account for cell-cell communication, as well as a method for determining cell monolayer confluence to ensure proper cell behavior. Unfortunately, the most commonly used aperture for measurements involving the integrity of a cell layer is the diffusion cell, which does not account for the shear stress due to blood flow, or the presence of blood. The ability to measure cell monolayer integrity, however, is easily accomplished in diffusion cells by measuring TEER or performing permeation studies, which has become common practice.

The shortcomings of conventional vascular mimics are well addressed with microfluidic systems, as it is possible to mimic the small distance between the blood vessel and the endothelium.[19] Blood flow is also easily accomplished by incorporation of channels that have diameters similar to resistance vessels (capillaries and arterioles) found *in vivo*.[19] For these reasons, microfluidic systems have been employed for shear-related endothelial cell

experiments involving cell-cell communication, such as studies on migration[20], adhesion[15], and shear-induced NO production[18]. The advantages of using microfluidic technologies to model the vasculature have been realized as indicated by numerous reports of microfluidic devices capable of mimicking the vasculature.[21, 22] However, the ability to measure cell monolayer confluence on a microfluidic device was yet to be accomplished at the start of this work. Very recently, however, microfluidic devices have been developed to monitor cell monolayer permeation [23] and measure TEER [24, 25], illustrating the importance of such devices.

The integrated microfluidic TEER system reported in Chapter 2 is capable of mimicking the vasculature by enabling the flow of RBCs past an immobilized layer of endothelial cells whose barrier integrity has been characterized by the integrated TEER system. This device is the first microfluidic vascular mimic capable of determining cell monolayer confluence, and also the first microfluidic device capable of measuring TEER that also enables flow.[26, 27] This device provides a vascular mimic with multiple cell types separated by physiological distances, allowing for cell-cell communication. Additionally, this device incorporates flowing blood to account for shear stress, as well as a method for determining TEER to ensure cell monolayer confluence prior to experimentation. Importantly, the TEER measurement capabilities of the device allow for a confirmation of monolayer barrier integrity and confluence of cell layers cultured within the wells of the device prior to experimentation. Measuring TEER to verify layer confluence and barrier integrity prior to cellular investigations helps ensure physiologically appropriate cellular responses of cultured cells, thus improving reproducibility between experiments and also increasing the value and accuracy of experimental results, as well as conclusions stemming

from these results. These benefits are particularly favorable when studying cell-cell communication, cell monolayer permeation, or any other cellular response involving the monolayer. As such, cell monolayer confluence was confirmed prior to experiments carried out during the course of this work.

3.2 - The Potential Role of C-Peptide in Vessel Dilation

C-peptide is a 31 amino acid peptide produced in the pancreas and released in equimolar amounts with insulin as discussed in Chapter 1.[28, 29] In brief summary, for the first few decades after its discovery in the late 1960's, C-peptide was thought to have minimal physiological effects after release into the bloodstream.[30] However, numerous reports since the mid 1990's have confirmed that C-peptide is a bioactive peptide that can have significant beneficial effects in organs, tissue, and even cultured cells such as endothelial cells.[31-33] Studies involving Type 1 diabetic subjects who are unable to naturally produce C-peptide have shown that C-peptide improves nerve conduction and regeneration[34], renal function[35], inflammation,[36] and blood flow[37, 38] via unknown mechanisms.

In vivo, the endothelium plays a vital role in regulating blood flow and pressure throughout the entire vascular system. It is able to produce and release NO, a potent vasodilator that can participate in the relaxation of the smooth muscle cells surrounding blood vessels.[31, 39-41] In smooth muscle cells, NO produced by the endothelium stimulates the activation of soluble guanylyl cyclase (sGC) that converts guanidine triphosphate (GTP) to cyclic guanidine monophosphate (cGMP), resulting in relaxation of the smooth muscle and subsequent dilation of the vessel.[42, 43] Indeed, if C-peptide is capable of stimulating endothelial NO production, it

could account for the C-peptide induced improvement in blood flow observed in Type 1 diabetic subjects.

A relationship between C-peptide and the enzyme responsible for regulating endothelial NO concentration, namely endothelial nitric oxide synthase (eNOS), has been reported in many different types of complications associated with diabetes, as well as in various tissues and organs, both *in vivo* and *in vitro*.[44, 45] Reports of C-peptide-stimulated NO production in the endothelium could have great importance, especially in the pulmonary endothelium, where the flow of RBCs through the pulmonary bed allows re-oxygenation of the RBCs prior to delivery of that oxygen to organs and tissues throughout the body. In accordance with the importance of NO production, Sprague *et al*. has shown that ATP derived from RBCs stimulates NO production in the pulmonary circulation.[46] Interestingly, C-peptide stimulates the release of ATP from RBCs.[47] In this construct, C-peptide may have the ability to stimulate NO production in the endothelium directly and indirectly, as mediated by C-peptide stimulated release of ATP from RBCs via a mechanism proposed and elaborately discussed within Section 1.2.4. Importantly, the potential involvement of RBC derived ATP in the proposed mechanism again highlights the importance of flow, as flowing RBCs under the influence of shear stress release more ATP than static RBCs.[48-51] Elucidating these potential mechanisms of cell-cell communication will be a primary focus of the work presented in this chapter.

3.3 - Effects of Metal Binding on C-Peptide Bioactivity

Recently, our group has shown that if C-peptide is incubated in a solution containing divalent metal ions prior to addition to a RBC solution, the resulting metal activated C-peptide was able to facilitate glucose uptake into, and increase ATP release from RBCs.[47, 52]

Interestingly, these results could not be reproduced in the absence of a metal, indicating that C-peptide must first be introduced to a metal source for some, if not all bioactivity. This was further supported when mass spectrometric analysis of a solution containing active C-peptide not deliberately introduced to a metal, revealed that the peptide had indeed formed an at least one adduct with a metal.[47, 53] C-peptide has been shown to be active in the presence of multiple metal ions[47, 52, 54, 55], however it has been shown that zinc is present at millimolar levels within insulin secretory granules where C-peptide is produced and cleaved from proinsulin.[56] Therefore, Zn^{2+} is used to activate C-peptide throughout this work because when C-peptide is produced *in vivo*, zinc is the most bioavailable metal source, increasing the probability that zinc binds C-peptide for bioactivity in the body.

3.4 - Measuring Intracellular Nitric Oxide

The production and release of NO from bPAECs has been observed by the Spence group frequently, by electrochemistry [57, 58] and through the use of the fluorogenic probes DAF-FM DA[17-19, 59] and DAF-FM[60]. Electrochemistry is a useful technique for measuring NO because it provides direct detection of the analyte as opposed to a derivative. However, electrode fouling is often an issue in biological systems, which is compounded by the high oxidizing potentials required for NO detection. Also, the electrochemical detection of NO is not entirely selective, often resulting in the detection of peroxynitrite and nitrite in addition to NO. Furthermore, the relatively poor detection limits that are typical for electrochemical techniques could also be problematic. As a result of these shortcomings, electrochemistry was not chosen as a method for measuring NO during this work.

The use of fluorogenic probes to measure NO is an indirect detection method often requiring long derivatization times. However, a fluorogenic determination of NO provides the significant advantage of detection by fluorescence microscopy or flow cytometry, which is easily achieved in a common laboratory. Additionally, since NO can be measured optically by this method, it is amenable to high throughput screening, an advantage easily taken advantage of when coupled with microfluidic technology. Also, DAF-FM and DAF-FM DA have been reported to have extremely low detection limits at around 3 nM.[61] It should also be noted that DAF probes have been shown to be susceptible to reductants such as ascorbate, 2-mercaptoethanol, and glutathione, thereby diminishing NO induced fluorescence.[62] However, DAF-FM DA, a cell permeable probe, has been shown to produce emission that is highly dependent on intracellular NO concentration, as it is not sensitive to O_2^-, NO_2^-, NO_3^-, H_2O_2, or $ONOO^-$, all of which are common interferences in most methods for determining NO.[63]

DAF-FM reacts with NO in the presence of oxygen to form triazole derivatives, which emit green fluorescence similar to fluorescein as shown in Figure 3.1. This DAF probe is not cell permeable, and therefore is used in our group to measure changes in NO release from cells. Alternatively, DAF-FM DA has an identical structure to DAF-FM, with the addition of two acetate groups as shown in Figure 3.2. The acetate groups of DAF-FM DA increase cell permeability compared to DAF-FM, allowing DAF-FM DA to enter the cell where the acetate groups are cleaved by intracellular esterases, rendering the molecule confined to the cell with a structure identical to DAF-FM. The DAF-FM which has been confined to the cell can then react with NO in the same fashion described previously, yielding fluorescence that is proportional to the intracellular NO concentration. The DAF probe is confined to the cell in large quantities and,

therefore, any NO subsequently produced by the cell will react with the probe, enabling the detection of intracellular NO production in response to a given stimulus.

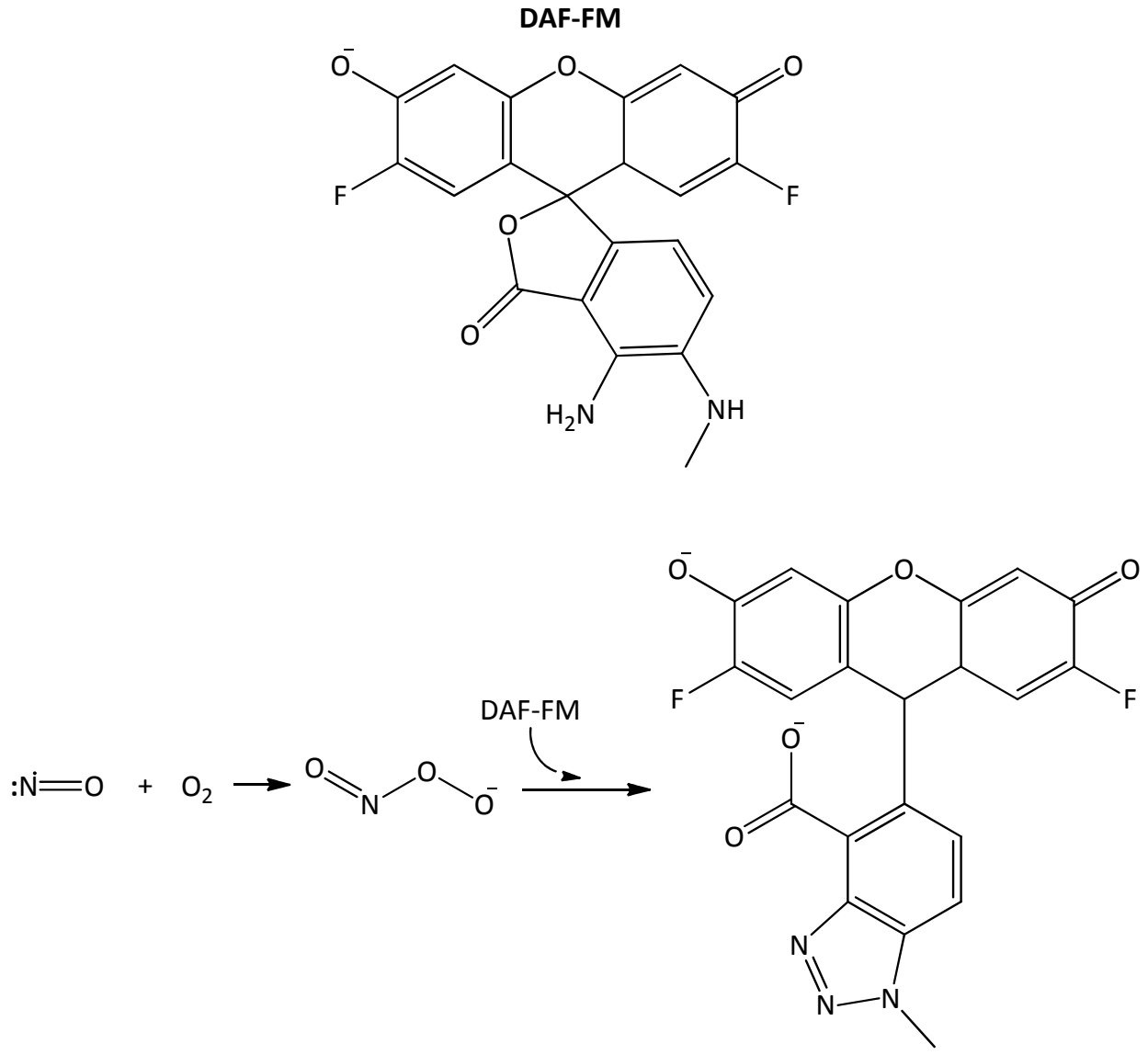

Figure 3.1 - Shown in the top of the image is the structure of DAF-FM, a fluorogenic probe for NO. Below is a potential mechanism for the formation of fluorescent DAF-FM-NO. This mechanism illustrates the reaction between NO and molecular oxygen to form a peroxynitrite intermediate before forming DAF-FM-NO. DAF-FM-NO fluorescence is detectable at wavelengths similar to fluorescein, with an excitation wavelength of 485 nm and emission of 515 nm.

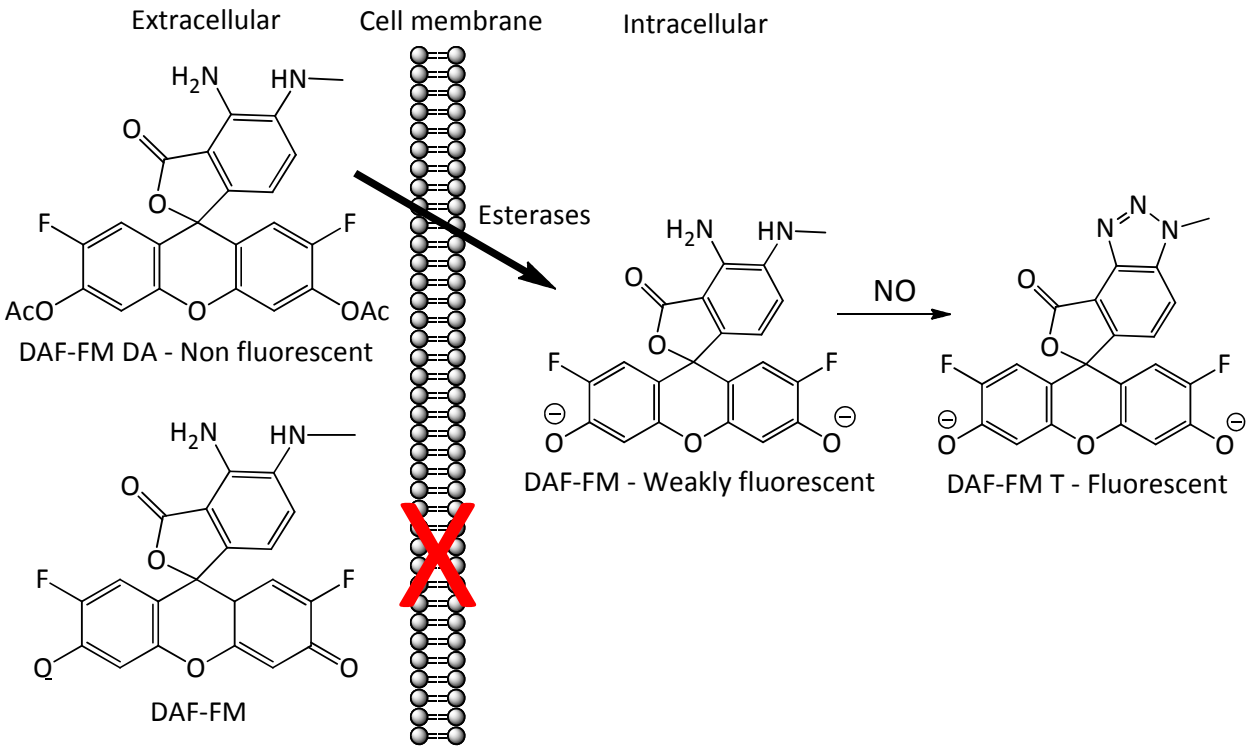

Figure 3.2 - The structures of DAF-FM and DAF-FM DA are shown on the left, the difference being the acetate groups of DAF-FM DA. As illustrated here, in contrast to DAF-FM, DAF-FM DA is capable of penetrating the cell membrane to the intracellular space where esterases cleave the acetate groups, which results in intracellular DAF-FM. Nitric oxide can then react with intracellular DAF-FM, producing the fluorescent DAF-FM T in amounts proportional to intracellular NO concentration.

DAF-FM DA was selected to determine whether endothelial NO production is altered by cell monolayer confluence, or by the actions of Zn^{2+}-activated C-peptide in the bloodstream. As discussed previously, it is hypothesized that Zn^{2+}-activated C-peptide can ultimately increase endothelial NO production by increasing ATP release from RBCs via a mechanism which involves cell-cell communication between the RBC and the endothelial cell. Since we could not predict the magnitude of C-peptide induced endothelial NO production, DAF-FM DA was a desirable choice for NO determination as a result of optimal detection limits that enable the observation of even slight changes in NO production. Also, due to the permeability of PDMS to gas, NO can diffuse in any direction from the endothelial monolayer and avoid detection by an extracellular probe, so an intracellular probe was desired. Additionally, optical detection schemes easily integrate with microfluidic technology, enabling simple measurements in a high-throughput fashion using common laboratory instrumentation.

3.5 - Methods

3.5.1 - Device Fabrication

The microfluidic device developed during the work described in Chapter 2 was used to accomplish the research presented throughout this chapter. Section 2.2.1 details the fabrication of the microfluidic vascular mimic. All polycarbonate membranes had a pore size of 0.6 µm.

3.5.2 - bPAEC Culture

The methods for maintaining bPAEC cultures, as well as the subsequent seeding and culture of these cells within microfluidic devices, are described in detail in section 2.2.3.

3.5.3 - TEER to Verify bPAEC Monolayer Confluence in Device

TEER measurements were performed routinely prior to flow experimentation to ensure bPAEC monolayer confluence. Section 2.3.1 includes the method used for acquiring TEER measurements, including the associated software and data manipulation. Cell monolayer confluence was confirmed by multiple sustained TEER measurements.

3.5.4 - Sample Preparation

Human blood samples were obtained from healthy volunteers by venipuncture. All procedures were followed according to approved Michigan State IRB protocol. Briefly, whole blood was collected from the donor into plastic blood collection vials (Becton, Dickinson and Company), each containing 158 USP units of spray-dried lithium heparin to prevent coagulation. The whole blood was then consolidated and centrifuged. After removal of the plasma and buffy layer by aspiration, RBCs were washed 3 times with a physiological salt solution (PSS, pH 7.4) containing (all from Sigma-Aldrich): 4.7 mM KCl, 2.0 mM $CaCl_2$, 140.5 mM NaCl, 12.0 mM $MgSO_4$, 21.0 mM tris(hydroxymethyl)aminomethane, 5.6 mM glucose, and 5% bovine serum albumin.[47] Crude C-peptide (Genscript) was purified by HPLC and prepared in distilled and deionized water (DDW, 18.2 MΩ), resulting in an 8.3 µM stock solution with is stored at 4°C. For samples containing Zn^{2+}-activated C-peptide, a 2.0 µM working solution of human C-peptide was prepared in DDW and combined with the same volume of a 2.0 µM Zn^{2+} solution also prepared in DDW.[47] For samples containing C-peptide without Zn^{2+}, only C-peptide was added, followed by the same volume of DDW in the absence of Zn^{2+}. Similarly, samples lacking C-peptide contain only the desired volume of Zn^{2+} solution with an equal volume of DDW. For

samples lacking C-peptide and Zn^{2+}, a volume of DDW was added equaling the volume of the other samples, ensuring that the volume of DDW was constant throughout all samples used for a given experiment. After the Zn^{2+} and C-peptide solutions were allowed to rest for around 5 min, PSS was added to the solution, immediately followed by the appropriate volume of washed RBCs, resulting in a solution of RBCs at 7% hematocrit. The appropriate volumes of 2.0 µM Zn^{2+} and 2.0 µM C-peptide working solutions were added so that final concentrations in the 7% RBC samples were always 20 nM. For samples lacking RBCs, PSS was added in lieu of RBCs to yield a 20 nM C-peptide solution.

3.5.5 - PPADS to Inhibit Purinergic Signaling

PPADS (pyridoxalphosphate-6-azophenyl-2',4'-disulfonic acid) (Sigma-Aldrich) is dissolved in Hanks balanced salt solution (HBSS) for a 100 µM stock solution. The stock solution was stored at -20°C as single use aliquots to prevent repetitive thawing. Aliquots were thawed at room temperature immediately before use and diluted in HBSS for a 10 µM working solution. Selected bPAECs were incubated with 10 µL of 10 µM PPADS solution for 30 minutes. After the incubation period, the solution was removed and rinsed with HBSS multiple times to remove color prior to the addition of DAF-FM DA. Care was taken to prevent light exposure by PPADS, as it is a light sensitive molecule.

3.5.6 - Sample Introduction in Microfluidic Flow Experiments

Syringe pumps (Harvard Apparatus) are employed to drive 500 µL Hamilton Gastight syringes for controlled flow of solution in the microfluidic channels. Tygon tubing is interfaced to the syringes using an adapter connecting a male luer syringe to a female 1/16 in.

compression fitting (Upchurch/IDEX scientific). The Tygon tubes are interfaced with the microfluidic device using 20 gauge stainless steel tubing (New England Small Tube Company), which fits securely into both the Tygon tubing and the microfluidic inlets described in previously in Section 2.2.1. RBC samples were prepared as described above and propelled via syringe pump at a rate of 1.0 µL·minute^{-1} for 30 minutes in all flow experiments. The syringes were rotated periodically throughout experiments to prevent RBC settling.

3.5.7 - Measuring NO Production of bPAECs Immobilized on Device

For measurements of intracellular NO production in endothelial cells immobilized in the wells of a microfluidic device, the cell permeable fluorescent probe DAF-FM DA (Invitrogen) was used. DAF-FM DA is dissolved in anhydrous dimethyl sulfoxide (DMSO) for a 5 mM stock solution that could be stored at -20°C, but was often used immediately in experiments. A 100 µM working DAF-FM DA solution was prepared immediately before experimentation by diluting stock solution in HBSS. 10 µL of DAF-FM DA working solution were added to each well and allowed to incubate with bPAECs for 30 minutes. After incubation, the probe was removed and replaced with phosphate buffered saline (PBS), prior to flow of the RBCs.

Fluorescence images of the bPAECs were obtained using an Olympus MVX10 microscope (Olympus America Inc.) prior to flow, and again after flow completion, and the difference in mean gray value analyzed. The difference in fluorescent signal is presented as the average gray value intensities of the integrated areas taken from each acquired image. Images acquired before and after flow for each well were analyzed sequentially so that the areas chosen for both integrations were the same. Figure 3.3 displays an image of the microfluidic vascular mimic during bPAEC NO determination via fluorescence microscopy.

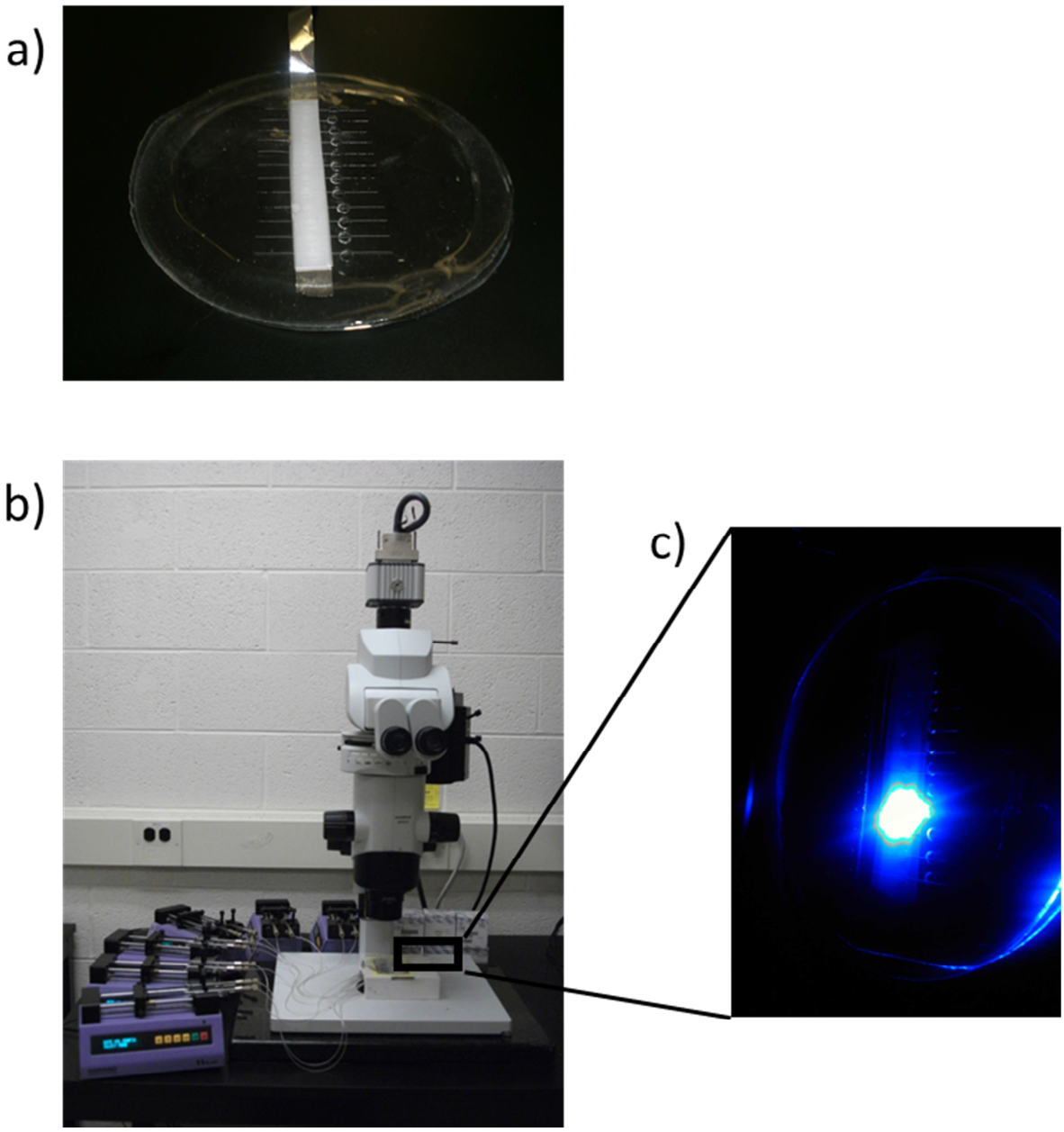

Figure 3.3 - An integrated microfluidic TEER device is shown in (a) prior to use. Panel (b) shows the microfluidic TEER device during a flow experiment prior to using fluorescence microscopy to study confluent cells cultured in the wells of the device. An examination of intracellular NO production of cells cultured in the wells of the microfluidic TEER device by fluorescence microscopy is shown in (c).

3.6 - Results

3.6.1 - Meeting bPAEC Culture Requirements

The success of the work described here requires complete confluence of bPAEC monolayers, as well as the observation of cell-cell communication, requiring proper and reproducible behavior of the cultured cells. Due to these requirements, bPAEC culture was held to high standards as shown in Figure 3.4. Prior to immobilization in a microfluidic device, bPAECs cultured in tissue flasks were examined to confirm optimal confluence, proper morphology, absence of bacteria, and minimal vacuoles, which is generally indicative of healthy cells. Also, since bPAEC monolayers were cultured on a polycarbonate membrane, the cells could not be imaged because the polycarbonate membrane is not optically clear, again highlighting the advantages of TEER capabilities on a microfluidic device. TEER was used to ensure confluence, but full coverage of the membrane by bPAECs was also often confirmed by cell staining with a nuclear dye, Hoechst 33342. This dye binds to the nuclear material of viable cells, allowing for visualization of the cells by optical microscopy when excited with 350 nm light and resulting in emission at 461 nm. Cells were often stained with this dye in addition to DAF-FM DA because their optical properties do not interfere. This method can be used to confirm full coverage of the polycarbonate membrane by bPAECs, but is incapable of confirming confluence as it does not allow for the confirmation of tight junctions between the cells.

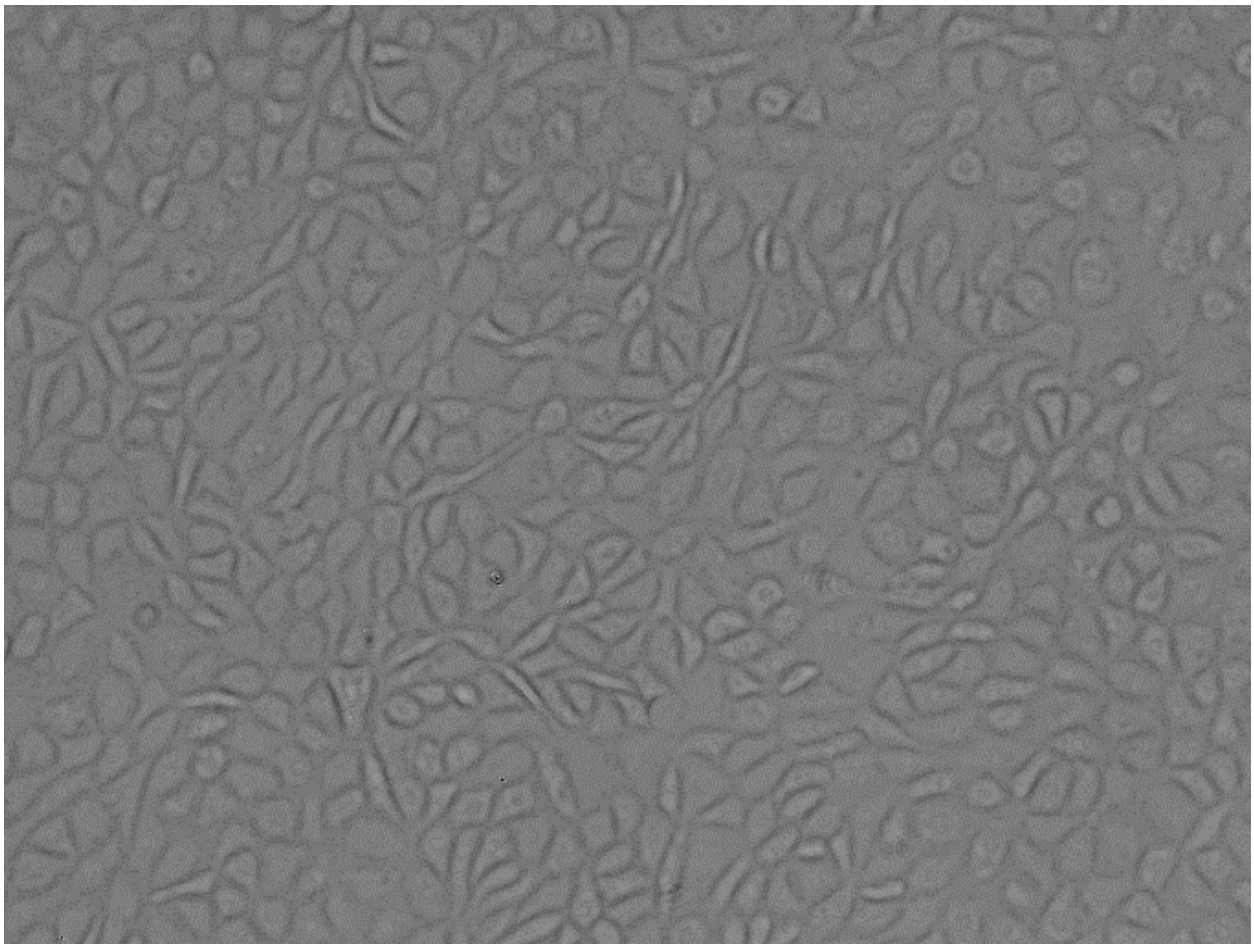

Figure 3.4 - A bright-field image of a monolayer of endothelial cells is shown. Cells were cultured to a high degree of confluence and verified to have the appearance shown here prior to seeding in microfluidic wells. During examination, the cells are checked for a cobblestone appearance, a lack of vacuoles (generally indicates healthy cells), as well as a lack of any visible bacteria.

3.6.2 - bPAEC Monolayer Confluence Influences NO Production

In order to display the importance of confirming cell monolayer confluence, a real physiological event was monitored, namely intracellular NO production within bPAEC monolayers of varying confluence as determined by the TEER system. Cells were allowed to adhere for either 1.5 h or 8 h, and their barrier integrity, or lack thereof, was verified via TEER measurements. After barrier integrity was confirmed, human RBCs were hydrodynamically pumped through the channel underlying the endothelial cell-modified membrane for 30 min at a flow rate of 1.0 $\mu L \cdot min^{-1}$. The movement of the RBCs through these channels has been shown by our group to stimulate the release of ATP from the RBC.[19, 48] This released ATP is able to migrate through the pores of the membrane and interact with the endothelial cell, stimulating the resultant production of NO by the endothelium as shown in Figure 3.5.

Intracellular NO production was measured using DAF-FM DA as the fluorogenic intracellular probe in conjunction with fluorescence microscopy. The NO production was measured in endothelial cells that had not reached confluence (1.5 h after seeding on the membrane) and for cells that were deemed confluent by the TEER measurement (8 h after seeding on the membrane). The difference in NO production (as indicated by fluorescence emission intensity) prior to pumping the RBCs to that 30 min after was measured. As shown in figure 3.5, those cells that had reached confluence (8 h post-seeding) produced 34% more NO than those cells that had not reached confluence (1.5 h post-seeding), a difference that is statistically significant ($p<0.05$). Importantly, data not shown here also demonstrated that measurements of NO production obtained at various points after confluence had been reached showed statistically insignificant changes.

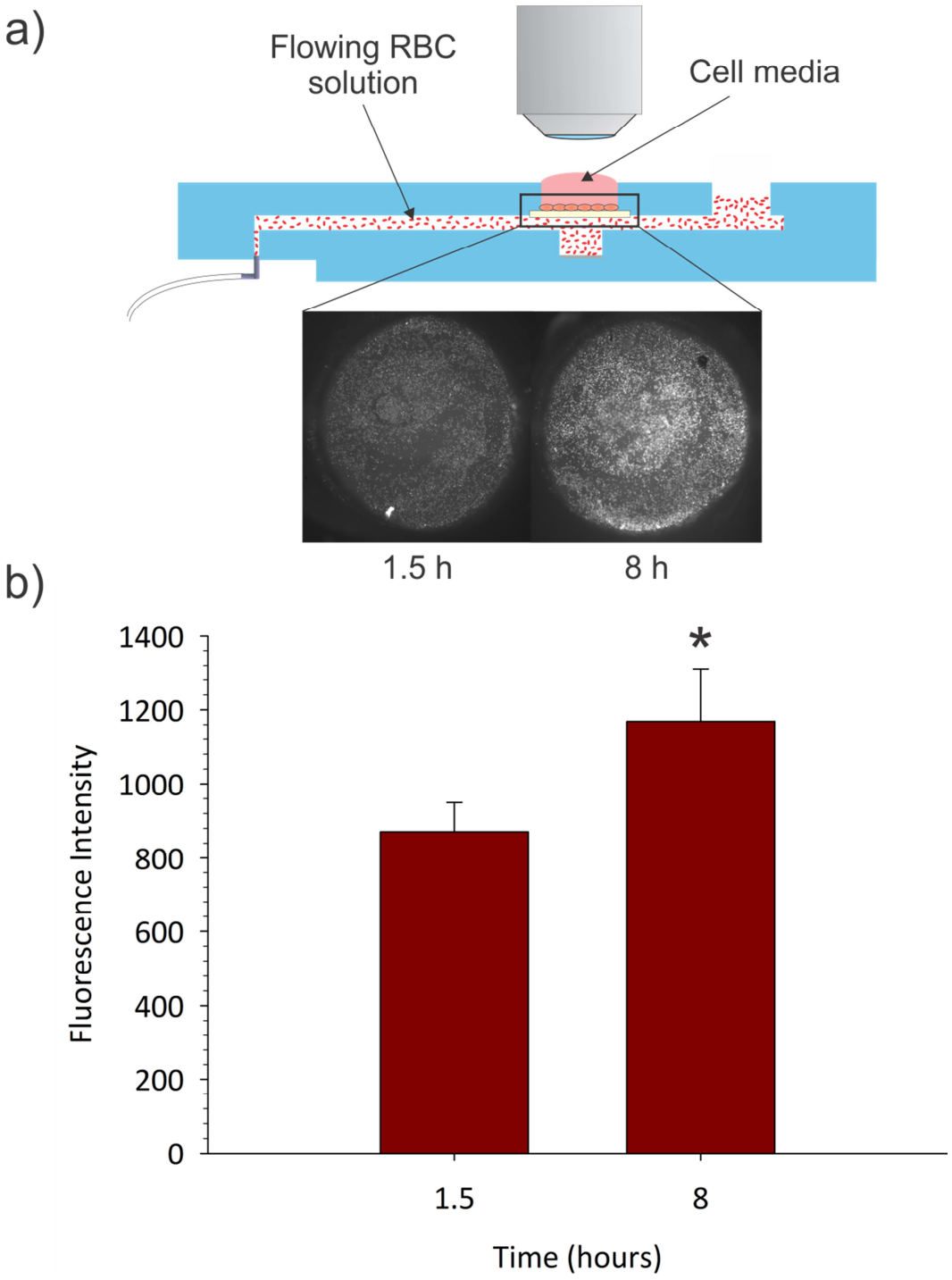

Figure 3.5 - A side view of the measurement system utilized to detect NO in the endothelial layer is shown in (a). A solution of RBCs in PSS is pumped under a membrane containing an endothelial layer cultured for 1.5 or 8 h. A significant increase ($P < 0.05$, $n = 3$, errors are SD) in NO production is observed when the cells reached confluence at 8 h, as shown in the inset bar graph.

3.6.3 - Mechanism Determination: C-peptide Stimulated Endothelial NO Production

Using the microfluidic vascular mimic, RBCs treated with 20 nM C-peptide and Zn^{2+} (RBC + Zn + C-peptide), 20 nM C-peptide (RBC + C-peptide), and 20 nM Zn^{2+} (RBC + Zn) were pumped beneath bPAECs cultured on a polycarbonate membrane as shown in Figure 3.6. PSS containing 20 nM C-peptide with Zn^{2+} was also pumped beneath bPAECs to determine if the mechanism leading to NO production is RBC-mediated. Fluorescence images were taken prior to flow, and again after flow completion and the difference in mean gray value was analyzed. The difference in fluorescent signal is presented in Figure 3.6 as the average gray value intensities of the integrated areas taken from each acquired image. It was observed that the endothelial cells that were allowed to interact with RBCs treated with C-peptide and Zn^{2+} had an 88.6 ± 7.5% increase in fluorescence intensity, indicative of NO production, when compared to untreated RBCs. The RBCs treated with only C-peptide or only Zn^{2+} did not generate statistical change in intracellular NO production within the endothelial cells when compared to untreated RBCs. Also, a statistically significant decrease in endothelial NO production was observed in the absence of RBCs ($p<0.02$) (Buffer + C-peptide + Zn). To confirm the possibility that the increase in endothelium NO production was due to ATP binding to the endothelial P2Y receptor, PPADS, a purinergic receptor inhibitor was incubated with the endothelial cells for 30 min prior to flow of RBCs that had been incubated with Zn^{2+}/C-peptide. This PPADS incubation resulted in a complete reversal of the increase in NO production measured when comparing the flow of RBCs incubated with Zn^{2+}/C-peptide to RBCs alone.

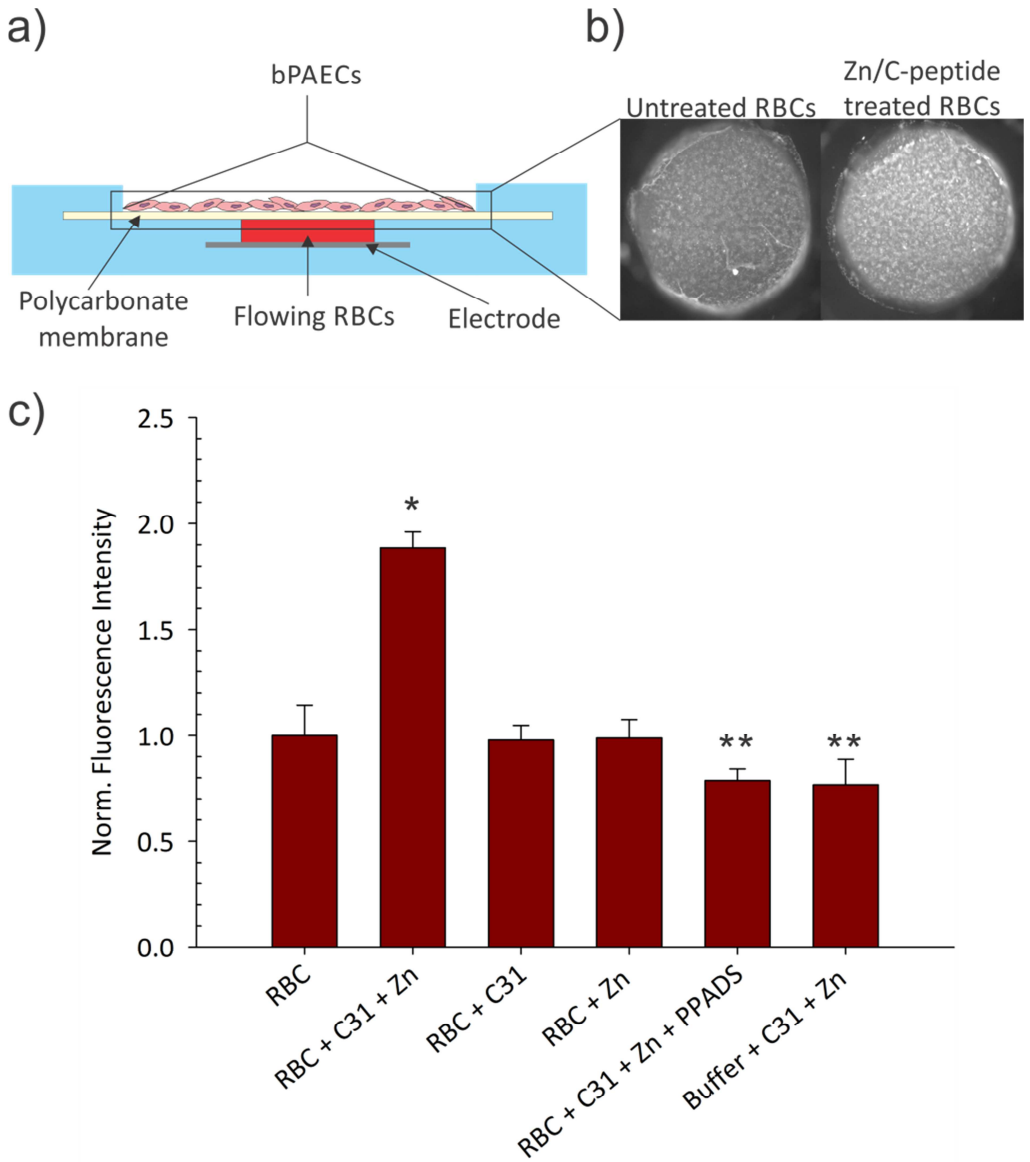

Figure 3.6 - A cross sectional view of a single channel of the microfluidic device utilized to detect NO produced by the endothelial layer is shown (a). Images of wells of a microfluidic device containing endothelial layers that had been exposed for 30 min. to untreated flowing RBCs, or flowing RBCs treated with Zn^{2+}/C-peptide, are compared in (b). An 88.6% ± 7.5% increase (n = 3, $p < 0.001$) in intracellular endothelial NO production was observed when RBCs were pumped in the presence of Zn^{2+}/C-peptide and compared to RBCs alone in (b). Interestingly, a statistical change in endothelial NO production was not observed when RBCs exposed to C-peptide alone or Zn^{2+} alone are compared to RBCs alone. A statistical decrease (n=3, $p<0.02$) in endothelial NO production was observed when comparing PSS lacking RBCs to RBCs alone. Additionally, when endothelial cells were incubated with PPADS, a purinergic receptor inhibitor, prior to flow of RBCs treated with Zn^{2+}-activated C-peptide, an increase in NO production was no longer observed. (* denotes $p<0.001$, ** denotes $p<0.02$)

3.7 – Discussion

As shown in figure 3.5, bPAECs that had reached confluence after 8 hours produced 34% more NO than those cells that had not reached confluence (1.5 h post-seeding), a difference that is statistically significant ($p<0.05$). Also, data not shown also demonstrated that measurements of NO production obtained at various points after confluence had been reached showed statistically insignificant changes. Coupled with the data in figure 3.5, the TEER measurements showing no changes in barrier integrity after confluence was reached represent the importance of TEER measurements prior to investigating the cellular activity of the layered cells. For example, the increase in fluorescence intensity could be due to improved cell-cell communication between the endothelium and the RBCs, altered endothelial cell behavior, or it could simply be due to more cells in the membrane after a small period of growth. In all likelihood, the behavior of the endothelial cells was altered, resulting in increased NO production upon reaching a confluent state, since eNOS activity has been shown to be associated with the presence of endothelial cell-cell contacts.[64] In any case, one seemingly indisputable experimental advantage to making the TEER measurements prior to the cellular investigation is having a quantitative measure of cell growth prior to addition of agonists or antagonists. Such knowledge has the potential to increase reproducibility of cellular assays performed on a specific cell type, as well as enhance precision between assays from different cultures. Performing TEER measurements prior to experiments with agonists or antagonists allows for more realistic, and in this case, enhanced cellular responses, allowing for more accurate conclusions stemming from experimental results.

The flow capabilities of this device enable hemodynamic shear stress on RBC's, creating a more biologically relevant mimic of the vasculature than conventional platforms capable of measuring TEER. Perhaps more beneficial is the ability to study cell to cell interactions and communication *in vitro*, while maintaining an environment that geometrically resembles the vasculature *in vivo*. In order to display the importance of performing TEER measurements prior to cellular investigations, we chose to study a cellular response that changes as a function of cell confluence, while showcasing the ability of the device to closely mimic and monitor biological events, namely endothelial intracellular NO production in response to flowing RBCs. However, we expect the ability to measure cellular barrier integrity, and relative changes in that integrity on a microfluidic platform, to enable studies in a broad variety of fields. Drug permeability studies, as well as elucidating the mechanisms of cellular barrier breakdown in disease states are some examples of studies made possible by this device. Additionally, since TEER measurements do not damage cells, or influence cell phenotype, this device could be used to monitor the influence of agonists or antagonists on cell barrier integrity in real time.

After it was determined that the TEER capability of the device allowed for an increase in reproducibility between cell assays and helped ensure proper cell behavior, we were prepared to elucidate the mechanism of C-peptide induced endothelial NO production, which would help clarify the observed improvements of blood flow in type 1 diabetic subjects since NO is a potent vasodilator. The first observation suggesting that C-peptide stimulates NO release was that in rat models of type 1 diabetes, C-peptide induced glucose utilization was altered by the inhibition of endothelial nitric oxide synthase (eNOS) via the eNOS inhibitor L-NNA.[65] It has also been demonstrated that C-peptide-mediated arteriolar vasorelaxation is dependent on

concentrations of NO in the vessel.[31, 66] Specifically, in the presence of insulin, C-peptide induced a vasodilatory effect in isolated rat cremaster muscle arterioles that could be reversed by L-NNA, again implicating eNOS in the mechanism.[31]

Subsequent to these findings, results from other studies have emerged that suggest a relationship between C-peptide and NO production. For example, in diabetic polyneuropathy, it has been shown that impaired expression of eNOS is the cause of decreased endoneurial blood flow resulting from decreased amounts of NO in diabetic models, ultimately resulting in slowed acute nerve conduction.[67-70] However, complete C-peptide replacement in these models normalized blood flow and vascular conductance.[67] Importantly, C-peptide had no effect on lipid peroxidation or superoxide dismutase activity, showing that the effects are not due to reduced oxidative stress and, instead, may be due to a NOS-related mechanism. Also, during the diabetic control and complications trial (DCCT), a relationship was established between circulating C-peptide and risk for vascular complications[71], which is thought to be primarily mediated by NO release from endothelial cells.[45, 72-74] Summarily, there is growing evidence that C-peptide improves blood flow of diabetic subjects by an eNOS dependent increase in NO production.

In previous microfluidic studies by our group, it was revealed that flowing RBCs are able to stimulate endothelial NO production.[19] In a separate microfluidic study conducted by our group, it was demonstrated that ATP could also stimulate endothelial NO production by a process that could be inhibited by L-NAME, a competitive inhibitor of NOS.[18] This work builds upon previous work demonstrating that the RBC itself can increase NO production by a process requiring RBC derived ATP, implicating the RBC as a regulator of vascular tone.[75-77]

Additionally, it has been shown that patients with pulmonary hypertension have impaired ATP release from their RBCs, further implicating RBC derived ATP in vasodilation.[78] Moreover, ATP release from diabetic RBCs is significantly less than that released from RBCs obtained from healthy, non-diabetic subjects.[79] However, C-peptide has been shown to normalize this release.[47] Interestingly, our group has revealed the ability of C-peptide to increase ATP release from RBCs, but only if C-peptide had first been carefully prepared in a solution containing Zn^{2+} prior to interaction with RBCs.[47, 52] Collectively, results from these studies suggest that C-peptide, upon zinc activation, could increase ATP release from RBCs that, in turn, could indirectly stimulate an increase in endothelial NO production.

The mechanism of ATP release from the RBC has been studied as discussed in Section 1.2.3. Also, the mechanism of ATP induced endothelial NO production has been elucidated, and is also described in depth in Chapter 1. Importantly, the purinergic P2Y receptor, located on the endothelial cell membrane[80], influences vasodilation in response to an agonist by producing smooth muscle relaxing factors, including NO, which seems to be the most potent.[41, 81-88] This activity of the P2Y purinoreceptor can be achieved by extracellular ATP levels, as ATP is an agonist of P2Y.[89, 90] Additionally, upon P2Y activation, an intracellular signaling cascade is initiated that results in the activation of eNOS [91-93], which has already been shown to play a role in C-peptide activity as discussed before. Understanding P2Y signaling is quite important for this work because the P2Y receptor is responsible for sensing and responding to extracellular signaling molecules, such as ATP, as is the case in the proposed mechanism for metal activated C-peptide induced endothelial NO production. Stated simply, the P2Y purinoreceptor is the proposed link between the RBC and the endothelium, and in order to

show that C-peptide can increase endothelial NO production as a result of increased ATP release from the RBC, the receptor will have to be implicated in the mechanism experimentally.

The proposed mechanism for endothelial NO stimulation by C-peptide is RBC mediated, and as such, is proposed to be an indirect, downstream consequence of C-peptide's action in the bloodstream. However, previous studies involving C-peptide application to cultured bovine aortic endothelial cells (bPAECs) resulted in an increased NO production and eNOS mRNA expression by an unknown mechanism not mediated by the RBC.[44] However, these results could not be replicated in our lab by directly applying C-peptide solutions at varying concentrations (physiologically relevant up to 10 times that amount) to cultured bPAECs. In contrast, results using other known stimuli such as ATP or a calcium ionophore did stimulate a significant production of NO, [44] thus providing evidence that the cells could produce NO which we could successfully measure.

Based on the importance of NO production in the pulmonary bed, it was somewhat surprising that C-peptide would evoke changes in aortic endothelium, but not in bPAECs. Unlike other organs, the lungs must accept the entire cardiac output, requiring the blood vessels in the lung bed to dilate and accept this output while simultaneously maintaining a reasonable blood pressure. Consequentially, the ability of the endothelial cells in the pulmonary bed to produce NO becomes especially important as all RBCs must return to the lungs for reoxygenation. Not surprisingly, there have been many reported stimuli of NO in the pulmonary endothelium, including but not limited to bradykinin, acetylcholine, prostacyclin, and adenosine triphosphate (ATP).[18, 94, 95] Regardless of the inability to directly stimulate NO production in bPAECs, C-peptide may be capable of indirect stimulation via its ability to

increase the release of ATP from RBCs as discussed previously. Of course, a system capable of investigating such cell to cell communication would be requisite to answer such a question.

The microfluidic TEER system introduced in chapter 2 enables the flow of blood components in a channel with dimensions mimicking a resistance vessel that is separated from a cultured endothelium by physiologically relevant distances. Therefore, ATP released from the flowing RBCs can diffuse to the endothelial layer, as it would *in vivo*. Here, RBCs in the presence and absence of C-peptide (with and without the addition of Zn^{2+}) were pumped underneath a monolayer of bPAECs that had been incubated with DAF-FM DA for NO detection. In the presence of Zn^{2+}-C-peptide, a significant increase ($p<0.001$) in NO production by the bPAECs was measured as shown in Figure 3.6. When RBCs with C-peptide alone (or Zn^{2+} alone) were pumped underneath the bPAECs, there was no increase in NO production observed. Furthermore, when a PSS solution containing Zn^{2+}-activated C-peptide, but lacking RBCs, was pumped beneath bPAECs, a decrease in NO production was observed when compared to basal levels produced by RBCs alone ($p<0.02$), proving that the Zn^{2+}-activated C-peptide induced NO production is mediated by the RBC. These results also suggest that flowing RBCs play a role in maintaining basal NO production in the bloodstream. Additionally, when bPAECs were incubated with PPADS to inhibit the P2 purinoreceptors, flowing RBCs containing Zn^{2+}-activated C-peptide could no longer cause an increase in NO production. Collectively, these results prove that C-peptide increases endothelial NO production by stimulating the release of a known endothelial P2Y agonist, ATP, from RBCs and thereby enhancing P2Y purinoreceptor activity by increasing levels of ATP antagonist, which stimulates purinergic signaling cascade known to

result in increased endothelial NO production. Therefore, even though C-peptide may not be able to stimulate NO directly in all cell types, its ability to stimulate the release of ATP from the RBC may enable C-peptide to stimulate NO production in certain types of endothelial cells through purinergic receptor signaling, just as it does in bPAECs.

C-peptide therapy has been shown to significantly reduce renal complications by increasing glomerular hyperfiltration,[96] microalbuminuria[35] and eNOS expression.[97] C-peptide also increases the Ca^{2+} influx to the renal tubular cells.[98] It is well-established that renal P2 receptors are determinants in the function of glomerular filtration and renal hemodynamics.[99] In light of the findings presented in Figure 3.6 showing the ability of C-peptide to influence purinergic signaling in bPAECs, it is quite possible that C-peptide influences renal function by purinergic signaling as well, potentially explaining the observed C-peptide induced improvements in diabetic renal function.

The potential impact of C-peptide's effect on ATP release and purinergic receptor-based signaling reaches beyond the endothelium alone. For example, previous studies have shown that C-peptide appears to have no direct effect on platelets.[100] To date, unpublished studies in our group involving platelets and C-peptide interacting directly, with our without any metal added, have resulted in similar conclusions. However, our group and others have recently reported that the P2X purinoreceptor on the platelet surface (an ATP-gated Ca^{2+} channel) may be play a more crucial role in platelet function than originally perceived.[101, 102] In this paradigm, the ability of C-peptide to stimulate ATP release from RBCs may indirectly affect purinergic receptor signaling on the platelet, similar to that shown here for the endothelium.[27] Indeed, recent reports have shown that RBC-derived ATP has a profound

effect on platelet adhesion to the endothelium, [15] and it is already well known that platelet activation is a result of purinergic signaling.[103-105]

Another important aspect of the results presented here is the role of the metal in C-peptide activity. It has been reported that chromium and iron have similar effects to zinc in rendering C-peptide "bioactive".[47] However, it is important to remember that the studies reported for all three of these metals are more pharmacological than physiological as they were performed *in vitro* where a metal was selected by researchers. Specifically, C-peptide is found in the bloodstream at single-digit nanomolar levels, and bioavailable levels of chromium and iron are sub-nanomolar concentrations as well. Assuming the metal binds C-peptide, at these concentrations, chromium, iron, or any other metal capable of binding to C-peptide's carboxylate-containing amino acids (glutamate and aspartate) could not outcompete sodium, potassium and other metals found in the bloodstream found at concentrations 6 orders of magnitude higher in the millimolar range. However, in the pancreatic beta cell granules where C-peptide is produced, the concentration of zinc is known to be in the millimolar range.[56] Therefore, it is possible that zinc would have the ability to bind to C-peptide after cleavage from the proinsulin C-peptide hormone in the beta cell granules prior to excretion into the bloodstream.

This work clearly shows that C-peptide is incapable of eliciting endothelial NO production unless Zn^{2+} is introduced, indicating that C-peptide can only influence purinergic signaling in the presence of a metal. Of course, most studies to date involving the exogenous addition of C-peptide to humans, animal models, and cell models have not directly co-administered a metal. Interestingly, some studies report no effects from C-peptide unless co-administered with

insulin, which often contains Zn^{2+} at levels as high as 0.5% by mass.[106] Additionally, our group has found by mass spectrometric analysis that C-peptide produced commercially often contains metal contaminants. It is feasible that C-peptide samples often unintentionally contain metals, frequently rendering C-peptide bioactive, which could explain the inconsistent activity observed in clinical trials.

3.8 - Conclusions

In summary, the results presented here show that the degree of pulmonary endothelial monolayer confluence is a determinant in NO production, where confluent cells produce more NO relative to non-confluent cells. This finding highlights the importance of performing TEER measurements prior to experimentation involving cell monolayers to ensure proper behavior, which adds credibility to results and increases reproducibility between experiments. Additionally, through a mechanism that has been expounded during this work, C-peptide is identified as another factor influencing NO production in the pulmonary endothelium. It was determined that C-peptide, only in the presence of Zn^{2+}, stimulates RBC mediated NO production resulting from purinergic signaling in a cultured pulmonary endothelium. C-peptide is able to increase ATP release from RBCs, and, as an agonist of the P2Y purinoreceptor, ATP is capable of triggering a purinergic signaling cascade resulting in endothelial NO production.

While the involvement of C-peptide in purinergic signaling provides an explanation for the improvements in blood flow observed in diabetic patients during C-peptide therapy, this involvement may provide an explanation for the collective bioactivity of C-peptide observed throughout the body. Additionally, the requirement of a metal for C-peptide activity could explain inconsistencies in activity observed in C-peptide clinical trials. After all, the proper

treatment of C-peptide with Zn^{2+} reproducibly increases RBC mediated NO production in pulmonary endothelial cells cultured *in vitro* within the microfluidic vascular mimic. Due to the well-established ability of NO derived from the endothelium to regulate vessel dilation *in vivo*, Zn^{2+}-activated C-peptide can potentially relieve, or prevent, the common type 1 diabetic ailments resulting from a compromised ability to properly regulate vessel tone and, therefore, would be a promising drug candidate. Furthermore, C-peptide may be a determinant involved in the fundamentally important role of maintaining appropriate vascular tone in healthy individuals, a potential activity that has been previously overlooked.

REFERENCES

REFERENCES

1. Gumbleton, M. and K.L. Audus, *Progress and Limitations in the Use of In Vitro Cell Cultures to Serve as a Permeability Screen for the Blood-Brain Barrier.* J. of Pharm. Sci., 2001. **90**(11): p. 1681-1698.

2. Crone, C. and S.P. Olesen, *Electrical resistance of brain microvascular endothelium.* Brain Res FIELD Full Journal Title:Brain research, 1982. **241**(1): p. 49-55.

3. Witko-Sarsat, V., et al., *Neutrophils: molecules, functions and pathophysiological aspects.* Laboratory Investigation, 2000. **80**(5): p. 617-53.

4. Mehta, D. and A.B. Malik, *Signaling mechanisms regulating endothelial permeability.* Physiological Reviews, 2006. **86**(1): p. 279-367.

5. Staehelin, L.A., *Further observations on the fine structure of freeze-cleaved tight junctions.* J Cell Sci, 1973. **13**(3): p. 763-86.

6. Wang, W., W.L. Dentler, and R.T. Borchardt, *VEGF increases BMEC monolayer permeability by affecting occludin expression and tight junction assembly.* American Journal of Physiology-Heart and Circulatory Physiology, 2001. **280**(1): p. H434-H440.

7. Madsen, K.L., et al., *Interleukin 10 prevents cytokine-induced disruption of T84 monolayer barrier integrity and limits chloride secretion.* Gastroenterology, 1997. **113**(1): p. 151-9.

8. Xu, M., et al., *Ethanol disrupts vascular endothelial barrier: implication in cancer metastasis.* Toxicol Sci, 2012. **127**(1): p. 42-53.

9. Nagaraja, S., A. Kapela, and N.M. Tsoukias, *Intercellular communication in the vascular wall: A modeling perspective.* Microcirculation, 2012.

10. Atencia, J. and D.J. Beebe, *Controlled microfluidic interfaces.* Nature, 2005. **437**(7059): p. 648-55.

11. Kuczenski, B., et al., *Probing cellular dynamics with a chemical signal generator.* PLoS ONE, 2009. **4**(3): p. e4847.

12. Ayliffe, H.E., A.B. Frazier, and R.D. Rabbitt, *Electric impedance spectroscopy using microchannels with integrated metal electrodes.* Journal of Microelectromechanical Systems, 1999. **8**(1): p. 50-57.

13. Borchardt, R.T., et al., *Models for Assessing Drug Absorption and Metabolism. [In: Pharm. Biotechnol., 1996; 8]*1996. 444 pp.

14. Davies, P.F., *Flow-mediated endothelial mechanotransduction.* Physiological Reviews, 1995. **75**(3): p. 519-60.

15. Ku, C.J., T. D'Amico Oblak, and D.M. Spence, *Interactions between multiple cell types in parallel microfluidic channels: monitoring platelet adhesion to an endothelium in the presence of an anti-adhesion drug.* Anal Chem, 2008. **80**(19): p. 7543-8.

16. Tissot Van Patot, M.C., et al., *Endotoxin-induced adhesion of red blood cells to pulmonary artery endothelial cells.* Am J Physiol, 1996. **270**(1 Pt 1): p. L28-36.

17. Letourneau, S., et al., *Evaluating the effects of estradiol on endothelial nitric oxide stimulated by erythrocyte-derived ATP using a microfluidic approach.* Anal Bioanal Chem, 2010. **397**(8): p. 3369-75.

18. D'Amico Oblak, T., P. Root, and D.M. Spence, *Fluorescence monitoring of ATP-stimulated, endothelium-derived nitric oxide production in channels of a poly(dimethylsiloxane)-based microfluidic device.* Anal Chem, 2006. **78**(9): p. 3193-7.

19. Genes, L., I., et al., *Adressing a Vascular Endothelium Array with Blood Components using Underlying Microfluidic Channels.* Lab on a Chip, 2007. **7**(10): p. 1256-1259.

20. Shamloo, A., et al., *Endothelial cell polarization and chemotaxis in a microfluidic device.* Lab on a Chip, 2008. **8**(8): p. 1292-1299.

21. van der Meer, A.D., et al., *Microfluidic technology in vascular research.* J Biomed Biotechnol, 2009. **2009**: p. 823148.

22. Wong, K.H., et al., *Microfluidic Models of Vascular Functions.* Annu Rev Biomed Eng, 2012.

23. Young, E.W., et al., *Technique for real-time measurements of endothelial permeability in a microfluidic membrane chip using laser-induced fluorescence detection.* Anal Chem, 2010. **82**(3): p. 808-16.

24. Douville, N.J., et al., *Fabrication of two-layered channel system with embedded electrodes to measure resistance across epithelial and endothelial barriers.* Anal Chem, 2010. **82**(6): p. 2505-11.

25. Ferrell, N., et al., *A microfluidic bioreactor with integrated transepithelial electrical resistance (TEER) measurement electrodes for evaluation of renal epithelial cells.* Biotechnol Bioeng, 2010. **107**(4): p. 707-16.

26. Vogel, P.A., et al., *Microfluidic transendothelial electrical resistance measurement device that enables blood flow and postgrowth experiments.* Anal Chem, 2011. **83**(11): p. 4296-301.

27. Halpin, S.T., et al., *The Red Blood Cell and Nitric Oxide: Derived, Stimulated, or Both?* The Open Nitric Oxide Journal, 2011. **3**(Suppl 1-M2): p. 8-15.

28. Steiner, D.F., et al., *Proinsulin and the biosynthesis of insulin.* Recent Prog Horm Res, 1969. **25**: p. 207-82.

29. Rubenstein, A.H., et al., *Proinsulin and C-peptide in blood.* Diabetes, 1972. **21**(2 Suppl): p. 661-72.

30. Hoogwerf, B.J., et al., *Infusion of synthetic human C-peptide does not affect plasma glucose, serum insulin, or plasma glucagon in healthy subjects.* Metabolism, Clinical and Experimental, 1986. **35**(2): p. 122-5.

31. Jensen, M.E. and E.J. Messina, *C-peptide induces a concentration-dependent dilation of skeletal muscle arterioles only in presence of insulin.* Am J Physiol, 1999. **276**(4 Pt 2): p. H1223-8.

32. Scalia, R., et al., *C-peptide inhibits leukocyte-endothelium interaction in the microcirculation during acute endothelial dysfunction.* FASEB J, 2000. **14**(14): p. 2357-64.

33. Young, L.H., et al., *C-peptide exerts cardioprotective effects in myocardial ischemia-reperfusion.* Am J Physiol Heart Circ Physiol, 2000. **279**(4): p. H1453-9.

34. Pierson, C.R., W. Zhang, and A.A. Sima, *Proinsulin C-peptide replacement in type 1 diabetic BB/Wor-rats prevents deficits in nerve fiber regeneration.* Journal of Neuropathology and Experimental Neurology, 2003. **62**(7): p. 765-79.

35. Maezawa, Y., et al., *Influence of C-peptide on early glomerular changes in diabetic mice.* Diabetes/metabolism research and reviews, 2006. **22**(4): p. 313-22.

36. Sima, A.A., et al., *Inflammation in Diabetic Encephalopathy is Prevented by C-Peptide.* Rev Diabet Stud, 2009. **6**(1): p. 37-42.

37. Lindstrom, K., et al., *Acute effects of C-peptide on the microvasculature of isolated perfused skeletal muscles and kidneys in rat.* Acta Physiol Scand, 1996. **156**(1): p. 19-25.

38. Hansen, A., et al., *C-peptide exerts beneficial effects on myocardial blood flow and function in patients with type 1 diabetes.* Diabetes, 2002. **51**(10): p. 3077-3082.

39. Ignarro, L.J., et al., *Endothelium-derived relaxing factor from pulmonary artery and vein possesses pharmacologic and chemical properties identical to those of nitric oxide radical.* Circulation Research, 1987. **61**(6): p. 866-79.

40. Furchgott, R.F. and J.V. Zawadzki, *The Obligatory Role of Endothelial-Cells in the Relaxation of Arterial Smooth-Muscle by Acetylcholine.* Nature, 1980. **288**(5789): p. 373-376.

41. Palmer, R.M., A.G. Ferrige, and S. Moncada, *Nitric oxide release accounts for the biological activity of endothelium-derived relaxing factor.* Nature, 1987. **327**(6122): p. 524-6.

42. Ignarro, L.J., et al., *Nitric oxide and cyclic GMP formation upon electrical field stimulation cause relaxation of corpus cavernosum smooth muscle.* Biochem Biophys Res Commun, 1990. **170**(2): p. 843-50.

43. Rapoport, R.M. and F. Murad, *Agonist-induced endothelium-dependent relaxation in rat thoracic aorta may be mediated through cGMP.* Circ Res, 1983. **52**(3): p. 352-7.

44. Wallerath, T., et al., *Stimulation of endothelial nitric oxide synthase by proinsulin C-peptide.* Nitric Oxide, 2003. **9**(2): p. 95-102.

45. Kitamura, T., et al., *Proinsulin C-peptide activates cAMP response element-binding proteins through the p38 mitogen-activated protein kinase pathway in mouse lung capillary endothelial cells.* Biochemical Journal, 2002. **366**(3): p. 737-744.

46. Sprague, R.S., et al., *Extracellular ATP signaling in the rabbit lung: erythrocytes as determinants of vascular resistance.* Am J Physiol Heart Circ Physiol, 2003. **285**(2): p. H693-700.

47. Meyer, J.A., et al., *Metal-activated C-peptide facilitates glucose clearance and the release of a nitric oxide stimulus via the GLUT1 transporter.* Diabetologia, 2008. **51**(1): p. 175-82.

48. Sprung, R.J., R.S. Sprague, and D.M. Spence, *Determination of ATP release from erythrocytes using microbore tubing as a model of resistance vessels in vivo.* Anal. Chem., 2002. **74**: p. 2274-2278.

49. Sprague, R.S., et al., *Deformation-induced ATP release from red blood cells requires cystic fibrosis transmembrane conductance regulator activity.* Am. J. Physiol, 1998. **275**: p. H1726-H1732.

50. Price, A., K., et al., *Deformation-induced release of ATP from erythrocytes in a poly(dimethylsiloxane)-based microchip with channels that mimic resistance vessels.* Analytical Chemistry, 2004. **76**(16): p. 4849-55.

51. Wan, J., W.D. Ristenpart, and H.A. Stone, *Dynamics of shear-induced ATP release from red blood cells.* Proc Natl Acad Sci U S A, 2008. **105**(43): p. 16432-7.

52. Meyer, J.A., et al., *Zinc-activated C-peptide resistance to the type 2 diabetic erythrocyte is associated with hyperglycemia-induced phosphatidylserine externalization and reversed by metformin.* Mol Biosyst, 2009. **5**(10): p. 1157-62.

53. Keltner, Z., et al., *Mass spectrometric characterization and activity of zinc-activated proinsulin C-peptide and C-peptide mutants.* Analyst, 2010. **135**(2): p. 278-288.

54. Brooks, P., J. Meyer, and D.M. Spence, *Metal (Zn2+) Activated C-Peptide Induced ATP Release Via Red Blood Cells with the Addition of Albumin.* Abstracts, 60th Southeast Regional Meeting of the American Chemical Society, Nashville, TN, United States, November 12-15, 2008: p. SERM-680.

55. Medawala, W., et al., *A Molecular Level Understanding of Zinc Activation of C-peptide and its Effects on Cellular Communication in the Bloodstream.* Rev Diabet Stud, 2009. **6**(3): p. 148-58.

56. Hutton, J.C., *The insulin secretory granule.* Diabetologia, 1989. **32**(5): p. 271-81.

57. Hulvey, M.K. and R.S. Martin, *A microchip-based endothelium mimic utilizing open reservoirs for cell immobilization and integrated carbon ink microelectrodes for detection.* Anal. Bioanal. Chem., 2009. **393**(2): p. 599-605.

58. Hulvey, M.K., et al., *Fabrication and evaluation of a 3-dimensional microchip device where carbon microelectrodes individually address channels in the separate fluidic layers.* Analyst, 2007. **132**(12): p. 1246-1253.

59. Ku, C.-J., et al., *Fluorescence Determination of Nitric Oxide Production in Stimulated and Activated Platelets.* Analytical Chemistry, 2007. **79**(6): p. 2421-2426.

60. Halpin, S.T. and D.M. Spence, *Direct Plate-Reader Measurement of Nitric Oxide Released from Hypoxic Erythrocytes Flowing through a Microfluidic Device.* Analytical Chemistry, 2010. **82**(17): p. 7492-7497.

61. Itoh, Y., et al., *Determination and bioimaging method for nitric oxide in biological specimens by diaminofluorescein fluorometry.* Anal Biochem, 2000. **287**(2): p. 203-9.

62. Nagata, N., K. Momose, and Y. Ishida, *Inhibitory effects of catecholamines and anti-oxidants on the fluorescence reaction of 4,5-diaminofluorescein, DAF-2, a novel indicator of nitric oxide.* J Biochem, 1999. **125**(4): p. 658-61.

63. Kojima, H., et al., *Direct evidence of NO production in rat hippocampus and cortex using a new fluorescent indicator: DAF-2 DA.* NeuroReport, 1998. **9**(15): p. 3345-8.

64. Govers, R., et al., *Endothelial nitric oxide synthase activity is linked to its presence at cell-cell contacts.* The Biochemical journal, 2002. **361**(Pt 2): p. 193-201.

65. Li, L., et al., *Rat C peptide I and II stimulate glucose utilization in STZ-induced diabetic rats.* Diabetologia, 1999. **42**(8): p. 958-964.

66. Joshua, I.G., et al., *Mechanisms of endothelial dysfunction with development of type 1 diabetes mellitus: role of insulin and C-peptide.* J Cell Biochem, 2005. **96**(6): p. 1149-56.

67. Stevens, M.J., et al., *C-peptide corrects endoneurial blood flow but not oxidative stress in type 1 BB/Wor rats.* Am. J. Physiol. Endocrinol. Metab., 2004. **287**(3): p. E497-505.

68. Cotter, M.A., et al., *Effects of proinsulin C-peptide in experimental diabetic neuropathy: vascular actions and modulation by nitric oxide synthase inhibition.* Diabetes, 2003. **52**(7): p. 1812-7.

69. Stevens, M.J., et al., *The linked roles of nitric oxide, aldose reductase and, (Na+,K+)-ATPase in the slowing of nerve conduction in the streptozotocin diabetic rat.* The Journal of clinical investigation, 1994. **94**(2): p. 853-9.

70. Kitamura, T., et al., *Proinsulin C-peptide increases nitric oxide production by enhancing mitogen-activated protein-kinase-dependent transcription of endothelial nitric oxide synthase in aortic endothelial cells of Wistar rats.* Diabetologia, 2003. **46**(12): p. 1698-705.

71. Steffes, M.W., et al., *Beta-cell function and the development of diabetes-related complications in the diabetes control and complications trial.* Diabetes Care, 2003. **26**(3): p. 832-6.

72. Delaney, C., J. Shaw, and T. Day, *Acute, local effects of iontophoresed insulin and C-peptide on cutaneous microvascular function in Type 1 diabetes mellitus.* Diabetic medicine a journal of the British Diabetic Association, 2004. **21**(5): p. 428-33.

73. Forst, T., et al., *Effects of proinsulin C-peptide on nitric oxide, microvascular blood flow and erythrocyte Na+,K+-ATPase activity in diabetes mellitus type I.* Clin Sci (Lond), 2000. **98**(3): p. 283-90.

74. Forst, T., et al., *Biological activity of C-peptide on the skin microcirculation in patients with insulin-dependent diabetes mellitus.* J. Clin. Invest., 1998. **101**(10): p. 2036-41.

75. Sprague, R.S., et al., *ATP: the red blood cell link to NO and local control of the pulmonary circulation.* Am. J. Physiol, 1996. **271**: p. H2717-H2722.

76. Ellsworth, M.L., et al., *The erythrocyte as a regulator of vascular tone.* Am. J. Physiol, 1995. **269**: p. H2155-H2161.

77. Dietrich, H.H., et al., *Red blood cell regulation of microvascular tone through adenosine triphosphate.* Am. J. Physiol, 2000. **278**: p. H1294-H1298.

78. Sprague, R.S., et al., *Impaired release of ATP from red blood cells of humans with primary pulmonary hypertension.* Experimental Biology and Medicine, 2001. **226**(5): p. 434-439.

79. Carroll, J., et al., *An altered oxidant defense system in red blood cells affects their ability to release nitric oxide-stimulating ATP.* Mol Biosyst, 2006. **2**(6-7): p. 305-11.

80. Olsson, R.A. and J.D. Pearson, *Cardiovascular purinoceptors.* Physiol Rev, 1990. **70**(3): p. 761-845.

81. Saenz de Tejada, I., et al., *Cholinergic neurotransmission in human corpus cavernosum. I. Responses of isolated tissue.* Am J Physiol, 1988. **254**(3 Pt 2): p. H459-67.

82. Kimoto, Y., R. Kessler, and C.E. Constantinou, *Endothelium dependent relaxation of human corpus cavernosum by bradykinin.* J Urol, 1990. **144**(4): p. 1015-7.

83. Kim, N., et al., *A nitric oxide-like factor mediates nonadrenergic-noncholinergic neurogenic relaxation of penile corpus cavernosum smooth muscle.* J Clin Invest, 1991. **88**(1): p. 112-8.

84. Azadzoi, K.M. and I. Saenz de Tejada, *Diabetes mellitus impairs neurogenic and endothelium-dependent relaxation of rabbit corpus cavernosum smooth muscle.* J Urol, 1992. **148**(5): p. 1587-91.

85. Burnett, A.L., et al., *Nitric oxide: a physiologic mediator of penile erection.* Science, 1992. **257**(5068): p. 401-3.

86. Trigo-Rocha, F., et al., *Nitric oxide and cGMP: mediators of pelvic nerve-stimulated erection in dogs.* Am J Physiol, 1993. **264**(2 Pt 2): p. H419-22.

87. Saiag, B., et al., *Study of the mechanisms involved in adenosine-5'-O-(2-thiodiphosphate) induced relaxation of rat thoracic aorta and pancreatic vascular bed.* Br J Pharmacol, 1996. **118**(3): p. 804-10.

88. Shalev, M., et al., *Stimulation of P2y purinoceptors induces, via nitric oxide production, endothelium-dependent relaxation of human isolated corpus cavernosum.* J Urol, 1999. **161**(3): p. 955-9.

89. Needham, L., et al., *Characteristics of the P2 purinoceptor that mediates prostacyclin production by pig aortic endothelial cells.* Eur J Pharmacol, 1987. **134**(2): p. 199-209.

90. Mitchell, J.A., et al., *Different patterns of release of endothelium-derived relaxing factor and prostacyclin.* Br J Pharmacol, 1992. **105**(2): p. 485-9.

91. Kalinowski, L., et al., *Third-generation beta-blockers stimulate nitric oxide release from endothelial cells through ATP efflux: a novel mechanism for antihypertensive action.* Circulation, 2003. **107**(21): p. 2747-52.

92. da Silva, C.G., et al., *Mechanism of purinergic activation of endothelial nitric oxide synthase in endothelial cells.* Circulation, 2009. **119**(6): p. 871-9.

93. Xu, H.L., et al., *Agonist-specific differences in mechanisms mediating eNOS-dependent pial arteriolar dilation in rats.* American journal of physiology. Heart and circulatory physiology, 2002. **282**(1): p. H237-43.

94. Chataigneau, T., et al., *Acetylcholine-induced relaxation in blood vessels from endothelial nitric oxide synthase knockout mice.* Br J Pharmacol, 1999. **126**(1): p. 219-26.

95. Osanai, T., et al., *Cross talk of shear-induced production of prostacyclin and nitric oxide in endothelial cells.* Am J Physiol Heart Circ Physiol, 2000. **278**(1): p. H233-8.

96. Samnegard, B., et al., *Effects of C-peptide on glomerular and renal size and renal function in diabetic rats.* Kidney Int, 2001. **60**(4): p. 1258-65.

97. Kamikawa, A., et al., *Proinsulin C-peptide abrogates type-1 diabetes-induced increase of renal endothelial nitric oxide synthase in rats.* Diabetes Metab Res Rev, 2008. **24**(4): p. 331-8.

98. Ohtomo, Y., et al., *Differential effects of proinsulin C-peptide fragments on Na+, K+-ATPase activity of renal tubule segments.* Diabetologia, 1998. **41**(3): p. 287-91.

99. Graciano, M.L., et al., *Purinergic receptors contribute to early mesangial cell transformation and renal vessel hypertrophy during angiotensin II-induced hypertension.* Am J Physiol Renal Physiol, 2008. **294**(1): p. F161-9.

100. Ekberg, K., et al., *C-Peptide replacement therapy and sensory nerve function in type 1 diabetic neuropathy.* Diabetes Care, 2007. **30**(1): p. 71-6.

101. Karunarathne, W., C.J. Ku, and D.M. Spence, *The dual nature of extracellular ATP as a concentration-dependent platelet P2X1 agonist and antagonist.* Integr Biol (Camb), 2009. **1**(11-12): p. 655-63.

102. Anderson, K.B., W. Karunarathne, and D.M. Spence, *Measuring P2X1 receptor activity in washed platelets in the absence of exogenous apyrase.* Analytical Methods, 2012. **4**(1): p. 101-105.

103. Clemetson, K.J., *Platelet activation: signal transduction via membrane receptors.* Thrombosis and haemostasis, 1995. **74**(1): p. 111-6.

104. Heemskerk, J.W., E.M. Bevers, and T. Lindhout, *Platelet activation and blood coagulation.* Thrombosis and haemostasis, 2002. **88**(2): p. 186-93.

105. Dorsam, R.T. and S.P. Kunapuli, *Central role of the P2Y12 receptor in platelet activation.* J Clin Invest, 2004. **113**(3): p. 340-5.

106. Shafqat, J., et al., *Proinsulin C-peptide elicits disaggregation of insulin resulting in enhanced physiological insulin effects.* Cell Mol Life Sci, 2006. **63**(15): p. 1805-11.

Chapter 4 - Determining Endothelial Permeability to C-peptide

4.1 - Biological Activity of C-peptide: Direct and/or Indirect Mechanisms

C-peptide has been shown to act *in vivo* to maintain general health, having influence in various organs and throughout the body. This is evident by C-peptide induced improvements in type 1 diabetic patients who are incapable of producing endogenous C-peptide, including improved nerve conduction and regeneration[1], renal function[2], inflammation,[3] and blood flow.[4] In spite of the importance and scope of these physiological actions, until the work that was presented in Chapter 3 elucidating a mechanism by which C-peptide can improve blood flow, the mechanisms by which C-peptide exerts its beneficial effects *in vivo* were largely unknown. Work presented in Chapter 3 describes how C-peptide is capable of indirectly stimulating NO production in the endothelium via its ability to enhance ATP release from the red blood cell. NO is unique in that it was the first gaseous signaling molecule, inducing vessel dilation by diffusing to the smooth muscle cells that surround blood vessels. C-peptide is secreted into the bloodstream with insulin, however it has never been determined if, like insulin, C-peptide can leave the bloodstream. The work presented in Chapter 3 shows that C-peptide is capable of influencing cell-cell communication and purinergic signaling, allowing C-peptide to expand its influence beyond the bloodstream. However, whether the entirety of C-peptide stimulated bioactivity is a result from its activity in the bloodstream, or if particular activity is a result of direct stimulation by C-peptide in tissue exterior of the bloodstream is still indefinite. In order to potentially influence biological functions directly, the ability of C-peptide to permeate the endothelium to exit the bloodstream will be of obvious importance.

It has been previously shown that C-peptide is able to specifically bind to endothelial cells, which is saturated concentrations of ~ 1 nM, which is of importance since the transport of macromolecules is generally transcellular and specific.[5] This specific binding, however, has not yet been shown by conventional radioligand binding. Currently, a specific receptor for C-peptide has not been identified as the alleged binding structure is elusive. Furthermore, the homology pattern of C-peptide is markedly different from most signaling peptides.[6] However, C-peptide has been shown to be internalized by endosomes to enter human endothelial cells.[7] Additionally, this internalization can be inhibited by nocodazole and monodansylcadaverine (MDC), signifying that C-peptide enters the cell by a mechanism which is receptor mediated (clathrin) and requires microtubule assembly. Interestingly, microtubules have been shown to facilitate transcellular transport and influence endothelial permeability and integrity.[8-11] Additionally, some endothelial cell types have been shown to express PEPT membrane proteins, which are proteins that promiscuously facilitate the transcellular transport of peptides.[12, 13] These results mutually suggest that C-peptide can potentially leave the bloodstream and directly stimulate various cell types exterior of the cardiovascular system. In addition to human endothelial cells, C-peptide can also enter fibroblasts and human embryonic kidney cells where it is capable of influencing gene transcription,[14, 15] suggesting that C-peptide is capable of directly influencing cells exogenous of the bloodstream and again demonstrating the ability of C-peptide to permeate cellular membranes. The ability or inability of C-peptide to permeate a cultured endothelium can provide insight as to whether some biological effects of the peptide are initiated directly, or if all of these effects are a result of activity in the bloodstream.

4.2 - Enzyme-Linked Immunosorbent Assay (ELISA) for C-peptide Detection

ELISA is a powerful method for the detection and quantification of proteins or peptides in complex biological samples. As shown in Figure 4.1, antibodies are used to bind a particular protein or peptide antigen that is of interest, allowing for their detection with great specificity. Briefly, at least one antibody with specificity for a particular antigen of interest is immobilized at the bottom of a well of a microtiter plate. A sample with an unknown amount of antigen is then added to the well where binding occurs to the antibody. After binding for a specific duration of time, the remaining sample is removed, leaving the antigen of interest bound to the antibody, thereby extracting it from often complex biological samples. In order to detect the antigen, generally a secondary antibody that has been bioconjugated to an enzyme is added, and the secondary antibody specifically binds the immobilized antigen. Subsequently, an enzymatic substrate is added to produce a detectable signal such as color change, which is proportional to the quantity of antigen in the sample. Described here is a sandwich ELISA, however other ELISA methods with similar general principles to exist. Importantly, ELISA not only detects proteins and peptides with high specificity, impressive lower detection limits are also commonly achieved. For example, detection limits as low as 200 pg/mL have been reported.[16] Since C-peptide exists at low nanomolar levels *in vivo*, ELISA is a suitable technique for the detection and quantification of C-peptide in complex physiological samples resembling those found in biological systems.

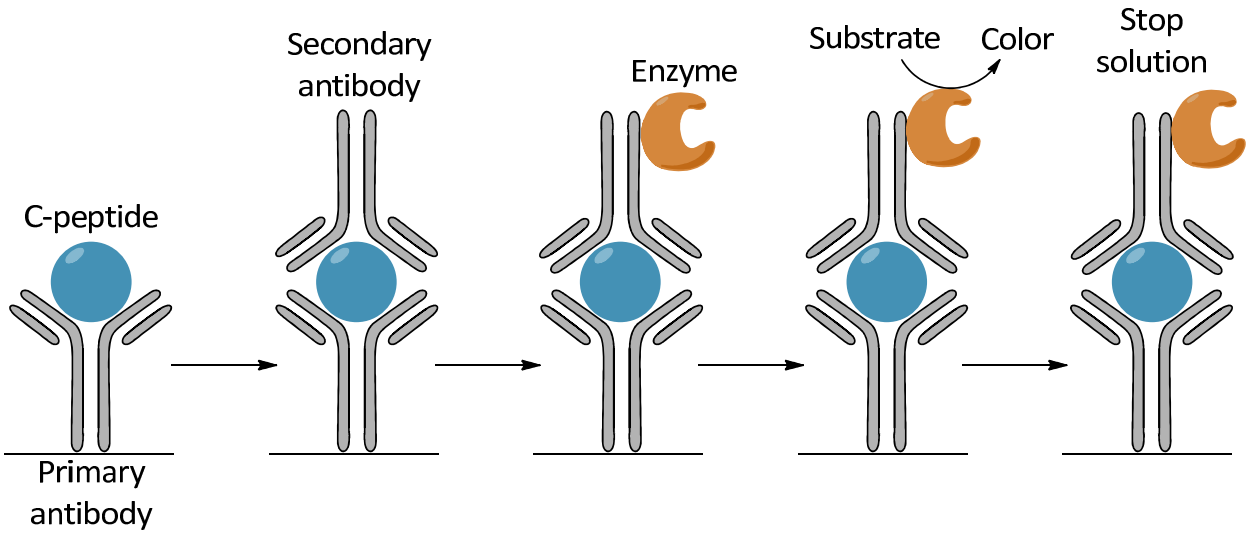

Figure 4.1 - Shown is a diagram illustrating C-peptide detection by sandwich ELISA. Complex biological samples containing C-peptide are added to wells of a 96-well plate, the bottoms of which have been coated with a primary antibody for human C-peptide. C-peptide is allowed to bind to the antibody for a period of time, after which a secondary antibody is added to the solution, which also binds to sandwich C-peptide between the two antibodies. Following incubation, an enzyme is added that binds to the secondary antibody and, subsequently, a substrate is added that allows the catalytic production of a detectable substance by the enzyme. In the case of C-peptide ELISA, this reaction yields a product which changes the color of the solution during the enzymatic process, which is stopped after an interval of time, causing the amount of color produced to be proportional to C-peptide concentration. The absorbance of the solution is read at 450 nm using a multiwell plate reader, allowing for quantification of C-peptide in complex biological samples.

4.3 - Methods

4.3.1 - Bovine Pulmonary Artery Endothelial Cell Culture

General methods for bPAEC culture are described in Chapter 2. Briefly, seeding cells in the wells of a microfluidic device or microtiter insert is accomplished by first coating the polycarbonate membrane with fibronectin. Fibronectin (Invitrogen) and dissolved in phosphate buffered saline (PBS) to prepare a 1000 μg/mL stock solution. The stock solution is aliquoted and frozen until use. When cell seeding is desired, an aliquot of stock solution is thawed and diluted to 100 μg/mL and 10 μL of solution are added to each microfluidic well, or 50 μL are added for microtiter inserts. The solution is allowed to completely evaporate to yield a fibronectin coating on the polycarbonate membrane.

As described in Section 2.2.3, bPAECs are cultured in T-75 tissue culture flasks, and are removed by pipetting 2 mL of a 0.25% trypsin solution onto the cells for 2 minutes. The trypsin solution is removed by aspiration and immediately replaced with 6 mL of cell media. The cells are repeatedly rinsed and the bottom of the flask is gently rapped to promote removal of the adhered cells. The resulting cell suspension is centrifuged at 500 *g* for 5 min. and the supernatant removed. The cells are then resuspended in 1 mL of cell media and 10 μL or 200 μL of the suspension are added to each well of the microfluidic device or microtiter insert, respectively. Cell media is replaced after 1.5 hours, and then again every 3 hours afterwards. For microtiter cell culture inserts, 450 μL of cell media is added for each replacement. If the cells are allowed to incubate overnight, 18 μL of cell media are added to each microfluidic well, and the device is stored in a covered petri dish with a Kimwipe saturated with water in order to

prevent evaporation of the cell media. Microtiter cell culture inserts are also incubated overnight with 450 µL of cell media.

4.3.2 - TEER Measurements

Immediately prior to TEER measurements or experimentation, 1 mL of media is added to each microtiter well containing an insert. Media contained in either the microtiter insert, microtiter well, or microfluidic well was replaced immediately prior to permeability assay or TEER measurement. TEER measurements on a microfluidic device were obtained using the integrated TEER system by methods described in Chapter 2. TEER evaluation of bPAECs cultured in microtiter cell culture inserts was accomplished using a commercially available TEER meter (Millicell-ERS, EMD Millipore). TEER values obtained by the device were normalized to the 1.13 cm^2 cell culture area of the microtiter cell culture inserts by multiplying each TEER value by the cell culture area. Prior to all permeability assays, TEER confirmation of bPAEC monolayer confluence was performed by measuring two sustained TEER measurements. Typically these measurements were obtained 1.5 hours apart, and upon a positive confirmation of cell monolayer confluence a permeability assay was subsequently performed, generally within the following hour.

4.3.3 - Microfluidic C-peptide Permeability Assay: Sample Preparation

Human blood samples were obtained from healthy volunteers by venipuncture. All procedures were followed according to approved Michigan State IRB protocol. Whole blood was collected from the donor into plastic blood collection vials (Becton, Dickinson and Company), each containing 158 USP units of spray-dried lithium heparin to prevent coagulation. The whole blood was then consolidated and centrifuged. After removal of the plasma and

buffy layer by aspiration, RBCs were washed 3 times with a physiological salt solution (PSS, pH 7.4) containing (all from Sigma-Aldrich): 4.7 mM KCl, 2.0 mM $CaCl_2$, 140.5 mM NaCl, 12.0 mM $MgSO_4$, 21.0 mM tris(hydroxymethyl)aminomethane, 5.6 mM glucose, and 5% bovine serum albumin.[17] Crude human C-peptide (Genscript) was purified by HPLC and prepared in distilled and deionized water (DDW, 18.2 MΩ), resulting in an 8.3 μM stock solution which is stored at 4°C. For samples containing Zn^{2+}-activated C-peptide, a 2.0 μM working solution of human C-peptide was prepared in DDW and combined with the same volume of a 2.0 μM Zn^{2+} solution also prepared in DDW.[17] For samples lacking C-peptide and Zn^{2+}, a volume of DDW was added equaling the volume of the other samples, ensuring that the volume of DDW was constant throughout all samples used for a given experiment. After the Zn^{2+} and C-peptide solutions were allowed to rest for around 5 min, PSS was added to the solution, immediately followed by the appropriate volume of washed RBCs, resulting in a solution of RBCs at 7% hematocrit. For samples lacking RBCs, PSS was added in lieu of RBCs to yield a 20 nM C-peptide solution. The appropriate volumes of 2.0 μM Zn^{2+} and 2.0 μM C-peptide working solutions were added so that final concentrations in the 7% RBC samples were always 20 nM.

4.3.4 - Microfluidic C-peptide Permeability Assay: Flow Studies

After bPAEC monolayer confluence was determined by the integrated TEER microfluidic device, existing media was removed from the well and replaced with 12 μL of fresh cell media. The solutions described above were propelled by syringe pumps (Harvard Apparatus) equipped with 500 μL Hamilton Gastight syringes for controlled flow of solution in the microfluidic channels. These solutions were propelled at a flow rate of 1.0 μL/min for 1 hour beneath the

cultured endothelial monolayers where C-peptide may permeate the bPAEC layers and finally reach the overlying cell media that is contained within the microfluidic wells as shown in Figure 4.2. During flow, the microfluidic device and a Kimwipe saturated with water were covered by a petri dish to prevent evaporation. After flow completion, 7 µL of solution were removed from each microfluidic well and diluted 11 or 12 fold in cell media prior to C-peptide determination by ELISA (EMD Millipore). The dilutions were performed so that the final concentration of the solutions rested within the linear range of the assay, typically 0 nM – 2 nM for these particular human C-peptide ELISA kits. ELISA was performed as instructed by included directions, though purified stock C-peptide solutions were used to prepare standard solutions as opposed to C-peptide standard solutions included with the kit in order to accurately represent the matrix of the experimental solutions. A calibration curve, with standards ranging from 0-2 nM, was obtained on each day that microfluidic permeability assays were performed, from which C-peptide concentrations were determined in the solutions within microfluidic wells. These solutions contain only C-peptide that successfully permeates the cultured endothelium from solution flowing in the underlying microchannel.

4.3.5 - Microtiter C-peptide Permeability Assay: Sample Preparation

For samples containing Zn^{2+}-activated C-peptide, a 2.0 µM working solution of human C-peptide was prepared in DDW and combined with the same volume of a 2.0 µM Zn^{2+} solution also prepared in DDW.[17] For samples lacking C-peptide and Zn^{2+}, a volume of DDW was added equaling the volume of the other samples, ensuring that the volume of DDW was constant throughout all samples used for a given experiment. After the Zn^{2+} and C-peptide

solutions were allowed to rest for around 5 min, appropriate amounts of cell media were added to achieve 10 nM, 20 nM, and 30 nM C-peptide solutions. Unfortunately, these experiments do not permit the use of blood samples since RBCs settle in static systems, rendering the system physiologically irrelevant and potentially adversely affecting analyte diffusion and permeation, again highlighting the advantages of microfluidic platforms for permeability assays and biological mimicry.

4.3.6 - Microtiter C-peptide Permeability Assay: Static Studies

Following the confirmation of bPAEC monolayer confluence by the Millicell-ERS TEER meter, the cell media contained in the microtiter inserts and wells was removed. The cell media removed from the cell culture insert was replaced by 450 µL of 10 nM, 20 nM, or 30 nM C-peptide solutions, resulting in the addition of 4.5 pmol, 9 pmol, or 13.5 pmol of C-peptide, respectively. After the addition of C-peptide to the cell culture inserts containing the bPAEC monolayers, 1.0 mL of cell media was added to the wells of the microtiter multiwell plate which contained the inserts, so that the added cell media surrounds the cell culture inserts, completing the diffusion cell as depicted in Figure 4.3. In this experimental platform, C-peptide is added to the apical region of the diffusion cell represented by cell culture inserts, and allowed to pervade the cultured endothelium to the basolateral region, represented by the microtiter wells. The microtiter multiwell plate is then sealed with a plastic multiwell plate sealer to prevent solution evaporation and then allowed to rest in the incubator (37°C) for 3.5 hours, during which C-peptide permeation from the apical region of the monolayer to the basolateral region.

Following this incubation, dilutions of the solutions contained within the cell culture inserts and microtiter wells were performed so that the resulting C-peptide concentrations fell within the linear range of ELISA. Typically, for example, if 4.5 pmol of C-peptide was added, the solutions in the cell culture insert were diluted 6 fold and the solutions from the surrounding wells were diluted 2 fold. Similarly, when a total of 9 pmol of C-peptide is added, the solutions in the microtiter inserts and wells underwent 11 fold and 2 fold, respectively. Finally, in cases where the amount of C-peptide added totaled 13.5 pmol, 18 fold and 3 fold dilutions of the solutions contained in the microtiter inserts and wells were performed, respectively. The C-peptide content of the solutions resulting from these dilutions was determined by ELISA and correlated back to determine the amount of C-peptide contained in the original solutions extracted from the diffusion cell prior to dilution.

4.4 - Results

4.4.1 - Microfluidic Assay of C-peptide Endothelial Permeability

The ability of C-peptide to permeate a cultured endothelium was investigated by the microfluidic vascular mimic, in conjunction with ELISA. Specifically, a physiological solution containing C-peptide was allowed to flow beneath a cultured monolayer of bPAECs for 1 hour, and C-peptide was allowed to permeate the cell layer to reach an overlying cell media solution contained by a microfluidic well that initially lacked C-peptide. Importantly, these bPAEC monolayers are characterized by the integrated TEER microfluidic system and deemed confluent by multiple sustained TEER measurements prior to permeability studies. Initially, a collective average TEER value for the bPAEC monolayers included in permeability assays of 3.69 ± 0.26 μC was obtained, followed by an average value of 3.67 ± 0.22 μC approximately 1.5

hours later, resulting in an average change in TEER of 0.15 ± 0.06 μC. The content of C-peptide contained by the basolateral solutions within the microfluidic wells was investigated by determining C-peptide concentration via ELISA. Any C-peptide contained within these basolateral solutions was capable of permeating the monolayer and, therefore, their C-peptide concentration was used to gauge ability of C-peptide to permeate the endothelium.

The C-peptide concentrations determined within these solutions are displayed in Figure 4.2. In the case where a 7% RBC solutions containing 20 nM C-peptide were flowed, the final C-peptide concentration of the basolateral cell media solutions overlying the confluent endothelial layers reached 17.09 ± 2.00 nM, as determined by ELISA. However, when a physiological solution lacking RBCs was streamed beneath the cultured endothelial layers, the overlying cell media solutions reached 18.91 ± 1.91 nM C-peptide concentrations. These 20 nM C-peptide solutions that either included RBCs, or lacked RBCs, were also flowed beneath bare polycarbonate membranes, and C-peptide that was allowed to permeate these membranes that were devoid of any bPAEC layers to finally reach the overlying cell media solutions. By flowing 20 nM C-peptide solutions containing 7% RBCs, the overlying solutions were verified by ELISA to contain 18.31 ± 1.93 nM C-peptide in the absence of bPAEC monolayers. Also, in the absence of RBCs, the flowing 20 nM C-peptide solution beneath bare polycarbonate membranes caused the basolateral solutions to reach 19.91 ± 1.62 nM C-peptide concentrations. In order to confirm that the biological matrices of the solutions investigated by ELISA were not influencing experimental results, a physiological solution lacking C-peptide, but containing RBCs at 7% hematocrit was flowed beneath the cell layer, and the basolateral solution overlying the bPAECs was found to contain 0.12 ± 0.69 nM C-peptide.

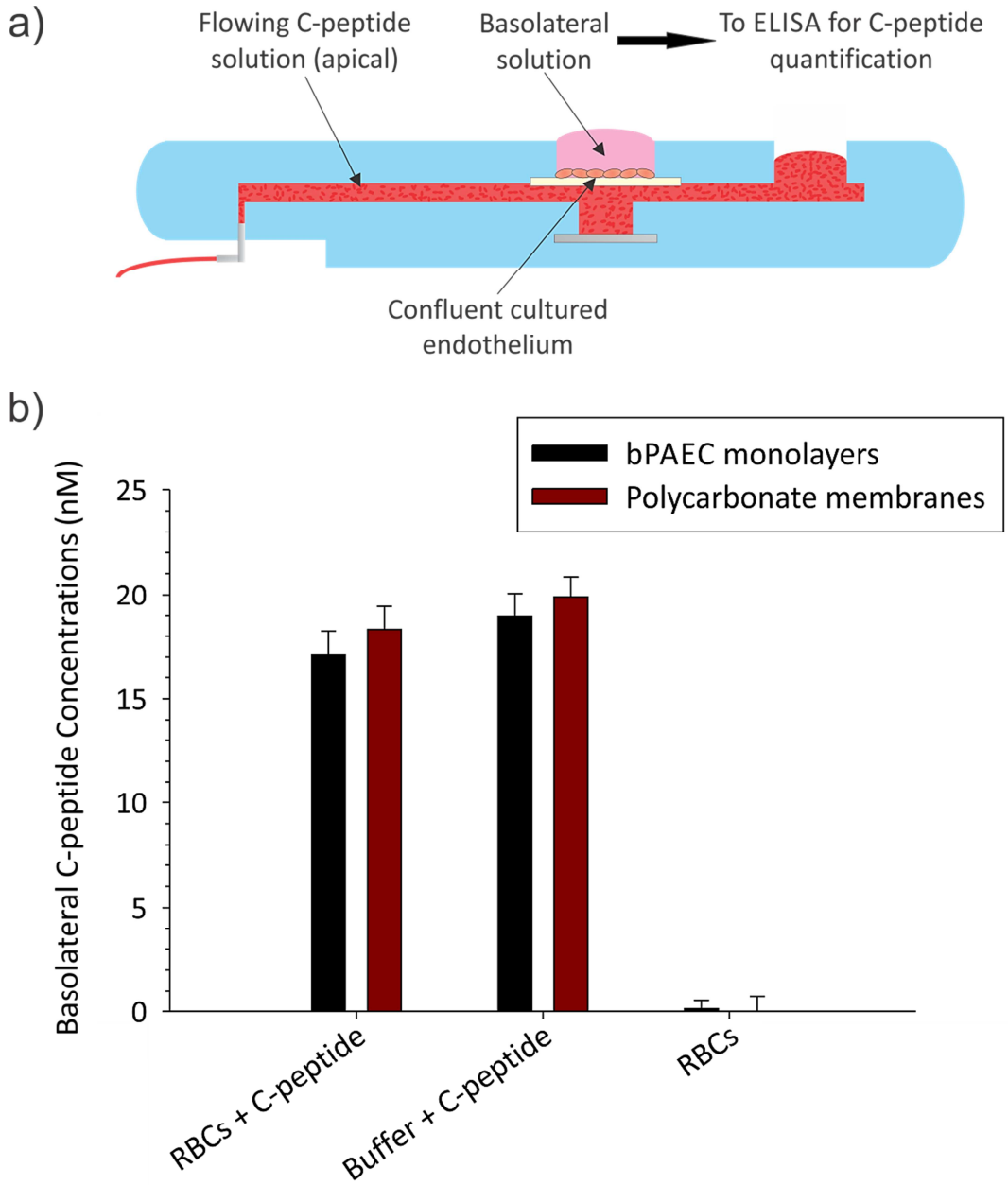

Figure 4.2 - A cross-sectional view of one channel of the microfluidic vascular mimic used to assess the permeability of a pulmonary endothelium to C-peptide under flow conditions is shown in (a). The permeation of C-peptide was monitored by detecting, via ELISA, C-peptide that permeates to basolateral solutions (in 30 minutes) from flowing apical solutions containing 20 nM C-peptide. As shown in (b), it was found that basolateral solutions overlying a cultured endothelium (black bars) reached 17.09 ± 1.16 nM and 18.91 ± 1.11 nM C-peptide concentrations when flowing C-peptide solutions either contained, or did not contain RBCs, respectively. Additionally, when endothelial layers were not cultured on polycarbonate membranes (red bars), and flowing apical solutions either contained, or did not contain RBCs, the basolateral solutions reached 18.31 ± 1.12 nM and 19.91 ± 0.94 nM C-peptide concentrations, respectively. Also, as a negative control, if C-peptide is not added to apical solutions, negligible C-peptide concentrations were found. (n=3, errors are SEM)

4.4.2 - Static Microtiter Assay of C-Peptide Endothelial Permeability

The ability of C-peptide to permeate a cultured endothelium was also investigated with microtiter techniques. In this construct, bPAECs were cultured in microtiter cell culture inserts, and confirmed confluent by multiple sustained TEER measurements obtained using a Millicell-ERS TEER meter. Collectively, initial TEER values to confirm bPAEC confluence averaged 190.26 ± 7.65 $\Omega \cdot cm^2$, which were followed by measurements obtained approximately 1.5 hours later, averaging 190.92 ± 4.90 $\Omega \cdot cm^2$, resulting in an average change in TEER of 4.90 ± 2.23 $\Omega \cdot cm^2$ over the specified time period. In contrast, for cell culture inserts not containing bPAEC monolayers, average TEER values of 139.74 ± 3.96 $\Omega \cdot cm^2$ were obtained. By using this experimental platform, solution flow and the inclusion of RBCs was not permitted. Instead, after TEER evaluation, 10 nM, 20 nM, and 30 nM C-peptide solutions prepared in cell media were added to the microtiter cell culture inserts, resulting in the total addition of 4.5 pmol, 9 pmol, or 13.5 pmol of C-peptide, respectively. For 3.5 hours following C-peptide addition, C-peptide was allowed to potentially permeate the confluent cell layer and reach the solution contained by the microtiter well in which the cell culture insert rests. C-peptide content was determined in the apical and basolateral compartments of the diffusion cell by ELISA and presented in Table 4.1.

When a total of 4.5 pmol of C-peptide is added to the diffusion cell, 4.11 ± 0.44 pmol are recovered from the apical region and 0.54 ± 0.6 pmol are recovered from the basolateral region after the allotted time period. Similarly, when 9 pmol of C-peptide is initially added, 7.67 ± 0.37 pmol and 1.12 ± 0.08 pmol of C-peptide is detected in the apical and basolateral regions, respectively. Finally, when 13.5 pmol is initially added to the apical region of the diffusion cell,

11.92 ± 0.46 pmol and 1.57 ± 0.26 pmol of C-peptide is ultimately detected in the apical and basolateral regions, respectively. Alternatively, in diffusion cells not containing cultured bPAEC monolayers, if 9 pmol of C-peptide is added to the apical side of the bare polycarbonate membrane, the amounts of C-peptide detected in the apical and basolateral regions totaled 5.50 ± 0.27 pmol and 3.98 ± 0.27 pmol, respectively.

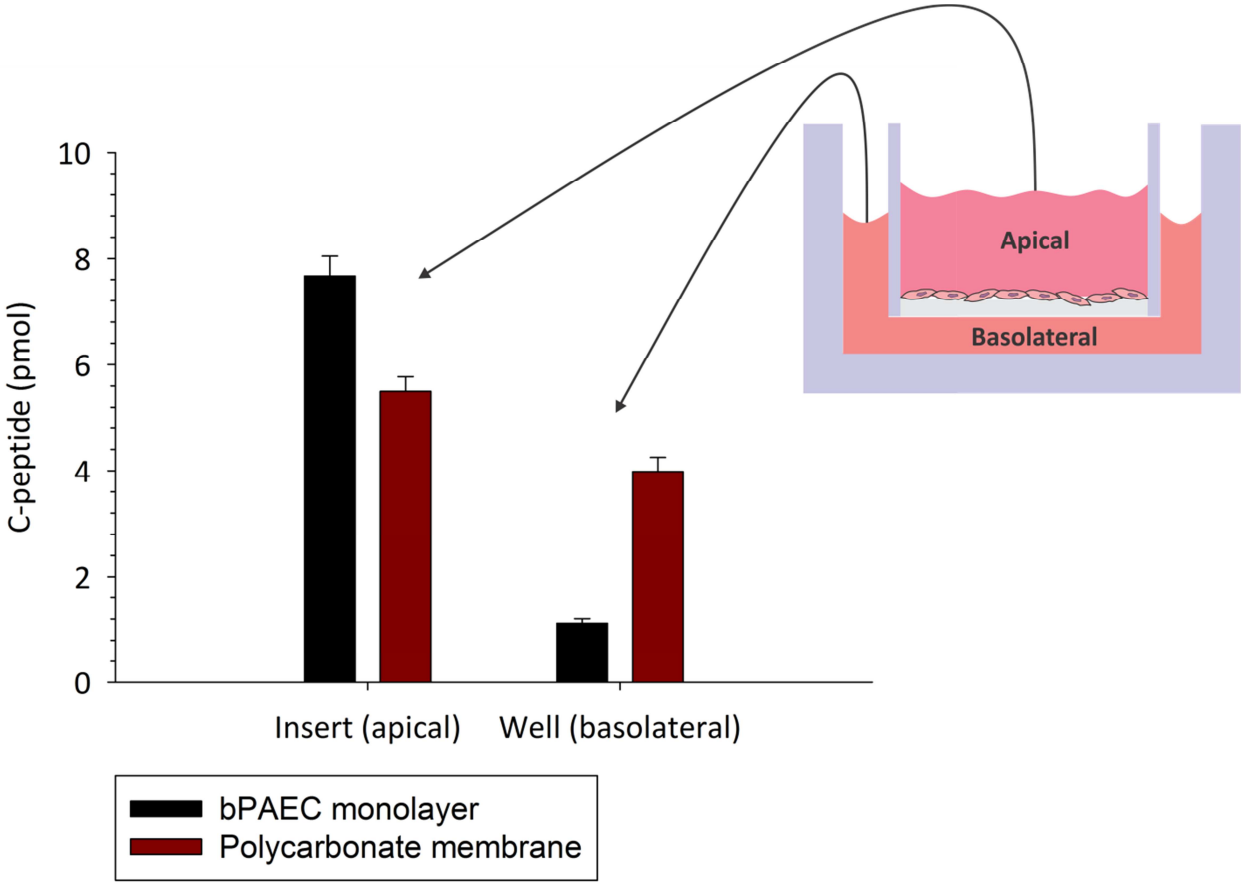

Figure 4.3 - The permeability of the pulmonary endothelium to C-peptide was investigated by monitoring C-peptide permeation from the apical compartment of a microtiter diffusion cell, pictured in the upper right, to the basolateral compartment. 9 pmol of C-peptide is added to the apical compartment and, after 3.5 hours of rest, C-peptide in each compartment is quantified by ELISA and reported. As the graph shows, when 9 pmol of C-peptide is initially added and allowed to permeate a confluent bPAEC layer (black bars), 7.67 ± 0.37 pmol and 1.12 ± 0.08 pmol of C-peptide is detected in the apical and basolateral regions, respectively. However, if 9 pmol of C-peptide is added to the apical side of a bare polycarbonate membrane (red bars), the amounts of C-peptide detected in the apical and basolateral regions totaled 5.50 ± 0.27 pmol and 3.98 ± 0.27 pmol, respectively. (n=4, Errors are SD)

Table 4.1 - The permeability of an endothelial monolayer to C-peptide was investigated by performing microtiter permeability assays, the results of which are reported here. C-peptide was quantified in the basolateral and apical compartments via ELISA 3.5 hours after adding varying quantities of C-peptide to apical compartments. Prior to each permeability assay, proper bPAEC barrier function was confirmed by measuring TEER. (n=4, Errors are SD)

C-peptide added (pmol)	bPAECs	Apical C-peptide (pmol)	Basolateral C-peptide (pmol)	Average TEER ($\Omega \cdot cm^2$)
4.5	yes	4.11 ± 0.44	0.54 ± 0.06	190.4 ± 5.4
9	yes	7.67 ± 0.37	1.12 ± 0.08	188.1 + 6.4
13.5	yes	11.92 ± 0.046	1.57 ± 0.26	194.2 ± 6.2
9	no	5.50 ± 0.27	3.98 ± 0.27	-

4.5 - Discussion

Determining the ability of C-peptide to permeate an endothelial layer *in vitro* would be a significant contribution towards determining if the peptide can escape the bloodstream *in vivo*. Importantly, since C-peptide is confirmed to be a bioactive peptide,[18] and is important for regulating many fundamental biological functions throughout the body as discussed earlier, a mechanistic understanding of these activities could be quite lucrative, scientifically. However, most of the discovered anatomically diverse biological impacts of C-peptide on the cardiovascular system and other organs are not currently understood mechanistically, or otherwise. In fact, aside from the work presented in Chapter 3, it has not yet been determined if C-peptide acts to induce biological events in various anatomical locations by directly interacting with the cell types that are primarily responsible for a specific event, or if these events are indirect consequences of C-peptide activity in the blood stream. The capability of C-peptide to act by direct mechanisms throughout the body is dependent on the ability of C-

peptide to permeate the endothelium *in vivo*. Therefore, all direct mechanisms can potentially be ruled out by showing that C-peptide is incapable of penetrating an endothelial layer since such findings would strongly suggest that C-peptide is confined to the bloodstream *in vivo*. For these reasons, in addition to the results presented in Chapter 3 showing that C-peptide acts indirectly to influence purinergic signaling, the ability of C-peptide to permeate a cultured endothelium was investigated.

In order to determine the ability of C-peptide to permeate an endothelial layer, a microfluidic vascular mimic was used in conjunction with conventional microtiter techniques. These two platforms have stark differences however, with microfluidic technology allowing for the flow of RBCs and, in contrast, microtiter technology is a static system and, therefore, does not permit flow. Additionally, the inclusion of RBCs is physiologically irrelevant in a static system, especially considering the tendency of RBCs to sink in static solutions, which would cause RBCs to coat the apical membrane and influence the diffusion and permeation of analytes between the apical and basolateral compartments. Furthermore, the work presented in Chapter 3 describes how RBCs can drastically influence endothelial cells, namely by their ability to release ATP, which ultimately stimulates endothelial nitric oxide synthase (eNOS). Importantly, eNOS has been shown to play a predominant role in regulating vascular permeability *in vivo*,[19-21] and furthermore, flowing RBCs have been shown to release more ATP than static RBCs.[22, 23] Since endothelial barrier integrity is the primary determinant of vascular permeability,[24] flowing RBCs will ideally be present in a vascular model, an important shortcoming to consider when performing microtiter based permeability assays.

Perhaps the most important aspect of a physiologically relevant vascular model is the incorporation of shear stress generated by flowing blood. For instance, shear stress has been shown to increase eNOS activity that, as stated earlier, plays a role in vascular permeability by influencing the barrier integrity of the endothelium. Also, in addition to increasing ATP release from RBCs, shear influences the metabolic state of RBCs,[25] as well as interactions between flowing RBCs that can lead to changes in viscosity and aggregation.[26] While the ability to increase eNOS activity is of fundamental importance, especially for permeation research, shear stress impacts endothelial cell behavior even more drastically. For example, shear stress alters endothelial morphology,[27] tissue factor expression,[28] signal transduction between adjacent endothelial cells,[29] intracellular signaling,[30, 31] and gene expression.[32, 33] Collectively, this myriad of influences makes shear stress a principal determinant of endothelial cell behavior and health.[34] Summarily, in contrast to microfluidic systems, microtiter technology does not account for the dramatic role of the RBC or shear stress in vascular function.

Furthermore, a microfluidic platform enables the flow of a solution with a specific C-peptide concentration which, in this case, is more physiologically correct than adding a finite amount since the concentration of circulating C-peptide is relatively constant *in vivo*. For these reasons, recovered C-peptide is reported as a concentration and an amount for microfluidic and microtiter permeability studies, respectively. Not surprisingly, the inherent differences between the two platforms influence experimental results, as well as perception of these results. For example, when employing the microfluidic vascular mimic to determine the ability of C-peptide to permeate a cultured endothelium, a 20 nM C-peptide solution flowing apical to the cell monolayer and not containing RBCs resulted in enough C-peptide permeating the cultured

endothelium to ultimately raise the overlying basolateral solution, which initially lacks C-peptide, to 18.91 ± 1.91 nM within an hour. In contrast, after adding a 20 nM C-peptide solution also not containing RBCs, for a total of 9 pmol, to the apical compartment of a microtiter diffusion cell, 1.12 ± 0.08 pmol of C-peptide successfully permeated the endothelial monolayer to the basolateral compartment in 3.5 hours.

Interestingly, the microfluidic permeability assay provides the unique perception that the basolateral solution nearly equilibrates with the apical flowing solution within an hour. In contrast, in over triple the time allotted for the microfluidic assay, the microtiter permeability assay reveals that only about 10% of the total C-peptide added to the apical compartment of the diffusion cell successfully reaches the basolateral compartment, which actually contains a higher volume of solution than the apical compartment. In fact, this was the case for each microtiter based permeability assay, regardless of the quantity of C-peptide added. However, these results are to be expected since shear has been shown to influence changes in endothelial permeability.[35] As an example, one study shows that shear stress can increase the permeability of a cultured endothelium 4-fold compared to an endothelium under static conditions.[36] Interestingly however, since the microfluidic wells contained only 12 µL of solution, only about 0.23 pmol of C-peptide would have to permeate the endothelial layer to result in a 19 nM solution. Hypothetically, if it took a full hour for this to occur, only 0.8 pmol would permeate to the basolateral solution in the same timeframe allotted in the microtiter permeability assay, suggesting the two results may not be so contrasting and also further highlight the varying perspectives that each platform provides. Obviously, in order to confirm this, the kinetics of this equilibration would need to be determined for the basolateral solution

in the microfluidic vascular mimic. Regardless, due to the small sample volumes typical of microfluidic systems, C-peptide permeation can be determined in a shorter duration than with microtiter systems. However, even considering the short duration of the microfluidic permeability assay, the ability of the endothelial monolayer to hinder C-peptide permeation to the basolateral region was not observed as it was microtiter permeability assay when 1.12 ± 0.08 pmol of C-peptide was detected in the basolateral chamber when the diffusion cell contained a cultured endothelium, compared to 3.98 ± 0.27 pmol detected when it did not.

Another aspect of the microfluidic approach towards studying permeation is the ability to determine the influence of blood or other common biological matrices on analyte permeation. For example, if blood was included in the flowing physiological C-peptide solution, the basolateral solution reached 17.09 ± 2.00 nM, compared to 18.91 ± 1.91 nM for a flowing solution lacking RBCs. While not statistically different, the basolateral solutions slightly differed in concentration by around 2 nM, depending on the presence of RBCs. This effect was again observed when bPAECs were not cultured on the polycarbonate membrane and the flowing 20 nM C-peptide solutions containing RBCs, or lacking RBCs, resulted in basolateral solution concentrations of 18.31 ± 1.93 nM and 19.91 ± 1.62 nM, respectively. Interestingly, unpublished data from our group has reproducibly shown that in a RBC solution at 7% hematocrit, C-peptide is able to interact with the RBC and thus lower the concentration of free C-peptide in the solution by 2 nM. Collectively, these data suggest that interactions between the RBC and C-peptide may act to lower the concentration of bioavailable C-peptide *in vivo*, which may be considerable since C-peptide is typically found at single-digit nanomolar levels in the bloodstream. Similarly, a small change can be observed that is dependent on the presence

of endothelial cells. While not statistically significant, after 1 hour of flow in the absence of endothelial cells, each measurement of C-peptide concentration in basolateral solutions is approximately 1 nM lower than in the presence of endothelial cells. While this change is slight, it is interesting that C-peptide has been shown to specifically bind to endothelial cells via an event that is saturated at approximately 1 nM levels.[5, 37]

Despite such vast differences, a strength shared by each platform is the ability to confirm endothelial monolayer confluence and barrier integrity. Clearly, a confirmation of barrier integrity is incredibly advantageous, especially for permeability assays, adding significant credibility to experimental results and conclusions stemming from these experimental results. In the permeability studies presented, multiple sustained TEER measurements were obtained as verification of bPAEC confluence. These measurements, typically obtained 1.5 hours apart, yielded dismal changes over time, averaging to 0.15 ± 0.06 μC and 4.90 ± 2.23 $\Omega \cdot cm^2$ for the microfluidic and microtiter assays, respectively. These confirmations that every cultured endothelium used to assay C-peptide permeation formed confluent barriers increase the likelihood that results derived from these assays will correlate to true activity *in vivo*.

An additional similarity between the two experimental platforms is that each technique conclusively confirms that C-peptide is capable of permeating a cultured endothelium. These results suggest that C-peptide may be able to perform biological functions by direct and indirect stimulation of cell types throughout the body. If C-peptide is truly capable of escaping the bloodstream, it may act as an important hormone that functions universally in the body, similar to insulin. This activity would support the recent concept that type 1 diabetes is actually a double-hormone deficiency disorder, with late complications potentially being derived from

chronic lack of C-peptide.[18] These results, in conjunction with the ability of C-peptide to specifically bind,[5, 37] and also become internalized by endothelial cells,[7] suggest that C-peptide likely has an endothelial transcellular transport mechanism. This is further supported by C-peptide's ability to be internalized by,[7, 14] and induce biological events in cell types exterior to the bloodstream.[15]

4.6 - Conclusions

In summary, these results are the first to suggest that C-peptide is capable of permeating the endothelium *in vitro*, implying that C-peptide can likely also permeate the endothelium in vivo. These findings suggest that, in addition to indirect influences shown in Chapter 3, C-peptide may have direct influences on various cell types throughout the body. Since C-peptide has never been detected exterior of the bloodstream, these novel findings suggest that C-peptide may have a much more comprehensive role in physiology and health than is currently assumed.

REFERENCES

REFERENCES

1. Pierson, C.R., W. Zhang, and A.A. Sima, *Proinsulin C-peptide replacement in type 1 diabetic BB/Wor-rats prevents deficits in nerve fiber regeneration.* Journal of Neuropathology and Experimental Neurology, 2003. **62**(7): p. 765-79.

2. Maezawa, Y., et al., *Influence of C-peptide on early glomerular changes in diabetic mice.* Diabetes/metabolism research and reviews, 2006. **22**(4): p. 313-22.

3. Sima, A.A., et al., *Inflammation in Diabetic Encephalopathy is Prevented by C-Peptide.* Rev Diabet Stud, 2009. **6**(1): p. 37-42.

4. Lindstrom, K., et al., *Acute effects of C-peptide on the microvasculature of isolated perfused skeletal muscles and kidneys in rat.* Acta Physiol Scand, 1996. **156**(1): p. 19-25.

5. Rigler, R., et al., *Specific binding of proinsulin C-peptide to human cell membranes.* Proc. Natl. Acad. Sci., 1999. **96**: p. 13318-13323.

6. Henriksson, M., et al., *Separate functional features of proinsulin C-peptide.* Cell Mol Life Sci, 2005. **62**(15): p. 1772-8.

7. Luppi, P., et al., *C-peptide is internalised in human endothelial and vascular smooth muscle cells via early endosomes.* Diabetologia, 2009. **52**(10): p. 2218-28.

8. Minshall, R.D. and A.B. Malik, *Transport across the endothelium: regulation of endothelial permeability.* Handb Exp Pharmacol, 2006(176 Pt 1): p. 107-44.

9. Minshall, R.D., et al., *Vesicle formation and trafficking in endothelial cells and regulation of endothelial barrier function.* Histochem Cell Biol, 2002. **117**(2): p. 105-12.

10. Lossinsky, A.S. and R.R. Shivers, *Structural pathways for macromolecular and cellular transport across the blood-brain barrier during inflammatory conditions. Review.* Histol Histopathol, 2004. **19**(2): p. 535-64.

11. Le Sueur, L.P., C.B. Collares-Buzato, and M.A. da Cruz-Hofling, *Mechanisms involved in the blood-brain barrier increased permeability induced by Phoneutria nigriventer spider venom in rats.* Brain Research, 2004. **1027**(1-2): p. 38-47.

12. Groneberg, D.A., et al., *Distribution and function of the peptide transporter PEPT2 in normal and cystic fibrosis human lung.* Thorax, 2002. **57**(1): p. 55-60.

13. Meredith, D. and C.A. Boyd, *Dipeptide transport characteristics of the apical membrane of rat lung type II pneumocytes.* Am J Physiol, 1995. **269**(2 Pt 1): p. L137-43.

14. Lindahl, E., et al., *Cellular internalization of proinsulin C-peptide.* Cell. Mol. Life Sci., 2007. **64**: p. 479-486.

15. Lindahl, E., et al., *Proinsulin C-peptide regulates ribosomal RNA expression.* J Biol Chem, 2010. **285**(5): p. 3462-9.

16. Leith, A.G., G.D. Griffiths, and M.A. Green, *Quantification of ricin toxin using a highly sensitive avidin/biotin enzyme-linked immunosorbent assay.* J Forensic Sci Soc, 1988. **28**(4): p. 227-36.

17. Meyer, J.A., et al., *Metal-activated C-peptide facilitates glucose clearance and the release of a nitric oxide stimulus via the GLUT1 transporter.* Diabetologia, 2008. **51**(1): p. 175-82.

18. Wahren, J., K. Ekberg, and H. Jornvall, *C-peptide is a bioactive peptide.* Diabetologia, 2007. **50**: p. 503-509.

19. Fukumura, D., et al., *Predominant role of endothelial nitric oxide synthase in vascular endothelial growth factor-induced angiogenesis and vascular permeability.* Proc Natl Acad Sci U S A, 2001. **98**(5): p. 2604-9.

20. Hutcheson, I.R., B.J. Whittle, and N.K. Boughton-Smith, *Role of nitric oxide in maintaining vascular integrity in endotoxin-induced acute intestinal damage in the rat.* Br J Pharmacol, 1990. **101**(4): p. 815-20.

21. Fukumura, D., et al., *Role of nitric oxide in tumor microcirculation. Blood flow, vascular permeability, and leukocyte-endothelial interactions.* Am J Pathol, 1997. **150**(2): p. 713-25.

22. Sprung, R.J., R.S. Sprague, and D.M. Spence, *Determination of ATP release from erythrocytes using microbore tubing as a model of resistance vessels in vivo.* Anal. Chem., 2002. **74**: p. 2274-2278.

23. Price, A., K., et al., *Deformation-induced release of ATP from erythrocytes in a poly(dimethylsiloxane)-based microchip with channels that mimic resistance vessels.* Analytical Chemistry, 2004. **76**(16): p. 4849-55.

24. Cines, D.B., et al., *Endothelial cells in physiology and in the pathophysiology of vascular disorders.* Blood, 1998. **91**(10): p. 3527-61.

25. Murphy, J.R., *Erythrocyte Metabolism. Vi. Cell Shape and the Location of Cholesterol in the Erythrocyte Membrane.* J Lab Clin Med, 1965. **65**: p. 756-74.

26. Brooks, D.E., J.W. Goodwin, and G.V. Seaman, *Interactions among erythrocytes under shear.* Journal of applied physiology (Bethesda, Md. 1985), 1970. **28**(2): p. 172-7.

27. Davies, P.F., *Flow-mediated endothelial mechanotransduction.* Physiol Rev, 1995. **75**(3): p. 519-60.

28. Grabowski, E.F. and F.P. Lam, *Endothelial cell function, including tissue factor expression, under flow conditions.* Thrombosis and haemostasis, 1995. **74**(1): p. 123-8.

29. Lehoux, S. and A. Tedgui, *Signal transduction of mechanical stresses in the vascular wall.* Hypertension, 1998. **32**(2): p. 338-45.

30. Li, Y.S., J.H. Haga, and S. Chien, *Molecular basis of the effects of shear stress on vascular endothelial cells.* J Biomech, 2005. **38**(10): p. 1949-71.

31. Lehoux, S., Y. Castier, and A. Tedgui, *Molecular mechanisms of the vascular responses to haemodynamic forces.* Journal of internal medicine, 2006. **259**(4): p. 381-92.

32. Malek, A.M. and S. Izumo, *Control of endothelial cell gene expression by flow.* J Biomech, 1995. **28**(12): p. 1515-28.

33. Resnick, N., et al., *Endothelial gene regulation by laminar shear stress.* Adv Exp Med Biol, 1997. **430**: p. 155-64.

34. Chatzizisis, Y.S., et al., *Role of endothelial shear stress in the natural history of coronary atherosclerosis and vascular remodeling: molecular, cellular, and vascular behavior.* J Am Coll Cardiol, 2007. **49**(25): p. 2379-93.

35. Jo, H., et al., *Endothelial albumin permeability is shear dependent, time dependent, and reversible.* Am J Physiol, 1991. **260**(6 Pt 2): p. H1992-6.

36. Sill, H.W., et al., *Shear stress increases hydraulic conductivity of cultured endothelial monolayers.* Am J Physiol, 1995. **268**(2 Pt 2): p. H535-43.

37. Pramanik, A., et al., *C-Peptide Binding to Human Cell Membranes: Importance of Glu27.* Biochem. Biophys. Res. Comm, 2001. **284**: p. 94-98.

Chapter 5 - Conclusions and Future Directions

5.1 - Conclusions

5.1.1 - Microfluidic TEER Measurement Device

Since the 1980s, microfluidic technologies have filled important niches in many scientific fields.[1, 2] More recently, microfluidics have been shown to be very useful for *in vitro* cell based assays, in particular the study of cellular monolayers or single cells, due to their unsurpassed ability to control cellular environments and mimic biological systems found *in vivo*.[3-7] However, *in vitro* cell culture and analysis is a longstanding science that has been consistently advancing since the 1910s,[8, 9] with cellular monolayers being cultured and studied as early as the 1920s.[10, 11] Over time, as the understanding of the physiological importance cellular monolayers increased, monolayer barrier integrity became a well-studied research topic by the 1950s, especially in regards to the impact of confluence and barrier integrity on cell behavior.[12-14] To meet this demand, TEER measurement devices have been made commercially available since the mid-1980s and have been further developed for the high throughput analysis of monolayer barrier integrity. However, regardless of the knowledge acquired from ongoing work building on research initiated in the 1950s showing the importance of quantitatively measuring barrier integrity to ensure appropriate cellular behavior and response, the copious amounts of microfluidic assays of cellular monolayers have not included such measurements. This is especially surprising since cellular monolayers have been routinely cultured in microfluidic devices for over a decade.[15, 16] Within the past two years, the first microfluidic devices capable of determining barrier integrity by measuring analyte

permeability,[17] or TEER,[18-21] have appeared in literature, which includes the microfluidic TEER system presented in Chapter 2, indicating the necessity for such devices.

Collectively, these devices and the microfluidic TEER measurement device presented in Chapter 2 finally addresses the long withstanding need for a microfluidic platform with monolayer barrier characterization capabilities. However, the microfluidic device presented in Chapter 2 is novel as it is the first microfluidic capable of measuring barrier integrity that serves as a vascular mimic, and also the first microfluidic device capable of monitoring barrier integrity that has been further utilized to observe real biological events.[21] For example, work presented in chapter 3 shows that confluent endothelial cells, as determined by the microfluidic TEER system, are capable of producing significantly more nitric oxide (NO) in response to flowing red blood cells (RBCs) than non-confluent cells, a difference that is statistically significant. These results highlight the importance of confirming monolayer confluence prior to investigations involving the monolayer, since important physiological responses are sometimes drastically altered by the extent of cell layer confluence.

Additionally, the simplicity of the design and construction of the device adds to its novelty, as similar devices are considerably more complicated in comparison, facilitating the unique potential for the successful integration of the TEER system with preexisting microfluidic platforms via the same design strategy employed during this work to develop the TEER device. Since measuring TEER of a cellular monolayer cultured in a microfluidic device can provide the same fundamental information and physiological accuracy as in conventional platforms, it is expected that the development of this technology has provided the necessary foundation so that TEER measurements can, and optimistically will be, used as extensively and routinely in

microfluidics as they are in other platforms. In any event, the work described throughout involving cellular monolayers is benefitted by the TEER measurement capabilities of the microfluidic vascular mimic. Given the ability to confirm and monitor cell monolayer confluence, cellular responses were consistently of optimal physiological relevance and occasionally enhanced, such as it was for RBC stimulated NO production in confluent endothelial cells mentioned previously. Additionally, a dramatic increase experimental reproducibility was accomplished as a result of the ability to investigate cellular responses with consistently optimal physiological relevance, which surely enhances the accuracy and applicability of conclusions stemming from these investigations, adding credibility to the work. While these advantages illustrate the importance of confirming monolayer confluence prior to experimentation, they also exhibit the ability of this particular device to mimic the vasculature with unparalleled biological accuracy as a result of its integrated TEER measurement capabilities.

5.1.2 - C-peptide Induced Vasodilation

Previously, C-peptide has been shown to improve blood flow in diabetic patients by an unknown mechanism.[22, 23] Interestingly, separate studies have shown that, diabetic complications related to blood flow are related to endothelial dysfunction,[24] and a potent vasodilator, nitric oxide.[25] Also previously, our group has established that C-peptide, if activated by Zn^{2+}, is capable of increasing ATP release from RBCs.[26] Interestingly, ATP has been shown to bind endothelial P2Y, a purinoreceptor capable of initiating a purinergic signaling cascade which results in endothelial nitric oxide synthase (eNOS) activation, the enzyme responsible for producing and regulating NO in the endothelium. Mindful of these

previous findings, it was hypothesized that C-peptide is capable of indirectly participating in purinergic signaling, as mediated by C-peptide stimulated release of ATP from RBCs, which ultimately results in increased endothelial NO production. Since NO derived from the endothelium has been identified as one of the most potent vasodilators yet discovered,[27] if C-peptide was determined to increase endothelial NO production, it would provide an explanation for C-peptide induced improvements in diabetic blood flow. The microfluidic vascular mimic with integrated TEER capabilities developed during the work presented in Chapter 2 was employed to examine the proposed mechanism of C-peptide induced endothelial NO production in work described in Chapter 3.

In order to examine the proposed mechanism, RBC solutions containing Zn^{2+}-activated C-peptide were flowed in the channels of the vascular mimic beneath a cultured endothelium, and intracellular endothelial NO production was measured and compared to NO production resulting from flowing RBC solutions not containing C-peptide. It was determined that flowing RBC solutions containing Zn^{2+}-activated C-peptide are capable of increasing endothelial NO production by almost 90% relative to RBC solutions lacking C-peptide. Interestingly, this effect was not observed if physiological RBC solutions containing only Zn^{2+}, or only C-peptide were flowed beneath the endothelial layer. This result shows that C-peptide requires Zn^{2+} to stimulate endothelial NO production, adding to other findings in the Spence group demonstrating the necessity of a metal for C-peptide bioactivity.[26, 28-30] Additionally, it was discovered that C-peptide is indeed capable of increasing endothelial NO production, however these results alone do not show conclusively that this NO production is a result of purinergic

signaling mediated by ATP released from RBCs as a result of Zn^{2+}-activated C-peptide stimulation. Instead, the RBC was revealed to mediate the NO production when physiological solutions lacking RBCs, but still containing Zn^{2+}-activated C-peptide did not stimulate an increase in NO production when flowed beneath the cultured endothelium. In order to show that RBC derived ATP is involved in the proposed mechanism, endothelial cellular monolayers were incubated with PPADS, a P2Y purinoreceptor inhibitor, flowing solutions containing RBCs and Zn^{2+}-activated C-peptide were no longer able to increase NO production, resulting in a complete reversal of the increase in NO production measured when comparing the flow of RBCs incubated with Zn^{2+}/C-peptide to RBCs alone. Collectively, these results prove that Zn^{2+}-activated C-peptide increases endothelial NO production by stimulating the release of a known endothelial P2Y agonist, ATP, from RBCs and thereby enhancing P2Y purinoreceptor activity by the stimulated increase in ATP antagonist levels, which prompts a purinergic signaling cascade known to result in increased endothelial NO production.

The novel findings, presented in Chapter 3, revealing the involvement of C-peptide in purinergic signaling and endothelial NO production provides an explanation for the observed improvements in blood flow of diabetic patients. Additionally, these findings show the potential for C-peptide as a drug candidate for the treatment of type 1 diabetes. Of course, in order to elicit these desired effects as a drug, C-peptide would have to be properly introduced to a metal, particularly Zn^{2+}, prior to administration. Unfortunately, this vital step has been overlooked previously, potentially explaining irreproducible activity of C-peptide observed during clinical trials that contrast with the reproducible stimulation of endothelial NO

production by Zn^{2+}-activated C-peptide. Plausibly, since C-peptide is often co-administered with insulin, and insulin often contains substantial (0.5% by mass) zinc impurities, C-peptide may be unintentionally introduced to a metal source eliciting varying degrees of biological activity upon administration, ultimately leading to inconsistent and irreproducible outcomes. Nevertheless, this work conclusively shows that, only in the presence of Zn^{2+}, C-peptide stimulates nitric oxide production in a cultured pulmonary artery endothelium via RBC-mediated purinergic signaling.

Interestingly, the ability of C-peptide to treat diabetic complications suggests that a chronic lack of C-peptide leads to the development of these complications and, more importantly, C-peptide plays a vital physiological role in maintaining human health. Therefore, C-peptide may not only improve diabetic blood flow, but it may be vital for regulating vascular tone in healthy individuals via the mechanism confirmed by this work. As a result, C-peptide may be of far more physiological importance than originally thought, which is supported by the discovered involvement of C-peptide in purinergic signaling, since purinergic signaling is responsible for regulating numerous biological processes throughout the body.[31] For these reasons, RBCs may play an equally important role in regulating vascular tone. As discussed in Chapter 1, it is well-known that NO produced in the blood vessel is primarily responsible for the fundamentally important task of regulating vessel tone, however the source of this NO is debated in the literature. Generally, the consensus is that this NO is produced in vascular regions of high shear stress generated by flowing blood, such as in resistance vessels. However, generally these regions are also where oxygen is exchanged from the blood to the surrounding tissues in response to hypoxia, which has been shown to cause NO release from RBCs. In this construct, NO is either derived from RBCs in response to hypoxia, or from the endothelium in response to

shear stress, however the mechanism by which the endothelium is still under discussion. However, one promising hypothesis largely developed by Sprague *et al*. links NO production in the endothelium to the RBC by ATP,[32] specifically by the ability of the RBC to release ATP. This hypothesis is supported by the known vasodilatory effects of circulating ATP achieved by stimulating NO production in the endothelium via the same purinergic signaling event involved in mechanism elucidated during this work for C-peptide stimulated NO production. Also supporting this hypothesis is work performed in the Spence lab showing that flowing RBCs release more ATP than static RBCs.[33] Collectively, these results, and others not discussed, support the hypothesis that ATP released from RBCs in response to shear stress is able to stimulate endothelial NO production by purinergic signaling.[34]

Further supporting this hypothesis are the results discussed earlier, and obtained while investigating endothelial NO production in the microfluidic vascular mimic during work presented in Chapter 3. Specifically, when a physiological solution not containing RBCs was allowed to flow beneath the cultured endothelium, a significant decrease in endothelial NO production was observed ($p<0.1$) in comparison to NO production resulting from a flowing solutions that contain RBCs. This result shows that flowing RBCs under the influence of shear stress can cause an increase in NO produced in the cultured endothelium. However, this activity, which was reported by the Spence group previously,[35] does not conclusively show that this NO is produced as a result of the previously identified ability of shear stress to stimulate ATP release from RBCs. In the same study, however, if selected endothelial layers were incubated with PPADS, a purinergic receptor inhibitor, the NO production in response to flowing solutions containing RBCs was statistically the same as NO produced in uninhibited

endothelial layers in response to flowing physiological solutions not containing RBCs. Collectively, these results suggest that shear induced ATP released from RBCs is capable of stimulating NO production in the pulmonary endothelium via purinergic signaling.

In summary, these studies show that C-peptide, in the presence of Zn^{2+}, is capable of indirectly stimulating NO production in the pulmonary endothelium by mechanism mediated by the red blood cell. Furthermore, these studies display the involvement of C-peptide in purinergic signaling, and since purinergic signaling is involved in numerous biological processes, it may be by this mechanism that C-peptide accomplishes vast biological activity throughout the body. Additionally, since C-peptide is capable of stimulating NO production in the endothelium, the peptide may play a crucial and overlooked role in maintaining basal NO levels in the bloodstream and regulating vascular tone. Also, by the same purinergic mechanism, RBCs under the influence of shear stress are capable of stimulating endothelial NO production. The source of shear induced NO production is under considerable debate in the literature, however this work shows reveals that sheared RBC are at least partially responsible for generating shear induced NO, and it is by this mechanism that RBCs may regulate vascular tone.

5.1.3 - Endothelial Permeability to C-peptide

Determining the ability of C-peptide to permeate an endothelial layer *in vitro* would be a significant contribution towards determining if the peptide can escape the bloodstream *in vivo*. This is important to determination since, aside from the work presented in Chapter 3, it has not yet been determined if C-peptide acts to induce biological events in various anatomical locations by directly interacting with the cell types that are primarily responsible for a specific event, or if these events are indirect consequences of C-peptide activity in the blood stream.

Since the capability of C-peptide to act by direct mechanisms throughout the body is dependent on the ability of C-peptide to permeate the endothelium *in vivo*, an *in vitro* study was performed to determine the likelihood that C-peptide can escape the bloodstream to act by direct mechanisms, or if the peptide is likely confined to the bloodstream, implying that all bioactivity is carried out indirectly by influences within the vasculature. To accomplish this investigation, the ability of C-peptide to permeate an endothelial layer was observed using the microfluidic vascular mimic in conjunction with conventional microtiter techniques.

Despite such vast differences between these models, a strength shared by each platform is the ability to confirm endothelial monolayer confluence and barrier integrity. As such, complete endothelial monolayer confluence was determined prior to each permeability assay, thereby ensuring the cultured cells most accurately mimic the true pulmonary endothelium. In work presented in Chapter 4, each experimental platform conclusively shows that C-peptide is capable of permeating a cultured endothelium. These results suggest that C-peptide may be able to perform biological functions by direct and indirect stimulation of cell types throughout the body. For example, work discussed previously suggests that C-peptide is capable of indirectly stimulating smooth muscle cell to induce vasorelaxation as a result of activity in the bloodstream. However, if C-peptide is truly capable of escaping the bloodstream, it may act as an important hormone that functions universally in the body by direct and indirect mechanisms, similar to insulin. This activity would support the recent concept that type 1 diabetes is actually a double-hormone deficiency disorder, with late complications potentially being derived from chronic lack of C-peptide.[36] The ability of C-peptide to induce biological events in cell types exogenous of the bloodstream has been previously shown,[37] however it is

currently unclear if C-peptide is capable of reaching these cells. These results suggest that C-peptide may indeed be capable of direct interactions with cells external of the cardiovascular system as indicated by the ability to permeate a cultured endothelium. Since C-peptide has never been detected exterior of the bloodstream, these novel findings suggest that C-peptide may have a much more comprehensive role in physiology and health than is currently assumed.

5.2 - Future Directions

5.2.1 - Microfluidic TEER System

Currently, a strongpoint of the TEER system is the simplicity of device design and fabrication, which is easily accomplished by using soft lithography for the rapid prototyping of polydimethylsiloxane (PDMS) devices as discussed in Chapter 2. While PDMS offers many advantages for microfluidic cell based assays and culture, as a material for microfluidic fabrication PDMS has several disadvantages,[38, 39] such as hydrophobicity, absorption and adsorption of substances, as well as high flexibility. These disadvantages render PDMS microfluidic devices undesirable in various situations. For example, a future direction of the TEER device is to study the pharmacokinetics and pharmacodynamics (PK/PD) of various drugs, however unpublished data from the Spence lab shows that several drugs absorb in PDMS, rendering the current device incapable of analyses of those drugs. Additionally, the flexibility of PDMS facilitates unintentional wrinkling of the polycarbonate membranes, which leads to leaking in the microfluidic device. Another issue regarding the current device design not related to PDMS as a fabrication material is the throughput attained using a single moving top electrode for TEER determination. Currently, the electrode must be manually inserted in the solution overlying the cultured cells for each measurement. This method does not achieve the

desirable high throughput generally accomplished by microfluidic analyses. However, these disadvantages may be addressed by compromising simplicity, a tradeoff likely favorable in this case.

5.2.1.1 - Polystyrene (PS) as a Material for Microfluidic Fabrication

Recently, methods for micromolding and rapid prototyping of PS by soft lithography have been accomplished by work performed in the lab of Nancy Albritton,[40] as well as in the labs of Dana Spence and Scott Martin that was recently submitted for publication. PS is amenable to cell culture and is very well characterized for such, as it is the material most commonly used to construct tissue culture flasks and Petri dishes. Remarkably, PS is capable of alleviating the current disadvantages of PDMS as the material used to construct the microfluidic TEER system, such as absorption of small molecules and high degrees of flexibility. PS would greatly increase the robustness of the device and surely decrease the frequency of leaking, however the construction of PS microfluidic devices is substantially more complicated and time consuming than constructing PDMS devices. However, this issue is alleviated by the robustness of PS microfluidic platforms, potentially allowing the device to be reused for multiple experiments. Of course, a method for high throughput TEER analysis would need to be developed for the PS microfluidic device.

Recent advances in the Spence and Martin labs have showed promise for the successful development of a PS microfluidic device capable of high throughput TEER analysis. Figure 5.1 shows a potential design for such a device, which includes an array of electrodes integrated into a bottom layer of PS for use in in the microfluidic TEER measurement system 2.0. While microfluidic-based TEER systems have been reported, these systems have yet to be used in an

array format allowing for high throughput analysis. Here, it is proposed that such an array can facilitate proper timing of cell subculturing in the microfluidic system that will allow for the culture of cells over a period of time that may extend from days to weeks, during which various cell based assays are possible, including PK/PD determinations for drugs of interest.

The approach shown in Figure 5.1 can be used to integrate TEER measurement capabilities in a PS device. As is shown in Figure 5.1, the group of Scott Martin has recently been able to embed microelectrode arrays in polystyrene-based microchips. This was accomplished by melting polystyrene powder in the presence of a gold SEM grid that was affixed to a connecting wire. Once the chip was cooled, it could be polished to a flat surface. Subsequently, it was found that these embedded electrode arrays can be used for amperometric detection in polystyrene-based microchips, suggesting that they can be used to successfully determine TEER. In this study, the arrays will be made to reside below each reservoir (Figure 5.1), and a separate set of reservoir electrodes (conventional wires) will be directed through a relay (controlled by LabView) into the reservoir so that the TEER value for each reservoir can be monitored in an automated fashion. This separate set of reservoir electrodes will be used to replace the single moving top electrode described previously, and importantly, these reservoir electrodes will be arranged in an array format. By using relays, a specific relay can be triggered, completing the circuit and allowing for the TEER reading for that particular reservoir to be attained.

The successful development of this proposed microfluidic TEER system would increase the robustness of the current design to a great extent. The proposed device would likely be reusable and prevent the absorption of small molecules into the device. Most importantly, the

throughput of the proposed device would be greatly increased relative to the current TEER system, since an array of reservoir electrodes can be used in lieu of the single moving reservoir electrode requiring the tedious manual placement in each reservoir for every TEER measurement. In contrast, reservoir electrodes in an array format would allow for automated high throughput TEER analysis without human involvement. Collectively, this increase in throughput, in addition to minimal absorption and increased device sturdiness will likely greatly increase the utility and applicability of the microfluidic TEER device.

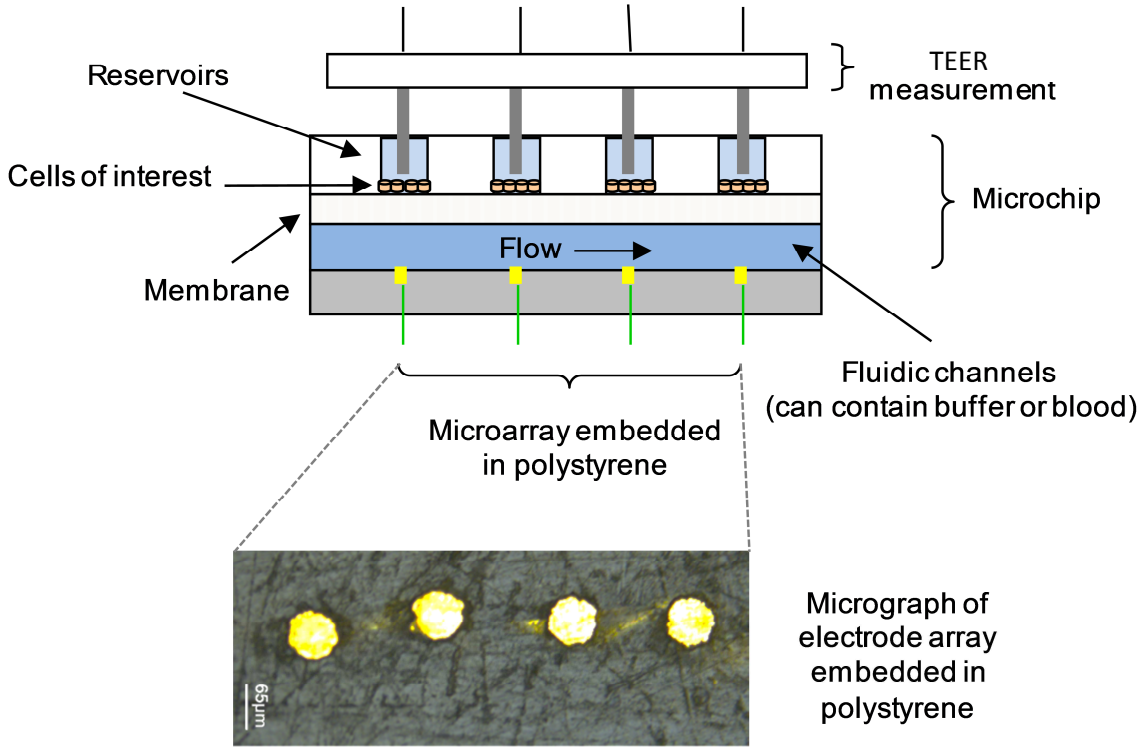

Figure 5.1 - Side-view of microchip with integrated TEER measurement. For simplicity, a 4-reservior array is shown. Also shown is a micrograph of a 4-microelectrode (gold) array that is embedded in polystyrene, which was fabricated in the lab of Scott Martin. The potential of the preliminary 4-microelectrode gold array as an effective platform for TEER analysis is illustrated by the previous utilization of the array in a microfluidic platform to detect analytes by amperometry, an electrochemical technique that is experimentally similar to the method used to determine TEER.

5.2.2 - C-peptide Induced Vasodilation

5.2.2.1 - Elucidate Zn^{2+}/C-peptide Interactions

The specifics of how Zn^{2+} is capable of rendering C-peptide capable of biological activity are currently unknown. Speculatively, Zn^{2+} is capable of binding C-peptide, possibly inducing a biologically active conformation of the peptide. In support of this proposed interaction, circular dicrhroism (CD) spectroscopic analysis performed in the Spence lab of Zn^{2+}-activated C-peptide and C-peptide alone suggest that in the presence of Zn^{2+}, a conformational change may occur. Also, a Scatchard binding curve has been obtained in the Spence lab for Zn^{2+} binding to C-peptide, which suggests that a single Zn^{2+} atom is capable of binding C-peptide. Additionally, mass spectrometric analysis of the active complex has revealed that C-peptide was likely bound to a metal, as discussed in Chapter 1. Aside from these results, as well as the observed change in the biological activity of C-peptide in the presence of Zn^{2+}, there is no further evidence for Zn^{2+}/C-peptide binding. These results do have not identified specific binding regions, or conclusively shown that binding results in an active conformation of the peptide.

As shown in Figure 5.2, C-peptide exhibits five negatively charged residues *in vivo* that are likely capable of Zn^{2+} binding and, therefore, provide insight as to where Zn^{2+} may bind the peptide. However, since preliminary data shows that only 1 Zn^{2+} atom binds C-peptide, it is still unclear which residue or residues it may bind. In order to conclusively show that C-peptide does bind Zn^{2+} to achieve an active conformation, nuclear magnetic resonance (NMR)

spectroscopic analysis of C-peptide, as well as the Zn^{2+}/C-peptide complex should be obtained. NMR is commonly used for the structural analysis of proteins and peptides,[41, 42] and could be used to determine Zn^{2+} induced conformational changes, and even elucidate specific binding regions. If it is ultimately shown that Zn^{2+} does not bind C-peptide, other interactions are possible that may result in C-peptide bioactivity. For example, C-peptide may not itself be responsible for bioactivity. Instead, zinc may be responsible for this observed bioactivity and C-peptide could simply be a carrier of the metal, responsible for delivering zinc to various cell types and thereby facilitating zinc transport through the bloodstream and into cells. This hypothesis is supported by the vast and fundamental physiological roles of zinc, including links to diabetes and nitric oxide production.[43-45]

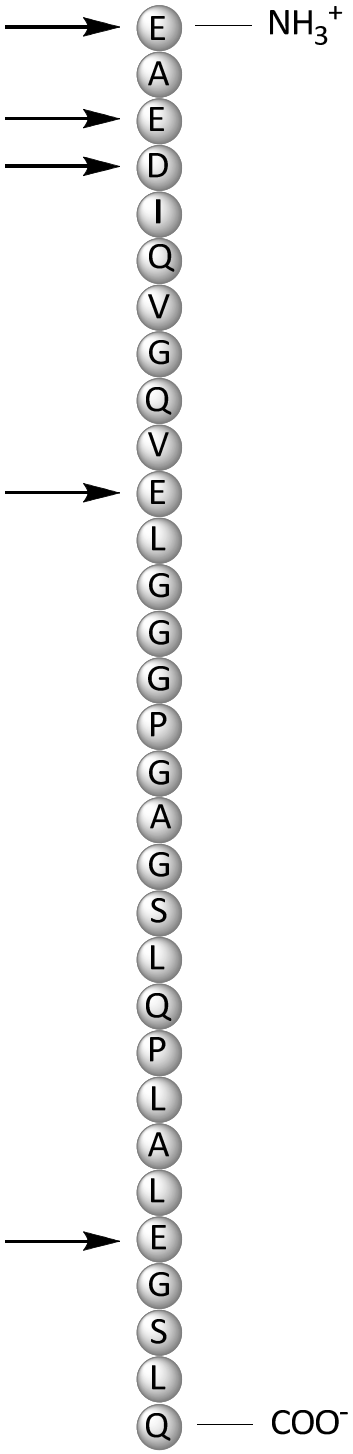

Figure 5.2 - The amino acid sequence of C-peptide is shown, which arrows highlighting residues that are negatively charged *in vivo*, and thus likely capable of binding free Zn^{2+} ions.

5.2.2.2 - Investigation of Zn^{2+}/C-peptide Activity *In Vivo*

Currently, several animal models of human type 1 diabetes exist.[46] To conclusively show the important potential bioactivity of C-peptide in the presence of Zn^{2+}, C-peptide should be administered alone, or co-administered with Zn^{2+} and the resultant physiological effects determined. Resulting improvements in blood pressure, nerve conduction, inflammation, etc. could be measured and attributed to Zn^{2+}-activated C-peptide. This study would be the first to determine the potential for Zn^{2+}-activated C-peptide as a drug for type 1 diabetes. Also, the necessity of zinc activation can truly be evaluated in a comparative clinical investigation for the first time. This investigation would be the most fundamental and conclusive method for determining the physiological effects of C-peptide, as well as the necessity of zinc activation.

5.2.3 - Endothelial Permeability to C-peptide

5.2.3.1 - Choosing Endothelial Cell Type

The work presented earlier revealing the ability of C-peptide to permeate a cultured pulmonary endothelium is novel in the sense that it is the first investigation into the potential ability of C-peptide to escape the bloodstream *in vivo*, and is, therefore, the first evidence suggesting that C-peptide does indeed leave the bloodstream *in vivo*. Since these results suggest that C-peptide may have a much more comprehensive role in physiology and health than is currently assumed, it is an important first step in determining the true scope of C-peptide's physiological influence throughout the body. However, to determine the true scope of biological activity, more research is required. These findings suggest that C-peptide is capable of permeating the pulmonary vasculature. However, it is well known that endothelial cells form

barriers of varying integrity, depending on their function in a specific organ or anatomical location.[47] In fact, endothelial permeability has been shown to be heterogeneous within the same organ.[48] Therefore, endothelial cell types that are specific to the particular organ or anatomical location influenced by C-peptide should be investigated to determine their particular permeability to C-peptide.

For example, C-peptide has been shown to improve diabetic neuropathy,[49] suggesting that C-peptide may be able to leave the bloodstream to enter the brain and directly improve nerved function. However, the endothelial cells lining blood vessels in the brain are highly specialized, forming an endothelial barrier called the blood brain barrier, which is far less permeable than endothelial layers found elsewhere in the body.[50] In consideration of this, in order to examine whether C-peptide directly facilitates improvements in nerve conduction and myelination, brain microvascular endothelial cells should be used to identify their permeability to C-peptide.

5.2.3.2 - Kinetics of Permeation and Comparisons

The kinetics of permeation of a particular analyte can be measured by the permeation coefficient of a particular analyte. The permeation assays reported in chapter 4 were performed merely to determine whether C-peptide was capable of penetrating a cultured endothelium. Since it was determined that C-peptide is capable of permeating the cultured pulmonary endothelium, permeation coefficients of C-peptide, as well as another well studied tracer molecules should be determined. By determining two permeation coefficients, the relative kinetics of permeation can be established, allowing for comparative studies. Several tracer molecules have been identified, such as phenol red and FITC-albumin, which are semi-

impermeable to endothelial monolayers.[51, 52] An experiment to support the results showing that C-peptide is capable of permeating an endothelium would be a comparative permeability assay, where the permeation coefficient of C-peptide obtained and compared to a semi-impermeable tracer molecule. If the permeability coefficient of C-peptide is higher than that of the semi-impermeable tracer, then it would be expected that C-peptide is able to permeate that particular endothelial cell type *in vivo*. However, since there exists no true negative control for endothelial permeation, or in other words, there is not a specific tracer molecule that is truly incapable of permeating endothelial cells *in vitro*, these semi-impermeable tracer molecules are generally used to monitor changes, or differences, in endothelial barrier integrity.

5.2.3.3 - Permeability of C-peptide Mutants

While a specific receptor for C-peptide has yet to be identified, it has been previously shown that C-peptide is able to specifically bind to endothelial cells by a binding event that is saturated at around 1 nM concentrations, which is of importance since the transport of macromolecules across the endothelium is generally accomplished by a transcellular and specific mechanism.[53] Also, C-peptide has been shown to be internalized by endosomes to enter human endothelial cells,[54] by a process which can be inhibited by nocodazole and monodansylcadaverine (MDC), signifying that C-peptide enters the cell by a mechanism which is receptor mediated and requires microtubule assembly. Interestingly, microtubules have been shown to facilitate transcellular transport and influence endothelial permeability and integrity.[55-58] These results suggest that there is a receptor responsible for trafficking C-peptide across the endothelium. In data not presented here, endothelial permeability to C-

peptide was shown not to be dependent on the presence of Zn^{2+}, suggesting that the proposed receptor may be promiscuous. However, in order to gain insight as to whether the mechanism of C-peptide transport is receptor mediated, the endothelial permeability to C-peptide mutants can be determined. Since receptors are often specific, the endothelial permeation of a C-peptide mutant may be halted or hindered due to inability to specifically bind the supposed receptor.

REFERENCES

REFERENCES

1. Kim, Y., W.C. Messner, and P. LeDuc, *Disruptive Microfluidics: From Life Sciences to World Health to Energy.* Disruptive Sciences and Technology, 2012. **1**(1): p. 41-53.

2. Whitesides, G.M., *The origins and the future of microfluidics.* Nature, 2006. **442**(7101): p. 368-73.

3. Szita, N., et al., *Microfluidic approaches for systems and synthetic biology.* Curr Opin Biotechnol, 2010. **21**(4): p. 517-23.

4. Shuler, M.L. and M.B. Esch, *Body-on-a chip: Using microfluidic systems to predict human responses to drugs.* Pure and Applied Chemistry, 2010. **82**(8): p. 1635-1645.

5. Genes, L., I., et al., *Adressing a Vascular Endothelium Array with Blood Components using Underlying Microfluidic Channels.* Lab on a Chip, 2007. **7**(10): p. 1256-1259.

6. Price, A.K., R.S. Martin, and D.M. Spence, *Circulation of erythrocytes through microfluidic channels: Investigations toward a circulatory vessel network on-chip.* Abstracts of Papers, 229th ACS National Meeting, San Diego, CA, United States, March 13-17, 2005, 2005: p. ANYL-208.

7. Spence, D.M., *Automation and Microfluidic Assays: In Vitro Models of the Mammalian Microcirculation.* Journal of the Association for Laboratory Automation, 2005. **10**(4): p. 270-275.

8. Carrel, A., *Pure Cultures of Cells.* J Exp Med, 1912. **16**(2): p. 165-8.

9. Carrel, A. and M.T. Burrows, *Cultivation of adult tissues and organs outside of the body.* Journal of the American Medical Association, 1910. **55**: p. 1379-1381.

10. Fischer, A., *Cultures of Organized Tissues.* J Exp Med, 1922. **36**(4): p. 393-7.

11. Fischer, A., *A Three Months Old Strain of Epithelium.* J Exp Med, 1922. **35**(3): p. 367-72.

12. Curtis, A.S. and M. Varde, *Control of Cell Behavior: Topological Factors.* J Natl Cancer Inst, 1964. **33**: p. 15-26.

13. Abercrombie, M. and J.E. Heaysman, *Observations on the social behaviour of cells in tissue culture. II. Monolayering of fibroblasts.* Exp Cell Res, 1954. **6**(2): p. 293-306.

14. Weiss, P., *Cell Contact*, in *International Review of Cytology*, G.H. Bourne and J.F. Danielli, Editors. 1958, Academic Press. p. 391-423.

15. Kaihara, S., et al., *Silicon micromachining to tissue engineer branched vascular channels for liver fabrication.* Tissue Eng, 2000. **6**(2): p. 105-17.

16. Andersson, H. and A. van den Berg, *Microfluidic devices for cellomics: a review.* Sensors and Actuators B-Chemical, 2003. **92**(3): p. 315-325.

17. Young, E.W., et al., *Technique for real-time measurements of endothelial permeability in a microfluidic membrane chip using laser-induced fluorescence detection.* Anal Chem, 2010. **82**(3): p. 808-16.

18. Ferrell, N., et al., *A microfluidic bioreactor with integrated transepithelial electrical resistance (TEER) measurement electrodes for evaluation of renal epithelial cells.* Biotechnol Bioeng, 2010. **107**(4): p. 707-16.

19. Douville, N.J., et al., *Fabrication of two-layered channel system with embedded electrodes to measure resistance across epithelial and endothelial barriers.* Anal Chem, 2010. **82**(6): p. 2505-11.

20. Booth, R. and H. Kim, *Characterization of a microfluidic in vitro model of the blood-brain barrier (muBBB).* Lab Chip, 2012. **12**(10): p. 1784-92.

21. Vogel, P.A., et al., *Microfluidic transendothelial electrical resistance measurement device that enables blood flow and postgrowth experiments.* Anal Chem, 2011. **83**(11): p. 4296-301.

22. Lindstrom, K., et al., *Acute effects of C-peptide on the microvasculature of isolated perfused skeletal muscles and kidneys in rat.* Acta Physiol Scand, 1996. **156**(1): p. 19-25.

23. Hansen, A., et al., *C-peptide exerts beneficial effects on myocardial blood flow and function in patients with type 1 diabetes.* Diabetes, 2002. **51**(10): p. 3077-3082.

24. Schalkwijk, C.G. and C.D. Stehouwer, *Vascular complications in diabetes mellitus: the role of endothelial dysfunction.* Clin Sci (Lond), 2005. **109**(2): p. 143-59.

25. Johansson, B.L., J. Wahren, and J. Pernow, *C-peptide increases forearm blood flow in patients with type 1 diabetes via a nitric oxide-dependent mechanism.* Am J Physiol Endocrinol Metab, 2003. **285**(4): p. E864-70.

26. Meyer, J.A., et al., *Metal-activated C-peptide facilitates glucose clearance and the release of a nitric oxide stimulus via the GLUT1 transporter.* Diabetologia, 2008. **51**(1): p. 175-82.

27. Ignarro, L.J., et al., *Endothelium-derived relaxing factor from pulmonary artery and vein possesses pharmacologic and chemical properties identical to those of nitric oxide radical.* Circulation Research, 1987. **61**(6): p. 866-79.

28. Brooks, P., J. Meyer, and D.M. Spence, *Metal (Zn2+) Activated C-Peptide Induced ATP Release Via Red Blood Cells with the Addition of Albumin.* Abstracts, 60th Southeast

Regional Meeting of the American Chemical Society, Nashville, TN, United States, November 12-15, 2008: p. SERM-680.

29. Medawala, W., et al., *A Molecular Level Understanding of Zinc Activation of C-peptide and its Effects on Cellular Communication in the Bloodstream.* Rev Diabet Stud, 2009. **6**(3): p. 148-58.

30. Meyer, J.A. and D.M. Spence, *A perspective on the role of metals in diabetes: past findings and possible future directions.* Metallomics, 2009. **1**(1): p. 32-41.

31. Burnstock, G., *Purinergic signalling.* Br J Pharmacol, 2006. **147 Suppl 1**: p. S172-81.

32. Sprague, R.S., et al., *ATP: the red blood cell link to NO and local control of the pulmonary circulation.* Am. J. Physiol, 1996. **271**: p. H2717-H2722.

33. Price, A., K., et al., *Deformation-induced release of ATP from erythrocytes in a poly(dimethylsiloxane)-based microchip with channels that mimic resistance vessels.* Analytical Chemistry, 2004. **76**(16): p. 4849-55.

34. Ellsworth, M.L., et al., *Erythrocytes: Oxygen Sensors and Modulators of Vascular Tone.* Physiology, 2009. **24**(2): p. 107-116.

35. D'Amico Oblak, T., P. Root, and D.M. Spence, *Fluorescence monitoring of ATP-stimulated, endothelium-derived nitric oxide production in channels of a poly(dimethylsiloxane)-based microfluidic device.* Anal Chem, 2006. **78**(9): p. 3193-7.

36. Wahren, J., K. Ekberg, and H. Jornvall, *C-peptide is a bioactive peptide.* Diabetologia, 2007. **50**: p. 503-509.

37. Lindahl, E., et al., *Proinsulin C-peptide regulates ribosomal RNA expression.* J Biol Chem, 2010. **285**(5): p. 3462-9.

38. Regehr, K.J., et al., *Biological implications of polydimethylsiloxane-based microfluidic cell culture.* Lab Chip, 2009. **9**(15): p. 2132-9.

39. Toepke, M.W. and D.J. Beebe, *PDMS absorption of small molecules and consequences in microfluidic applications.* Lab Chip, 2006. **6**(12): p. 1484-6.

40. Wang, Y., et al., *Benchtop micromolding of polystyrene by soft lithography.* Lab Chip, 2011. **11**(18): p. 3089-97.

41. Baldwin, A.J. and L.E. Kay, *NMR spectroscopy brings invisible protein states into focus.* Nat Chem Biol, 2009. **5**(11): p. 808-14.

42. Grzesiek, S. and H.J. Sass, *From biomolecular structure to functional understanding: new NMR developments narrow the gap.* Curr Opin Struct Biol, 2009. **19**(5): p. 585-95.

43. Prasad, A.S., *Clinical, immunological, anti-inflammatory and antioxidant roles of zinc.* Exp Gerontol, 2008. **43**(5): p. 370-7.

44. Pluth, M.D., E. Tomat, and S.J. Lippard, *Biochemistry of mobile zinc and nitric oxide revealed by fluorescent sensors.* Annu Rev Biochem, 2011. **80**: p. 333-55.

45. Jansen, J., W. Karges, and L. Rink, *Zinc and diabetes--clinical links and molecular mechanisms.* J Nutr Biochem, 2009. **20**(6): p. 399-417.

46. von Herrath, M. and G.T. Nepom, *Animal models of human type 1 diabetes.* Nat Immunol, 2009. **10**(2): p. 129-32.

47. Pries, A.R. and W.M. Kuebler, *Normal endothelium.* Handb Exp Pharmacol, 2006(176 Pt 1): p. 1-40.

48. Moldobaeva, A. and E.M. Wagner, *Heterogeneity of bronchial endothelial cell permeability.* Am J Physiol Lung Cell Mol Physiol, 2002. **283**(3): p. L520-7.

49. Johansson, B.L., et al., *Beneficial effects of C-peptide on incipient nephropathy and neuropathy in patients with type 1 diabetes mellitus.* Diabetic Medicine, 2000. **17**(3): p. 181-189.

50. Rubin, L.L. and J.M. Staddon, *The cell biology of the blood-brain barrier.* Annu Rev Neurosci, 1999. **22**: p. 11-28.

51. Wang, Y. and J.S. Alexander, *Analysis of endothelial barrier function in vitro.* Methods Mol Biol, 2011. **763**: p. 253-64.

52. Sun, M., et al., *A dynamic real-time method for monitoring epithelial barrier function in vitro.* Anal Biochem, 2012. **425**(2): p. 96-103.

53. Rigler, R., et al., *Specific binding of proinsulin C-peptide to human cell membranes.* Proc. Natl. Acad. Sci., 1999. **96**: p. 13318-13323.

54. Luppi, P., et al., *C-peptide is internalised in human endothelial and vascular smooth muscle cells via early endosomes.* Diabetologia, 2009. **52**(10): p. 2218-28.

55. Minshall, R.D. and A.B. Malik, *Transport across the endothelium: regulation of endothelial permeability.* Handb Exp Pharmacol, 2006(176 Pt 1): p. 107-44.

56. Minshall, R.D., et al., *Vesicle formation and trafficking in endothelial cells and regulation of endothelial barrier function.* Histochem Cell Biol, 2002. **117**(2): p. 105-12.

57. Lossinsky, A.S. and R.R. Shivers, *Structural pathways for macromolecular and cellular transport across the blood-brain barrier during inflammatory conditions. Review.* Histol Histopathol, 2004. **19**(2): p. 535-64.

58. Le Sueur, L.P., C.B. Collares-Buzato, and M.A. da Cruz-Hofling, *Mechanisms involved in the blood-brain barrier increased permeability induced by Phoneutria nigriventer spider venom in rats.* Brain Research, 2004. **1027**(1-2): p. 38-47.